CO_2 Absorption Rate Improvement of an Amino Acid Salt Solvent with an Inorganic Promoter

vorgelegt von
Dipl.-Ing.
Diego Andrés Kuettel
geb. in Madrid (Spanien)

von der Fakultät III - Prozesswissenschaften
der Technischen Universität Berlin
zur Erlangung des akademischen Grades

Doktor der Ingenieurwissenschaften

-Dr.-Ing.-

genehmigte Dissertation

Promotionsausschuss:
Vorsitzender: Prof. Dr. Felix Ziegler
Gutachter: Prof. Dr. George Tsatsaronis
Gutachterin: Prof. Dr. Tetyana Morozyuk
Gutachter: Prof. Dr. Klaus Görner

Tag der wissenschaftlichen Aussprache: 6. November 2015

Berlin 2016

Table of Contents

List of Figures

List of Tables

Nomenclature

Variables

Ap	Pipeline section [m]
a	Interfacial area [m^2/m^3]
[A]	Compound A concentration in the liquid phase [M]
*[A]**	Compound A equilibrium concentration in the liquid phase [M]
α	Cost index [-]
α_{rich}	Rich solvent carbonation ratio [mol/mol]
α_{lean}	Lean solvent carbonation ratio [mol/mol]
α_{CO2}	CO_2 loading [mol/mol]
BC	Bare cost [€]
C	Normalised cost [€]
C_o	Reference cost [€]
Cp	Heat capacity [kJ/kg·K]
CR	Capture rate [%]
ΔH_{Abs}	Heat of absorption [kJ/mol]
ΔT_{ln}	Logarithmic mean temperature [ºC]
E	Enhancement factor [-]
dp	Pipeline inner diameter [m]
dP/dt	Pressure derivative against time [mbar/s]
Ep	Performance enhancement factor [-]
f	Capacity factor [$Pa^{0.5}$]
FCI	Fixed capital investment [€]
HTF	Heat transfer factor [-]
IAF	Interfacial area factor [-]
L/G	Liquid to gas ratio [-]

M	Molar mass [kg/kmol]
MF	Module factor [-]
MPF	Material pressure factor [-]
n	Mol diffusion rate [kmol/h]
$O\&M$	Operation and maintenance cost excluding steam and power [€]
OMC	Operation and maintenance cost including steam and power [€]
P_A	Compound A partial pressure in the gas phase [bar]
P_A^*	Compound A equilibrium partial pressure in the liquid phase [bar]
pK_A	Acid dissociation constant [-]
Q	Heat transfer [kW]
q_{des}	Heat of desorption [kJ/kg]
q_{sen}	Sensible heat [kJ/kg]
q_{vap}	Heat of vaporisation [kJ/kg]
ρ	Density [kg/m^3]
R	Ideal gas constant [kJ/kmol·K]
R_A	Absorption rate [mol/m^2·s]
S	Capacity [-]
S_o	Reference capacity [-]
SED	Specific energy demand [MJ/kg]
t	Time [s]
T	Temperature [K]
TCI	Total capital investment [€]
U	Heat transfer factor [kW/(m^2·K)]
UF	Update factor [-]
$UMBC$	Updated module bare cost [€]
v	Fluid velocity [m/s]
V	Volume [m^3]
x	Mole fraction [mol/mol]

Abbreviations / Acronyms

AAS	Amino Acid Salt
BWT	Bundesamt für Wirtschaft und Technologie
CCS	Carbon Capture and Storage
CAPEX	Capital Investment Expenditures
ECHA	European Chemicals Agency
EOR	Enhanced Oil Recovery
ETS	Emission Trading Scheme
EUA	European Union Emission Allowance
FG	Flue Gas
G	Gas
GHG	Green House Gases
GV	Giammarco Vetrocoke
HPC	Hot Potassium Carbonate
HSS	Heat Stable Salt
L	Liquid
LNG	Liquefied Natural Gas
NG	Natural Gas
Oxo	Synthesis of oxo-alcohols from syngas
OPEX	Operation Expenditures
PCC	Post Combustion Capture
SCR	Selective Catalytic Reduction
TSA	Temperature Swing Absorption
V-l	Vapour-Liquid

Chemical Compounds

AAS^{2}	Secondary amino acid salt
AAS^{3}	Tertiary amino acid salt
$AASCOO^{-}$	Amino acid salt carbamate
$AASH^{+}$	Protonated amino acid salt
AMP	2-amino-2-methyl-1-propanol
As_2O_3	Arsenic trioxide
CCS^{+}	Siemens amino acid salt solvent
CO_2	Carbon dioxide
CO_3^{2-}	Carbonate anion
-COOH	Carboxyl group
COS	Carbonyl sulfide
CS_2	Carbonyl disulfide
DEA	Diethanolamine
H^{+}	Proton cation
HCN	Hydrogen cyanide
HCO^{3-}	Bicarbonate anion
H_2O	Water
H_2S	Hydrogen sulfide
KBO_3	Potassium borate
K_2CO_3	Potassium carbonate
M^{+}	Metal ion
MDEA	Methyldiethanolamine
MEA	Monoethanolamine
NH_3	Ammonia
NO_x	Nitrogen oxide
O_2	Oxygen
OH^{-}	Hydroxide anion

PROM-1	Absorption rate promoter 1
PROM-2	Absorption rate promoter 2
PZ	Piperazine
-R, -R_1, -R_2	Proton, alkyl or aryl functional group
R_1R_2NH	Primary or secondary amine formula
$R_1R_2NH_2^+$	Protonated primary or secondary amine
$R_1R_2NHCOO^-$	Amine carbamate
$R_1R_2RNCOOH$	Amino acid
$R_1R_2RNCOO^-M^+$	Amino acid salt
R-SH	Mercaptan
SO_2	Sulphur dioxide
SO_x	Sulphur oxide
V_2O_5	Vanadium (V) oxide

Units

bar	Bar (pressure)
ºC	Celsius degree (temperature)
€	Euro (price/cost)
g	Gram (weight)
h	Hours (time)
K	Kelvin (temperature)
kg/h	Kilogram per hour (mass flow)
kg/kg	Kilogram liquid per kilogram gas (L/G ratio)
kJ/mol	Kilojoules per mole (enthalpy)
kW	Kilowatt (power)
m	Meters (distance)
m^2	Square meters (area)
m^3	Cubic meters (volume)

mbar	Milibar (pressure)
MJ/kg	Megajoule per kilogram (steam demand)
ml	Mililiters (volume)
ml/h	Mililiter per hour (volume flow)
mm	Milimeter (distance)
μm	Micrometer (distance)
mmol	Milimole (mole quantity)
m^2/m^3	Square meters per cubic meter (specific area)
$m^3/(m^2 \cdot h)$	Cubic meter per square meter and hour (trickling density)
mol.%	Mole percent (concentration)
mol/mol	Mole CO_2 per mole amine (CO_2 loading)
MW_e	Megawatt electric (power)
MWh	Megawatt hour (energy)
Nm^3/h	Standard cubic meter per hour (volume flow)
$Pa^{0.5}$	Pascal square root (capacity factor)
ppm	Parts per million (concentration)
ppmv	Volumetric parts per million (concentration)
rev/min	Revolutions per minute (mixing speed)
t/d	Tones per day (mass flow)
vol.%	Volume percent (concentration)
W	Watt (power)
wt.%	Weight percent (concentration)

1. INTRODUCTION

Since fossil energy sources will remain the backbone of power generation worldwide for many years, Carbon Capture and Storage (CCS) is one of the short-term solutions to reduce carbon dioxide (CO_2) emissions, thus helping to mitigate global warming (IEA09). Among the major technologies for carbon capture, post-combustion is the most flexible option because it is not only suitable for new power plants, but can be retrofitted to existing power plants of any size that operate with any kind of fossil fuel.

In post-combustion carbon capture (PCC), carbon dioxide is removed downstream the combustion process. The removal process must be adequate for treating very large gas volumes with low carbon dioxide partial pressures in the presence of other impurities such as metal ions, oxygen sulphur and nitrogen oxides. The best option to achieve high removal efficiencies is carried out via absorption with chemical solvents. Gas scrubbing with chemical solvents is well known process to the gas purification industry, since it has been implemented in the removal of various types of acidic gases for the past eight decades.

The state of the art process uses an aqueous alkaline solution as a chemical absorbent, which undergoes an acid-base reaction to form soluble salt products. These salts are broken down by further heating in the solvent reactivation step. The most popular alkaline solutions nowadays are alkanolamines. Amino acid salts (AAS) were used in many gas scrubbing applications in the early stages of gas purification. Nowadays, AAS are no longer considered competitive in industrial processes (Koh97). The ionic nature of AAS has several operability benefits such as low vapour pressure and reduced solvent loss. They are considered as a potential solvent candidate for PCC plants. For the removal of carbon dioxide from other industrial gas mixtures at higher pressures, such as in the conditioning of synthesis gas, less reactive solvents like methanol and hot potassium carbonate (HPC) are preferred.

In the past few years Siemens has developed a post-combustion process, named PostCap™, designed to remove carbon dioxide from coal and gas fired power plants. This temperature swing absorption (TSA) process is operated with an aqueous amino acid salt solution, named CCS⁺. To further reduce the cost of the PostCap™ process, development and solvent improvement are currently under investigation.

It is the scope of this work to investigate potential chemical compounds, also known as absorption rate promoters, which added to CCS⁺ solvent accelerate the carbon dioxide absorption rate. The gas-liquid absorption basics dictate that for the removal of the same volume of gas, a promoted solvent requires less contact area and residence time, therefore smaller absorption equipment. A screening study was carried out to select the best promoter regarding toxicity, performance and cost. The benefit of the promoted solvent is further quantified in a laboratory mini plant and in a pilot plant that is retrofitted to a coal power plant combustion gas exhaust. The pilot results were fitted to a simulation model that estimates the packing height reduction potential with the promoted solvent. The process cost savings are finally calculated through an economic evaluation.

1.1. Evolution of Acidic Gas Treatment

Acidic gas treatment with alkaline solvents is a well-known process from its extensive implementation in petroleum and natural gas refining, coal gasification and hydrogen production. The evolution of this technology is marked by the variation in the industrial gas properties: temperature, pressure, composition and off-gas impurity specification. Technology developers need to select the nature of the chemical solvent and optimise the process design in order to fit each type of gas application, the sales gas specification and the other impurities present in the gas mixture. Table 1.1 compares the data gathered by Rolker et al. (Rolk12) on the CO_2 and H_2S specification and impurities of different gas applications treated with alkaline solvents with the values from combustion flue gas produced in coal and gas fired power plants after treatment with a post combustion CO_2 capture plant.

Table 1.1. Typical acidic gas specifications for various applications (Rolk12)

Application	CO_2 specification	H_2S specification	Further impurities
Natural gas (NG)	2 – 3 vol.%	< 4 ppm	> Hydrocarbons
LNG	< 50 ppmv	< 4 ppmv	
Syngas (Oxo)	10 – 100 ppmv	< 1 ppmv	O_2, SO_2, HCN, COS
Syngas (NH_3)	< 500 ppmv	-	
Refinery gas	-	4 – 150 ppmv	Hydrocarbons, sulphur components
*Biogas upgrading	2 – 3 vol.%	< 4 ppm	Hydrocarbons, O_2, NH_3, H_2S
Combustion flue gas	**0.35 – 1.6 vol.%	-	NO_x, SO_2, O_2

* Approximate values for injection in the natural gas grid

**After 90% removal from feed gas 3.5 vol-% (gas) to 13 vol-% (coal)

An acidic gas undergoes an acidic reaction in an aqueous solution and is later released unchanged upon sufficient heating of the water. Their removal from industrial gas mixtures is known as “gas sweetening”. This process involves a cyclic temperature swing absorption, in which an aqueous alkaline solvent chemically dissolves the acid absorbed component at low temperatures in the absorber and is later reactivated by high-temperature steam stripping in the desorber.

Other examples of acidic gas compounds removed by gas sweetening besides carbon dioxide are sulphur oxides (SO_x), nitrogen oxides (NO_x) hydrogen sulphide (H_2S), hydrogen cyanide (HCN), carbonyl sulphide (COS), carbon disulphide (CS_2) and mercaptans (R-SH). These acidic gas compounds are present in gas applications such as natural gas (NG), liquefied natural gas (LNG), refinery off-gas, synthesis gas, biogas and combustion flue gas.

1.1.1. Acidic Impurity Removal

In its early stages, gas sweetening was developed for mainly three reasons:

a) the presence of hydrogen sulphide and carbon dioxide reduces the heating value of natural gas, biogas and synthesis gas,

b) the mixture of acidic gases with moisture lead to metal corrosion and may damage pipelines, compressors, combustion equipment (e.g. gas turbine blades) and valves and

c) the separated hydrogen sulphide is fed to a Claus plant for the production of elementary sulphur.

The effect of strict product gas specifications in the end of the 1920s made the Girdler Corporation replace the usual absorbents, such as sodium and potassium carbonates used in the Seaboard process (Spe26), for aqueous alkanolamine solutions in their so-called “Girbotol Amine Process”. The alkanolamines demonstrated a higher gas solubility and absorption rate. For the treatment of the same volume of gas, amines required less solvent and smaller equipment. In the process, triethanolamine (TEA) was preferred due to its negligible vapour pressure and high viscosity, which leads to a minimum solvent loss during absorption or reactivation. A more detailed process description is to be found in Bottom’s US patent (Bot30).

Table 1.2. Types of Alkazid amino acid salt solvents and applications

Solvent	Properties	Application	Example
Alkazid “M”	Fast absorption reaction kinetics High working capacity	For efficient overall removal of CO_2 and H_2S	Syngas to be burned in a gas turbine Natural gas before transport in pipeline
Alkazid “Dik”	Slow absorption reaction kinetics with CO_2	Selective removal of H_2S	Refinery and coke oven gas to be fed in a Claus plant
Alkazid “S”	Stable in the presence of HCN, NH_3, CS_2, R-SH, dust and tar	Use with high impurity content off-gas	Off-gas from the gasification of a high impurity-containing raw material

At the same time, the I.G. Farbenindustrie patented the Alkazid process for the removal of acidic gases. To this process three different absorption solutions are known: Alkazid “M”, Alkazid “Dik” and Alkazid “S” (Table 1.2); all of which are formed from mixing a strong inorganic base (alkali-metal hydroxide) and a weak nonvolatile amino sulphonic or amino carbonic acid. The resulting amino acid salt (abbr. AAS) was intended to solve the main drawbacks of the alkanolamine processes. For instance, the high vapour pressure of the solution enriched with hydrogen sulphide disabled a complete cleanup to meet the product specifications. Moreover, the salt character of AAS reduced the solvent refill during operation (Bäh38).

1.1.2. Purification of Synthesis Gas

Since the 1950s, the growth of the demand for synthesis gas to be introduced in the ammonia, methanol, “Oxo” and Fischer-Tropsch synthesis extended the raw material spectrum to those with high sulphur contents. The extraction and exploitation of these resources was not profitable with the amine processes. Within the production of synthesis gas, large amounts of high pressure carbon dioxide were produced as a by-component in the water-gas shift reactor downstream the gasification. The carbon dioxide removal to concentrations lower than 0.1% is required so that the hydrogen consumption during methanation remains economically sustainable (Schi). A bulk carbon dioxide removal was to be combined with a fine scrubbing for which larger process equipment and higher energy demands were to be dealt with.

The Benfield process licensed by UOP (Ben56) proposed a new innovative configuration, which operates at a high temperature throughout the entire removal cycle. The absorption takes place at high pressures, and the carbon dioxide is later released by solvent flashing. The heat loss decreases, since no heat transfer between the rich and lean solvent is needed. The process runs with a hot potassium carbonate (HPC) solution, also known as “Hot Pot”. The high temperatures in the absorption column and high driving force make up for the poor absorption efficiency of the potassium carbonate absorbent. However, to enhance the absorption rate, proprietary compounds, also known as rate promoters or activators are added. Nowadays there are many licensed processes operated with different absorption promoters (Table1.3).

Table 1.3. Commercial synthetic gas purification processes with activated Hot Pot solvent

Process	Licensor	Rate Promoter
Benfield	UOP	Diethanolamine
Catacarb	Eickmeyer & Associates	$KBO_2 + V_2O_5$
Flexsorb HP	Exxon	Sterically hindered amines
GV / Arsen	Giammarco Vetrocoke	Arsenic trioxide
GV / Dual	Giammarco Vetrocoke	Glycine + Diethanolamine

At present, potassium carbonate is also considered as one of the potential solvents for carbon dioxide removal from combustion flue gases. However, the low gas partial pressures and the solvent’s kinetic limitation would lead to unfeasible equipment sizes. To compensate this kinetic limitation, there were several new rate promoters investigated by different authors (Cul04; Ste09; Tan11; Beh12).

1.1.3. Carbon Dioxide Recovery from Combustion Flue Gases

In the late 1970s, the recovery of carbon dioxide from power plant flue gases started to gain attention due to the higher demand for Enhanced Oil Recovery (EOR) and for the beverage industry. At that time, the most economic sources were gas wells and natural gas sweetening or synthesis gas purification, where carbon dioxide was obtained as a by-product. In remote locations where by-product carbon dioxide was unavailable, fossil fuel was combusted to produce low pressure flue gas. Carbon dioxide was then extracted by using a diluted monoethanolamine (MEA) solvent. Despite the fact that high oil prices made this production method economically feasible, it proved in the end to be a waste of energy. It was therefore targeted to recover carbon dioxide by retrofitting skid-mounted carbon capture plants on diverted power plant flue gas streams. However the recovery price was too high due to energy costs for solvent regeneration. The moment the oil price went down again, some plants were even closed down (Cha99).

Moreover, the worldwide scientific concern for climate change was finally materialised by the signing of the Kyoto protocol in 1997. In this meeting, it was for the first time internationally agreed upon that carbon emissions had to be significantly reduced, as a measure for combating against global warming (Wol94). Since coal, gas and oil are still to be maintained as main energy resources for the future, the carbon capture technology had to be improved to meet the requirements of large scale power plant flue gases (Table 1.4). First, the low carbon dioxide partial pressure in a combustion flue gas requires higher absorption efficiency in order for absorption to take place. Contrary to other high pressure gas feeds, such as synthesis and natural gas, combustion flue gases require a chemical absorbent. Secondly, combustion flue gases are composed of other gaseous products besides carbon dioxide, nitrogen and water vapour. By-components like sulphur oxides, nitrogen oxides and oxygen are also present and degrade the chemical absorbent (And12). The degraded solvent is refilled for a constant capture performance, which increases the operational costs of the process.

Table 1.4.Technological requirements for CO_2 recovery from flue gases

CO_2 application	Off-gas properties	Process specifications
Coal- and gas-fired power plants	Atmospheric pressure flue gas with low CO_2 concentrations (approx.13 vol.% for coal and 3.5 vol.% for gas), oxidative environment, intermediate gas inlet temperatures (50°C), large gas volumes (approx. 3000 Nm^3/h per 1 MW_e for a hard coal-fired power plant) and presence of NO_x, SO_x	90% CO_2 removal (only achievable with chemical absorbents), low total CO_2 capture cost

The amine processes had already gained a lot of operation experience in other industrial applications. Three similar processes were therefore developed for carbon dioxide recovery:

a) Kerr-McGee / ABB Lummus Crest Process

b) Kansai Mitsubishi - Carbon Dioxide Recovery (KM-CDR)

c) Fluor Daniel Econamine FG Process

The Kerr McGee process is an improved version of the Girbotol Amine Process. From the priority date on, it was widely used in the petroleum industry for purifying refinery and natural gases, and for recovery of hydrogen sulphide for sulphur manufacture. The low vapour pressure TEA had been substituted by the faster reacting MEA. With the focus on lowering the vapour pressure at the column head, Riggs' disclosed findings proposed lowering the temperature of the solvent to 26 - 35°C before entering the absorber, as well as keeping the amine concentration at 15-20% to maintain a high absorption rate (Rig89).

The Kansai and Mitsubishi technology developers were not satisfied with the low solvent concentrations, the low amount of carbon dioxide absorbed per mole of amine and the high energy requirements, characteristic of the MEA process. For this purpose, hindered amines such as 2-amino-2-methyl-propanol (AMP) and amino acid salts had been reported to be of advantage, in spite of their low absorption rate. However, this was improved by the addition of a fast reacting rate promoter, such as Piperazine (PZ). Moreover, in their Patent published in 1995 (Mim95), Kansai states that there is a very high risk of corrosion in the ethanolamine capture plant when recovering carbon dioxide from combustion gases with high oxygen content. A hindered amino acid salt activated with fast reacting piperazine was suggested as an adequate solvent, since the mixture was tested with low corrosion effects on carbon steel.

In 1989, Fluor Daniel bought the GAS/SPEC FT-1^{TM} process and licensed it under the name of Econamine FG^{SM}. This process had been previously developed and operated by Dow Chemical and Union Carbide in the early-1980s before the oil price downfall. The solvent used was a 30 wt-% aqueous MEA solution with an oxidation inhibitor. All of Fluor's commercial plants were retrofitted to gas-fired flue gases. The process has only been demonstrated under coal-fired conditions at a pilot-scale (San92).This process is considered as the state of the art technology for carbon dioxide recovery from combustion flue gases.

1.1.4. Carbon Capture and Storage (CCS)

At the start of the past decade, the actions to meet the carbon emission standards set in the Kyoto protocol were intensified. In 2005, the European Union put the Emission Trading System (ETS) into practice as an incentive for industrial installations to reduce their carbon emissions, and therefore reach the European reduction target set for 2020. According to the “cap and trade” theory, a limit was set to the total greenhouse gas emissions. At the start of the program, emission allowances, also known as EUAs were sold in auctions or allocated for free. Those installations with fewer emissions can trade their allowances to those who require higher emissions. In the middle of 2008 the emission of a metric ton of carbon dioxide cost 30€. A positive financial environment motivated private companies and public research and development entities to invest in reducing the cost of state of the art carbon capture technologies below this price. Much importance was given into increasing the absorption efficiency of capture solvents, in order to reduce the equipment size and regeneration energy demand. However, due to the economic crisis, the lower industrial activity decreased the demand for EUAs, and the allowance price decreased to 6€. With the current state of the art technology, it is unrealistic to try and achieve a lower capture price by means of cost reduction. This has put CCS activities “on hold”.

Although the ETS may have succeeded in reducing carbon dioxide emissions, it has failed to ensure a stable pathway towards a future decarbonisation of the energy and industry sectors. This target is only achievable through a large scale deployment of CCS systems. Due to the adverse economic situation, the European Commission asks for more commitment from the national governments and industry outside of the ETS, including those providing the fossil fuels. In their last communication from January 22, 2014, the European Commission proposed to set the greenhouse gas emission reduction target at 40% relative to emissions in 1990. This target shall be met by 2030. The main driver proposed to all member states is a controlled increase on the maximum annual permitted emissions (bel14).

1.2. The PostCap™ Process

In the past few years, Siemens has developed a post-combustion process, named PostCap™, designed to remove the carbon dioxide from coal and gas fired power plants. This temperature swing absorption (TSA) process is operated with an aqueous amino acid salt solution, named CCS⁺. To further reduce the cost of the PostCap™ process, development and solvent improvement are currently under investigation.

The four main factors in Siemens strategy towards climate change mitigation are increasing the power generation efficiency, expanding renewable energies, switching to more efficient fuels and CCS. Like many other companies driven by the introduction of the ETS at the start of the 21st century, Siemens developed a proprietary post-combustion carbon capture process, which was designed under the trade name PostCap™ for the separation of carbon dioxide from power plant flue gases. The absorption-desorption process has been fitted to operate with an improved amino acid salt solvent, CCS⁺. After years of intensive pilot-scale testing under the real flue gas conditions of Staudinger Block V coal-fired power plant, Post-Cap™ (Figure 1.1) is ready for large-scale demonstration (And11).

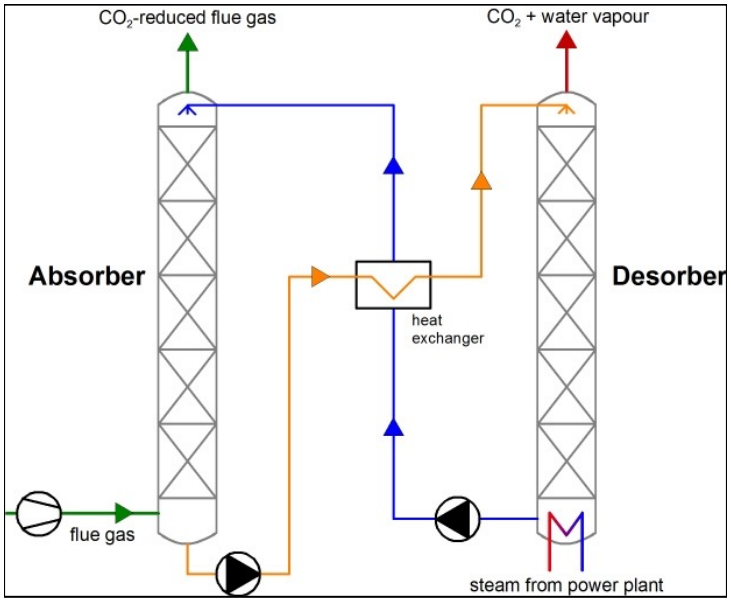

Figure 1.1. PostCap™ simplified flow diagram for CO_2 capture

Amino acid salts are the salt form of natural amino acids. They are therefore formed by neutralising an amino acid compound with an alkali metal hydroxide (Figure 1.2). Thus the alkalinity of the amine group is increased, i.e. the amino acid reacts selectively with acid gases such as carbon dioxide. Due to their ionic nature, both AAS and their absorption products are conveniently nonvolatile.

Amino acids derive from ammonia (NH_3), from which one, two or three hydrogen atoms are substituted by proton, alkyl and (or) aryl groups (-R, -R1, -R2). At least one of the substituents comprises a carboxylic group (-COOH). All aqueous solutions of amines are of alkaline nature. Hence, they react with acid gases through their free electron pair. Amino acids are normally found in detergents, fertilisers and cosmetics.

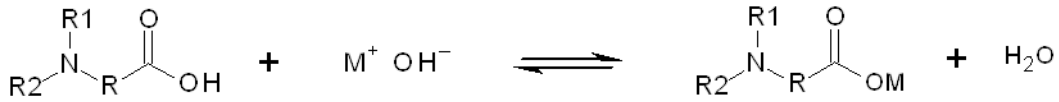

Figure 1.2. Amino acid neutralisation to amino acid salt

As shown by Eide-Haugmo et al. (Eid09), AAS have a high biodegradability. Their toxicity is an order of magnitude lower than any of the other alkanolamines, piperazine or ammonia. The components are considered as adequate solvents for carbon dioxide absorption.

To sum up, the main advantages from the CCS+ solvent are:

a) Comparable absorption reaction kinetics as alkanolamines

b) Low energy demand (demonstrated by current Siemens investigations)

c) Zero vapour pressure of the AAS

d) High biodegradability

e) Mainly nonvolatile degradation products, which remain in the liquid phase

The Siemens PostCap™ CO_2-capture process experiences in general have validated the numerous benefits amino acid salt based solvents potentially possess for the separation of CO_2 from power plant flue gases. Due to the ionic nature, the PostCap™ process has no solvent volatility losses during the operation of the capture plant. This significantly reduces additional process costs in comparison to state of the art alkanolamine processes. The formation of heat-stable salts due to the impurities in the flue gas current is well understood (Fis13) and is not a handicap for the PostCap™ process. These HSS and other hazardous products can be regenerated in the Siemens proprietary solvent reclaiming process.

1.3. Motivation and Scope

At the moment, the cost of separating one tone of carbon dioxide with the state of the art chemical amine solvent technology is by far higher than the price of a European emission allowance, or the CO_2 price dictated by the beverage industry and EOR applications. The reduction of the emission cap will increase the allowance price in the coming years and the continuous climb in the oil price will trigger the EOR deployment. This will give the industry sector a second chance of reducing the cost of carbon capture. Only a large scale deployment of CCS in the short to mid-term will provide with a realistic chance to fight against global warming, while maintaining fossil fuels as the backbone of power generation.

The main contributors to the cost of carbon capture are the size of the absorption equipment and the high energy demand for solvent regeneration. An improvement of the solvent's absorption efficiency, which contemplates both the kinetics and equilibrium properties of the carbon dioxide separation, is therefore the key factor to reducing costs.

In acidic gas removal from low pressure gas mixtures, the most used solvent thanks to its high absorption efficiency is MEA. Its main drawbacks, which include solvent stability, steel corrosion and carry-over losses, were solved through degradation inhibitors and technical improvements in the process layout. The CCS^+ solvent based on an amino acid salt is set out to be a potential replacement of MEA in carbon capture. Its favourable features due to its ionic nature and chemical structure significantly improve the operability of the capture process. Regarding absorption reaction kinetics, CCS^+ is at the same level as MEA. As it has already been verified and deployed for the slow reacting hot potassium carbonate and MDEA solvents, the absorption rate of carbon dioxide can be significantly enhanced by the addition of rate promoters. Organic promoters such as MEA and PZ were widely investigated and implemented at an industrial scale. Inorganic promoters were mainly investigated for the hot potassium carbonate process. Their implementation in amino acid salt solvents is still to be verified.

It is the purpose of this work to identify a potential rate promoter that suits the CCS^+ solvent's absorption properties. The selected promoter is to be further tested in the laboratory mini plant and in the Staudinger pilot plant to verify its effect on the absorption kinetics. The enhancement of the absorption rate is to be experimentally determined and modelled in the simulation program Aspen Plus®. In the end, an economic evaluation will determine the cost savings by introducing the promoter in a full scale carbon capture plant.

2. BASIC PRINCIPLES

Absorption is the phenomenon of taking up and dissolving a gaseous absorbed component into a liquid phase. In the process industry, absorption is used for removing gaseous solutes from gas mixtures using a liquid solvent as absorbent. This process is commonly known under “gas scrubbing or washing”. The liquid solvent is contacted in countercurrent with the gas mixture in an absorber. By means of V-L mass transfer, the gaseous solute is dissolved into the liquid solvent (Lew24). Afterwards, the loaded solvent is regenerated from the absorbed component by means of desorption, and again fed into the absorber to start a new cycle. This process allows the removal of unwanted components from gas mixtures; and by means of the subsequent regeneration, these components may be gained as a product. Chemical absorption occurs when the absorbed component is converted with the liquid reactant into reaction products. In case of fast reaction, the solute diffusion through the liquid film occurs parallel to the chemical reaction. The resistance of the film to mass transfer and the solute concentration are lowered, which increases the absorption rate. If the reaction belongs to the slow regime, the chemical reaction takes place in the liquid bulk. The absorption rate remains the same as physical absorption.

Enhancement of the absorption rate or absorption efficiency is higher for those solvents with bigger heats of absorption. These solvents possess a higher capacity of absorbed carbon dioxide per cycle and require smaller equipment sizing to meet low pressure gas specifications. Alkanolamines are the state of the art solvents for carbon dioxide removal in petroleum refining, coal gasification and hydrogen production. The increase in interest of flue gas scrubbing to reduce carbon dioxide emissions has increased the interest back to amino acid salt solvents due to their ionic nature. Chemical solvents with kinetic-limited operation conditions, either because of molecular structure or the loading range in the absorber may be promoted by adding absorption rate promoters. Fast-reacting alkanolamines are well known promoters. However, some may result unstable under post-combustion operation conditions. Weak oxyacids are proven to act as carbon dioxide hydration catalysts (Rou38). Their use in systems that operate close to equilibrium has been reported to be beneficial. The activation of amino acid solvents has not been fully investigated yet.

Carbon capture performance is defined as the amount of energy required to reach the desired gas specification. In the process operation, it is quantified by the capture rate and the solvent specific energy demand. Both variables depend on a series of key process parameters, which must be also considered when optimising the operation. For a given plant design, the energy requirement for a given capture rate can be lowered by adjusting the liquid-to-gas ratio. In order to combat against climate change, CCS must be deployed at a full scale. The state of the art technology has mainly been built for commercial purposes. However, reducing carbon emissions requires a big investment and operation cost savings. Testing of improved solvents and process optimisation occurs mainly at a pilot-scale. The next step is to demonstrate the progress at a large-scale.

2.1. Gas Absorption

A large number of gas absorption operations or processes have long been put into practice in the industry. In all of them, a liquid is contacted with a gas to transfer a soluble component from the vapour phase to the liquid absorbent. In post-combustion carbon capture, carbon dioxide is removed from a combustion flue gas stream exiting a coal or gas-fired power plant, and dissolved into an alkaline solution. Amine-based solvents are ideal for this gas mixture, since the low carbon dioxide partial pressure requires high absorption efficiency. The transport phenomenon is described in different hydrodynamic models such as the Film Theory (Lew24) and the Penetration Theory (Hig35), which was later revised by Prof. Danckwerts' Surface Renewal Model (Danc50). The Film Theory, the first and most simple of all models, is used in this work for better understanding of the principles of gas absorption.

2.1.1. Film Theory

In 1924, Lewis and Whitman established the Film Theory, which dictated that whenever a liquid and a gas come into contact, there exists on both sides of the interface a layer in which motion by convection is slightly compared to that in the bulk. The model considers the liquid and gas layers as stationary films, in which the diffusion of the gaseous solute takes place. The diffusion is driven by the molecule redistribution from higher to lower concentration regions. It is therefore common to speak of a concentration "driving force". Speaking in local mass transfer terms, the driving force is the difference between the bulk and the interface (i) concentration. Speaking in overall mass transfer terms, the driving force is the difference between the bulk and the equilibrium (*) concentration. An illustrative example of the Film Theory for an absorbed component A is given in Figure 2.1.

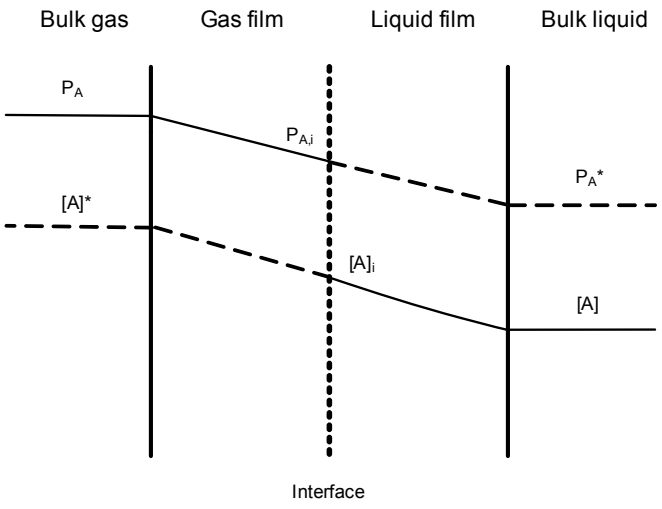

Figure 2.1. V-L concentration gradients of the absorbed component A

The Film Theory simplifies the understanding of the mass transfer process; however the authors pointed out that it should not be interpreted that there is a sharp line of demarcation between the stationary film and the bulk of the gas and liquid (Lew24).The absorbed component is distributed throughout the film forming a concentration profile. At the interface, the solute concentration is in thermodynamic equilibrium between both phases. In the gas and liquid bulk, mixing by convection causes the solute concentration to remain uniform at all points. The film is therefore where the resistance to the mass transfer of the absorbed component from one phase to the other is the controlling agent. In some cases the resistance in one film is so much greater, that the other is neglected. For example, in the case of absorbing a pure gas into a liquid, the resistance in the gas film is nonexistent. At a higher gas or liquid flow rate, the resistance to mass transfer decreases.

Equilibrium or saturation is the final state in which every gas-liquid system that is not in equilibrium advances to. After the equilibrium is reached, diffusion of the absorbed component stops. The system can be displaced from equilibrium by varying the temperature and/or the pressure. The rate at which the system advances towards equilibrium is sometimes more important in the practice than the equilibrium itself. These two factors are dependent on one another, in the sense that the rate is greater the further the system is from equilibrium. The equilibrium concentration gradient is illustrated with a discontinuous line. With the passage of time in a closed system, the concentration profiles on both sides of the interface would tend to move to the horizontal, where the absorbing component concentration in the bulk of the gas and the liquid are equal to equilibrium ($P_A^* \rightarrow P_A$ *and* $[A] \rightarrow [A]^*$). In a flowing system, Figure 2.1 would represent an instant at some point during countercurrent flow. In industrial applications, the contact time is not sufficient in order for the system to reach equilibrium.

2.1.2. Diffusion Rate

The diffusion rate with which an absorbed component is transferred from the gas to the liquid phase depends on the film resistance or diffusion rate coefficient, the V-L interface area and the displacement from the equilibrium or driving force (Equation 2.1):

$$Diffusion\ Rate = Diffusion\ Rate\ Coefficient \times Interfacial\ Area \times Driving\ Force \quad (2.1)$$

Empirical correlations in liquid-side controlled absorption have established that at constant hydrodynamic conditions (film thickness, viscosity), the overall diffusion rate coefficient is directly proportional to the square root of the absorbed component film diffusivity and to the gas solubility in the liquid (Ast67). The gas solubility is inversely proportional to the temperature and the ionic strength of the liquid (Kir04). The interface area is the effective contact area between the gas and liquid. In industrial absorbers, the contact area is maximised by placing structured or random packing in the column's internals. In V-L systems where the liquid film diffusion is the controlling step, the thin liquid film trickling down the packing reduces the resistance to mass transfer. The absorption driving force is equal to the gradient between the absorbed component partial pressure in the gas bulk P_A, and the equilibrium vapour pressure above the liquid absorbent P_A^*. According to the Van't Hoff equation, the equilibrium pressure variation with the inverse temperature is directly proportional to the absorption enthalpy characteristic of the absorbent (Equation 2.2).

$$\frac{\mathrm{d}lnP_{CO_2}}{\mathrm{d}\left(\frac{1}{T}\right)} = \frac{\Delta H_{abs\,CO_2}}{R} \qquad (2.2)$$

If the absorbed component partial pressure in the bulk is higher than the equilibrium, absorption occurs; if lower, the mass transfer is reversed and the solute is transported back to the vapour phase (Figure 2.2). Desorption can therefore be considered as a reversed absorption. In the practice, the solvent temperature is lowered before entering the absorber column to favour gas solubility. In the desorber, a stripping vapour stream is generated in the reboiler to heat up the solvent to its boiling point, providing the heat of desorption to break the chemical bonds with the solvent and reduce the carbon dioxide partial pressure in the gas bulk below the equilibrium pressure.

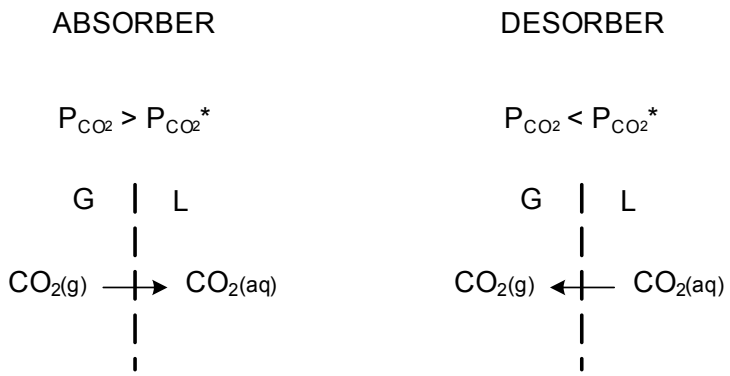

Figure 2.2. CO_2 absorption and desorption in practice

2.1.3. Enhancement of Mass Transfer with Chemical Reaction

If the absorbed component undergoes a chemical reaction in the liquid film, the absorption rate is substantially increased, because of two reasons: the absorbed component concentration in both the film and the bulk are reduced, which lowers the equilibrium pressure and results in a higher driving force; the resistance to mass transfer in the liquid film is lowered, assuming that the chemical reaction takes place in the liquid film (Figure 2.3). The effect of chemical reaction in the liquid film diffusion is represented by the enhancement factor *E*, or ratio between the diffusion rate with chemical reaction, n_{chem} and without chemical reaction, n_{phys} as expressed in Equation 2.3:

$$E = \frac{n_{chem}}{n_{phys}} \qquad (2.3)$$

Depending on the rate of reaction, the absorption rate is controlled either by the diffusion in the liquid film or by the chemical reaction.

In case of fast absorption reaction kinetics, the solute is consumed in the liquid film, which curves the concentration gradient (Figure 2.3). The enhancement factor is directly proportional to the reaction constant, so the diffusion rate coefficient increases linearly with absorption reaction kinetics (Ast83). If the reaction rate takes place instantaneously, the absorbed component and liquid-phase reactant cannot coexist in the liquid film. The enhancement factor reaches its maximum and the diffusion of the liquid phase reactant in the liquid film is the controlling step.

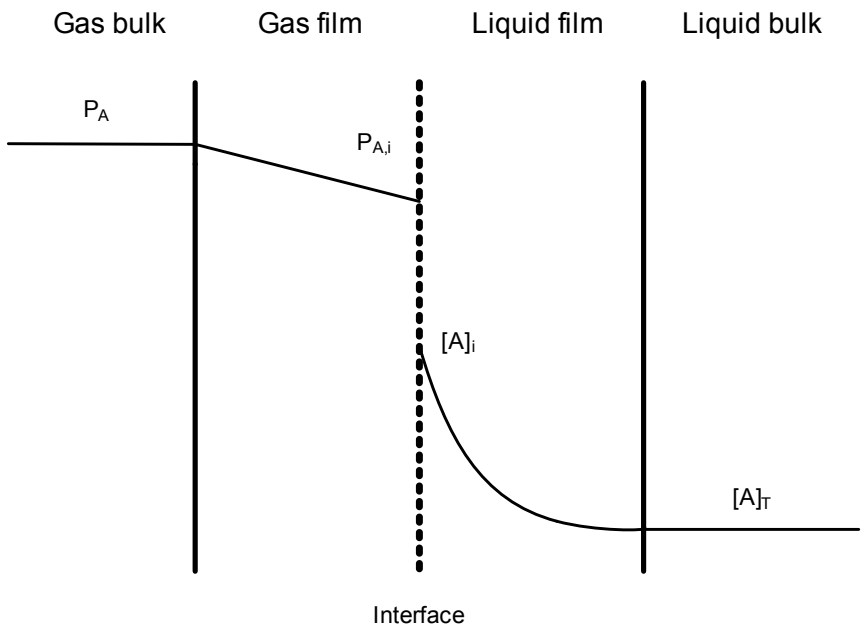

Figure 2.3. Concentration gradients of solute A with chemical reaction in the liquid film

In case of slow absorption reaction kinetics, the solute is transported through the liquid film, and the chemical reaction takes place in the liquid bulk. The concentration gradient in the film approaches linearity, and the chemical reaction no longer affects the film resistance to mass transfer. Within the slow reaction, two regimes can be differentiated:

- The kinetic regime for when the reaction rate is extremely slow. The liquid phase is completely saturated with the absorbed component.
- The diffusional regime for when the chemical reaction does not enhance the diffusion rate coefficient, i.e. the enhancement factor equals 1.

As can be seen in Table 2.1 in the practical example column, the variation of the temperature, the solvent strength and the carbonation ratio can cause that a same absorption system encounters three different chemical absorption regimes. After consumption of the absorbent's chemical capacity, the heat of absorption decreases, approaching the physical absorption enthalpy. The absorption efficiency decreases and the curve shown in Figure 2.3 would tend to move towards linearity at higher carbonation ratios for most chemical solvents.

In case of fast-reacting amines, the heat of absorption remains constant for carbonation ratios below a value of 0.5 mol/mol. At higher carbonation ratios the heat of absorption decreases linearly. Depending on the chemical nature of the solvent, the heat of absorption at higher carbonation ratios has a higher decreasing gradient.

Table 2.1. Chemical absorption regimes (Ast67)

Regime	Properties	Absorption rate = f(-)	Practical example
Kinetic	Very low reaction rate, liquid is saturated with absorbed component	Liquid holdup	CO_2 absorption with potash at room T and high carbonation ratios
Diffusional	*E=1*	Contact area, volumetric diffusion rate coefficient	CO_2 absorption with fast reacting amines at carbonation ratios higher than 0.5 mol/mol
Fast-Reaction	*E>1*	Contact area, reaction rate, driving force, rate promoter	CO_2 absorption with potash at high T and high $[CO_3^{2-}]$
Instantaneous	*E* ↑↑↑	Diffusion of the liquid reactant in the film	CO_2 absorption with fresh fast reacting amines

The solvent fed at the top of the absorber always contains a residual amount of carbon dioxide, since complete reactivation in the desorber would require excessive stripping steam. The chemical absorption regime within the absorber will therefore depend on the extent of solvent reactivation. The energetic optimum is reached when for a feasible absorber size the solvent is regenerated so that the desired gas specification can be met.

2.1.4. Conventional Chemical Solvents for CO_2 Capture

The use of aqueous chemical solvents is one of the major options for removing carbon dioxide from combustion flue gases. As seen in the previous decades, alkanolamines and hot potash have played a major role in removing carbon dioxide from industrial gases, such as in petroleum refining, coal gasification and hydrogen production (Roc01).In post-combustion capture, there are various factors regarding the process which influences the solvent selection. These were classified into three main groups: absorption efficiency, operability and toxicity.

The absorption efficiency is one of the most important factors in carbon capture because it determines the size of the absorption equipment and the steam economy. The absorption efficiency is a function of the carbon dioxide loading capacity and the gas uptake velocity. The absorption efficiency of a chemical solvent is directly proportional to its heat of absorption. The loading capacity is a measure of the amount of carbon dioxide absorbed per unit of solution per absorption cycle. Its numerical value is equal to the working capacity between the carbonation ratio at the bottom of the absorber and desorber (Figure 2.4).The loading capacity is in large measure a function of the equilibrium characteristics, i.e. how the equilibrium partial pressure varies with the carbonation ratio in the solvent. Solvents with higher heats of absorption achieve a higher loading capacity at a smaller temperature difference (absorber / desorber), i.e. they have a higher “temperature swing capacity”. Solvents with lower heats of absorption theoretically reach loadings closer to 1 mol/mol. However, their low temperature swing and absorption reaction kinetics requires high gas partial pressures.

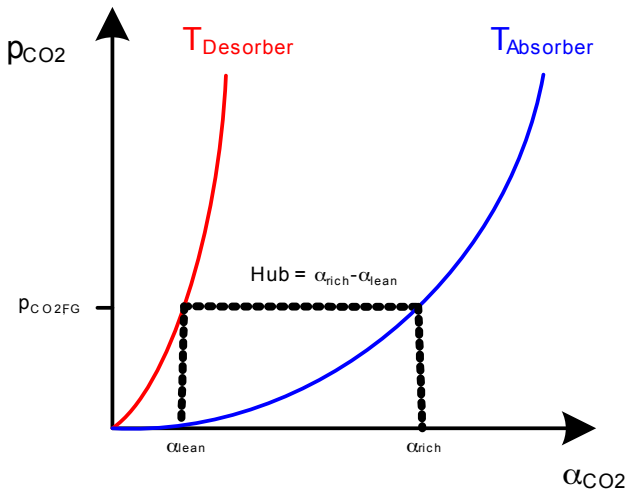

Figure 2.4. Loading capacity

The simple relationship between equilibrium and heat of absorption for various conventional alkanolamines has been recently discussed by Mathias et al. (Mat12). Under constant absorber conditions (temperature, lean carbonation ratio and solvent concentration), those solvents with higher heats of absorption achieve a lower equilibrium pressure. The gas uptake velocity is a measure of the speed with which the V-L system advances towards equilibrium. It is directly proportional to the heat of absorption, and is physically determined by the diffusion rate coefficient. Kinetic-limited amines require high gas pressures and absorber sizes to operate close to equilibrium. Their use in chemical absorption is only feasible when they are combined with an absorption rate promoter. Table 2.2 contains some examples of common alkanolamines investigated and used in the gas purification industry. The enthalpy of absorption from the reaction with carbon dioxide is related to the diffusion rate coefficient and temperature swing.

Table 2.2. Common alkanolmines used in the industry (Koh97; Mat12)

Alkanolamine	Heat of absorption, kJ/mol	Diffusion rate coefficient	Temperature Swing	Comments
PZ	-87	Very high	High	Used as activator in aMDEA™
MEA	-85	High	High	State of the art
DEA	-72	Intermediate	Intermediate	Used in refinery gases, inert to COS
AMP	-66	Low	Low	Hindered amine
MDEA	-59	Low	Low	Selective removal of H_2S
TEA	-48	Low	Low	First commercial amine

The operation costs of the capture process are increased by the liquid reactant loss due to thermal and oxidative degradation, solvent slip in the treated gas and heat stable salt (HSS) formation (Shao09). Those solvents which due to their chemical structure are more stable towards flue gas by-components (NO_x, SO_x and O_2), or require easier reclaiming methods, are therefore preferred. In order to ensure stable operation, the solvent loss must be continuously refilled, for which the solvent cost is a deciding factor. CO_2-loaded amine solutions are well known to corrode industrial construction material, mainly carbon steel (Ste06). The use of less corrosive solvents or the addition of an inhibitor omits the need of using costly metallurgies.

In carbon capture systems, the low toxicity has a priority over the cost effective factor. The introduction of fast reacting solvents or promoters that are hazardous to the environment is therefore excluded from this work, although they may have a very high cost reduction potential. Although a solvent itself may not be hazardous to the environment, the products that may result from scrubbing combustion flue gases might be. In the case of primary and secondary amines, it is well known that they react with nitrogen dioxide to form nitrosamines. Recently, the Norwegian Climate and Pollution Agency has directly addressed nitrosamines in amine scrubbing, restricting total nitrosamine levels (NCPA11). A proper control and management of the formed nitrosamines is required if the amine scrubbing technology is to be further considered as an important option to post-combustion carbon capture.

2.3. Amine-CO_2 Reaction Chemistry

During chemical absorption, carbon dioxide reacts with the amine to form salt products. The various reaction pathways that occur in the liquid depend mainly on the reaction rate, influenced by the chemical structure of the amine and the free amine concentration in the film. The absorption is followed by an amine-CO_2 interaction to form an adduct ($R_1R_2NHCOO^-$), which may undergo two different transformations. These transformations depend on the chemical structure of the amine solvent and determine the two possible reaction paths. If the N-C bond is strong, there will be a concominant depopulation of the N-H bonding orbital. If sufficiently strong, the depopulation of this orbital may lead to the loss of the proton and the formation of the carbamate species ($R_1R_2NCOO^-$) (Chak88). The released proton is accepted by another amine molecule to form the protonated amine species ($R_1R_2NH_3^+$). This first reaction pathway (Reaction 2.1) is known as the carbamate formation.

$$2 \cdot R_1R_2NH + CO_2 \Leftrightarrow R_1R_2NCOO^- + R_1R_2NH_2^+ \qquad \text{(R-2.1)}$$

Primary and secondary amines are able to form carbamates. According to the reaction stoichiometry, the maximum carbonation ratio in the CO_2-loaded solution (total moles of carbon dioxide absorbed per mol amine) possible is 0.5 moles CO_2 per mole amine. This is only in case the only product of reaction is the amine carbamate. In the following chapters, the carbonation ratio will generally be expressed in mol/mol units. Tertiary amines cannot react directly with carbon dioxide since the free electron pair is shielded by the nitrogen atom hydrocarbon substituents. The N-C bond is weak, and the acid-base adduct is hydrated. This second reaction is known as the bicarbonate formation. Sterically hindered primary and secondary amines also form carbamates. However, the carbamate stability decreases due to the steric hindrance of the free electron pair. The carbamate therefore more easily hydrolyses to bicarbonate in the presence of water. The reaction between carbon dioxide and water (Reaction 2.2) is the slowest of all reactions. The rate may be enhanced by the presence of a stronger base that accepts the free proton such as potassium carbonate or a tertiary amine.

$$CO_2 + H_2O \Leftrightarrow HCO_3^- + H^+ \qquad \text{(R-2.2)}$$

The reaction between carbon dioxide and hydroxide ion (Reaction 2.3) belongs to the instantaneous regime. However, at lean-solvent pH values (9 -10), the hydroxide concentration is too low to be considered. Primary and secondary amines predominantly form carbamate. Tertiary and some hindered amines act as bases to accept the free proton in the direct carbon dioxide hydration.

$$CO_2 + OH^- \Leftrightarrow HCO_3^- \qquad \text{(R-2.3)}$$

The carbamate also may undergo hydrolysis to form bicarbonate. The overall reaction(Reaction 2.4) is divided into 2 consecutive reactions: first the carbon dioxide hydration, followed by a base displacement reaction (reversed Reaction 2.1), in which the carbamate loses the COO^- group, and by recuperating its proton, it is once again regenerated to a free amine that diffuses back to the interface (Chak88). The overall balance enables every mole of carbon dioxide to form one mole of bicarbonate.

$$R_1R_2NCOO^- + H_2O \Leftrightarrow HCO_3^- + R_1R_2NH_2 \qquad \text{(R-2.4)}$$

The degree of carbamate hydrolysis is controlled by parameters such as free amine concentration, solution pH, and most important of all, by carbamate stability (Cap68; Ewi80; Chak88). The maximum absorption of carbon dioxide is achieved when all of the absorbed carbon dioxide exists as bicarbonate, and all the amine exists as the protonated species (Hoo97). It is therefore desired to achieve maximum carbamate hydrolysis in the absorber. There are mainly two limitations:

- a kinetic limitation due to the slow carbon dioxide hydration and
- an equilibrium limitation regarding carbamate stability.

2.4. Amino Acid Salt Solvents

After their use long ago in the Alkazid process, amino acid salt solvents were superseded in the gas scrubbing industry by the akanolamine solvents such as monoethanolamine and activated methyldiethanolamine for the treatment of natural gas, refinery and syngas. The latter solvents have demonstrated a higher solvent stability and regeneration energy requirement amongst other things. However, a new interest arising in carbon dioxide removal from combustion flue gases has set amino acid salt solvents back into the potential candidate solvent list (Fer01).

2.4.1. AAS properties

Amino acid salts exist in aqueous solution as totally dissociated salts, making them much less volatile than conventional alkanolamines. The big advantage of having a negligible vapour pressure is the reduction of solvent carry-over losses and the subsequent solvent refill cost. The comparison of degradation pathways of amino acid salts and conventional alkanolamines in carbon capture is discussed by Fischer (Fis13). It was observed in general that AAS such as potassium N,N-dimethylglycinate, taurate and sarcosinate demonstrated lower degradation rates and less volatile degradation product emissions in comparison to alkanolamines such as MEA and DEA. The catalytic effect of metal ions on the degradation pathways can be hindered with a solvent inhibitor.

The formation of bicarbonate at high pH values causes solid crystallisation in some amino acid salts. The precipitate may damage rotating equipment such as pumps and may cause blockages in pipelines, valves and column packing structures. The precipitation is enhanced at lower temperatures, higher carbonation ratios and AAS-concentrations (Hoo97). Crystallisation in amino acid salt solvents thus introduces some limitations in the carbon dioxide capture process:

- the absorber bottom temperature cannot be lower than the solubility limit of the rich solvent, which compromises the loading capacity and
- the AAS strength cannot exceed the limit marked by the optimum absorber operating temperature required to fulfil the treated gas specification.

Kumar (Kum02) gave evidence to the higher conversion rates when the reaction product from carbon dioxide absorption into aqueous potassium taurate precipitated. Crystallisation increases the loading capacity at a constant gas partial pressure, which would lower the regeneration energy demand. It is only required that the absorber is modified to be capable of processing the slurry. A spray absorber or plate tower would fit this purpose (Ver11).

2.4.2. CO_2 Absorption with AAS

In a solvent screening investigation for use in a submarine air purifying device, Hook (Hoo97) compared the carbon dioxide absorption efficiency of two conventional alkanolamines, MEA and AMP, with various types of AAS molecular structures. The purpose of his study was to quantitatively determine the effect of hydrocarbon substituents at the amino group and at the α-carbon on absorption reaction kinetics, loading capacity and crystallisation. MEA's counterpart in AAS is Glycine. Its fast absorption reaction kinetics with carbon dioxide have made it the low toxicity version (in substitution of arsenite) of the Giammarco Vetrocoke Dual process (Gia84).A strong steric hindrance clearly reduced the initial absorption rate. The amine centre is blocked by the hydrocarbon substituents avoiding the direct electrophilic attack by carbon dioxide. It also increased crystallisation at lower carbonation ratios.

The Siemens CCS^+ solvent is an aqueous mixture of a secondary hindered amino acid neutralised with a strong metal hydroxide base. The diffusion scheme of carbon dioxide into the solvent is depicted in Figure 2.5.

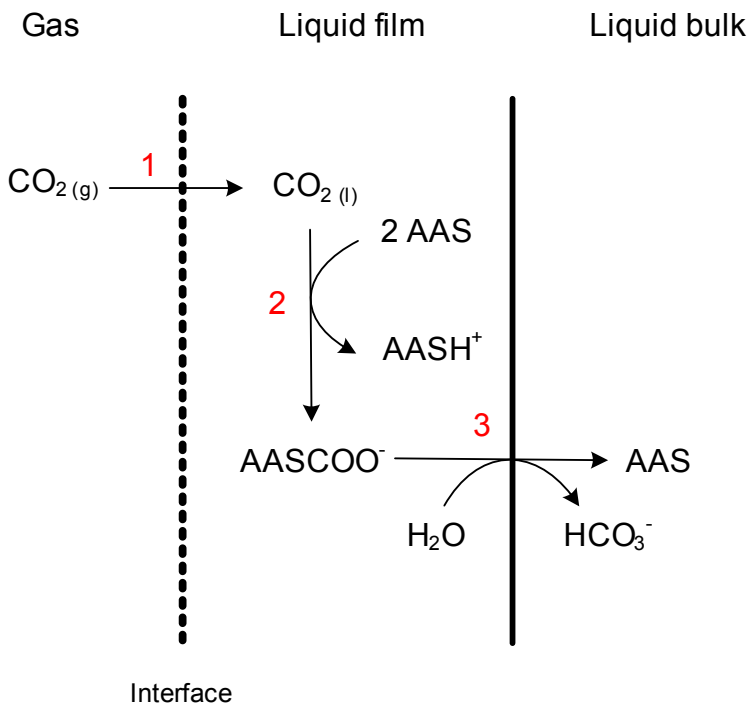

Figure 2.5. CO_2 diffusion scheme into CCS^+

The gaseous carbon dioxide is first absorbed into the liquid phase (step 1). As stated before, this stage is proportional to gas solubility and partial pressure in the gas mixture. The ionic nature causes the salting-out effect, which lowers the gas solubility under that of water. The solved carbon dioxide later reacts with the free amino acid salt molecule. The secondary amino group enables the fast carbamate formation (step 2). This reaction is favoured at low carbonation ratios and takes place in the liquid film, close to the interface. The steric effect lowers the carbamate stability, enabling the slow hydration reaction (step 3) to take place in the liquid bulk, to achieve higher carbonation ratios.

Step	Name	Proportional to	Rate
1	CO_2 Physical Absorption	Gas solubility, CO_2 partial pressure,	Fast
2	Carbamate formation	Absorption heat	Fast
3	Carbamate hydrolysis	Carbamate stability	Slow

Table 2.3. CO_2 mass transfer stages in aqueous CCS^+

From all three mass transfer stages, the carbamate hydrolysis is the slowest and therefore rate-controlling (Table 2.3). In the practice, in order to obtain high conversions to bicarbonate, high residential times in the absorber are required. The equipment costs are increased due to larger column and packing sizes.

2.4.3. Addition of an Absorption Rate Promoter

McNeil (McN67) established that in the absorption of carbon dioxide into aqueous amine solutions, the fast reaction in the liquid film leads to carbamate formation. The carbamate product diffuses through the film to the liquid bulk where it undergoes carbamate hydrolysis to form bicarbonate and free amine. Through the carbamate formation and posterior hydrolysis, carbon dioxide is transported through the film faster than if it diffused unreacted to the zone of slow reaction in the bulk. This absorption rate enhancement is called the “shuttle mechanism”.

fIn commercial absorption systems with fast reacting solvents, the residence time is not long enough to allow much carbamate hydrolysis to take place (McN67). The bulk liquid composition at the bottom of the absorber corresponds to the carbamate equilibrium. If the carbon dioxide hydration is catalysed by addition of a hydration promoter, such as sodium arsenite, carbamate hydrolysis is enhanced and the bulk composition tends to move towards the bicarbonate equilibrium". According to McNeil, if sodium arsenite is added to MEA, it is possible to operate closer at bicarbonate equilibrium. The catalyst enables the plant to operate at an increased working capacity of 0.2-0.6 mole CO_2/mole MEA. Compared to the standard 0.2-0.4 mol/mol loading range, the absorber size is higher in order to reach the maximum loading capacity. However, steam economy and solvent flow rate can be reduced, which also lowers pumping costs and the cross heat exchanger size.

The catalysis with buffer solutions of the slow carbon dioxide hydration was proposed by Roughton and Booth (Rou38). They investigated the mass transfer promoting effect of several oxyacid buffers when added into carbonate buffer solutions, in order to further investigate on the initial findings from Faurholt (Fau24). Weak acids with similar dissociating constants (pK_A) had a similar catalytic effect. The absorption enhancement effect was also seen for the rate of carbon dioxide output or desorption. This effect is therefore considered as catalytic, and was named "homogeneous catalysis".

Astarita et al. (Ast81) pointed out that both mechanisms (shuttle mechanism and homogeneous catalysis) are extreme cases of the same operation (absorption of a gas accompanied by two parallel reactions) and that the reaction rates determine which one is predominant. In practically most important situations neither of the two mechanisms is sufficiently accurate to describe this absorption operation.

Sharma (Sha63) encompassed the catalysis effect to all Brönsted bases. In this case a suitable rate promoter for the potassium carbonate solvent was searched for. After screening various contenders, they concluded that arsenite ion is the most effective due to its high catalytic power, high solubility, stability and favourable ionisation constant at the industrial practice range from 8.5 to 10. The addition of weak acid and base absorption rate promoters with pK_As within the industrial pH range in chemical solvents for acidic and alkaline gas absorption was further patented by Smith et al. (Smi78). Although the scope was aimed at other gas absorption processes rather than carbon dioxide absorption, they had found a positive relation between both factors and reported increased absorption rates and reduced operation costs.

Extended investigation work on the promotion effect of oxyacids on other chemical solvents such as amino acid salts has not yet been publicly presented. Mimura et al. (Mim98) patented the addition of piperazine to an amino acid salt solvent in order to accelerate the absorption rate of carbon dioxide from gas mixtures. Wagner et al. (Wag09) patented the addition of fast-reacting primary amines to tertiary amino acid solvents for enhanced carbon dioxide recovery from combustion flue gases. The advantage of tertiary AAS is their stability towards oxygen and that they do not form carcinogenic nitrosamines in the presence of NO_x. Vorberg et al. (Vor10) patented an acid promoter for AAS solvents. However the scope of this patent is preferred for selective hydrogen sulphide removal. Asprion et al. (Aspr11) patented the use of fast-reacting alkanolamines as rate promoters for amino acid salt solvents. The advantage of using an activated tertiary amino acid salt over a tertiary alkanolamine was investigated by Alvis et al. for use in carbon dioxide scrubbing during synthesis gas and LNG production (Alv12).

2.5. State of the Art CO_2 Recovery Plant

In post-combustion carbon capture, the plant is retrofitted at the tail end of the gas treatment chain. Upstream may be located: the selective catalytic reduction (SCR) of nitrogen oxides (NO_x) to molecular nitrogen, the electrostatic filter that precipitates most of the flue ash and the flue gas desulphurisation unit for removal of sulphur oxides (SO_x).

The basic configuration used in post-combustion carbon capture is illustrated in Figure 2.6. The flue gas to be treated (1) is introduced into the absorber, in which it is subjected, in counter flow, to an aqueous solution of an alkaline compound. This solution is loaded with a low carbon dioxide remainder, and is therefore known as “lean” solvent (2). In order to cool the gas down to the absorber operating temperature, a water quench is implemented upstream the absorber. Due to the concentration driving force, carbon dioxide is absorbed into the liquid, where it reacts with the alkaline molecules to form heat-labile salts. The absorber is equipped with structured packing segments in order to increase the V-L contact area, and enhance mass transfer. Structured packing is the most suitable option for this process since it combines a low pressure drop with a high interfacial area. Considering that power plant flue gases have near to atmospheric pressure, this fact reduces the size of the flue gas blower. On the other hand, a high contact area enhances the gas mass transfer and hence reduces the absorber and desorber packing height.

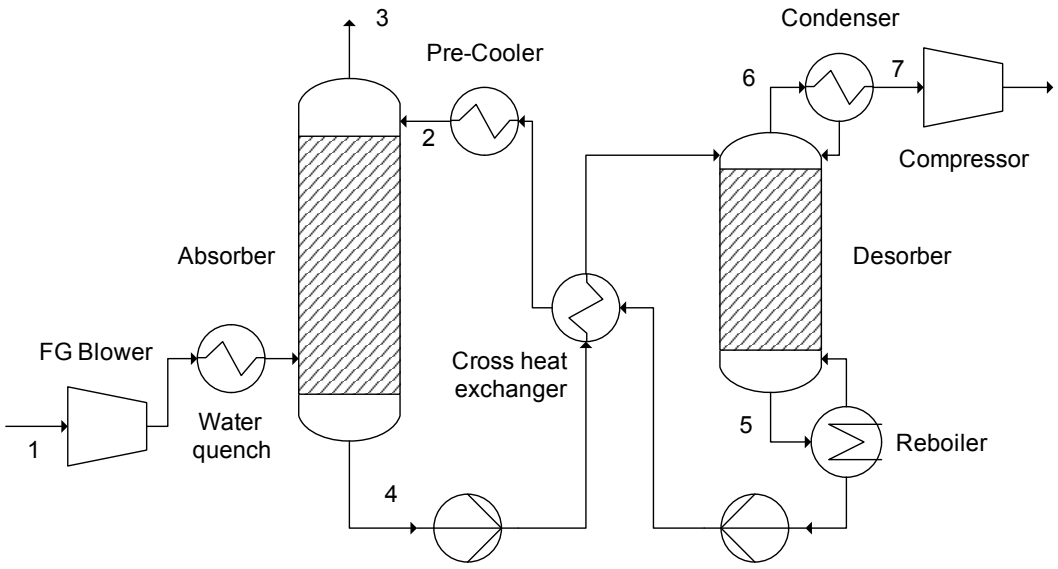

Figure 2.6. Absorber / Desorber process

The treated gas stream (3) is withdrawn from the absorber head and the salt-loaded aqueous solution, also known as “rich solvent” (4) from the sump. The rich solvent is pumped to the desorber for regeneration. In the cross heat exchanger placed between the absorber and the desorber, the heat of the lean solvent leaving the desorber bottom (5) is transferred to the rich solvent, until the desorber operating temperature is reached. The rich solvent is fed at the top of the desorber column, where the absorption reaction is reverted back to gaseous carbon dioxide and reactivated alkaline compound. The required reactivation energy is supplied by the upwards flowing stripping steam generated in the reboiler. The carbon dioxide is desorbed back into the vapour phase and exits the top of the desorber together with the aqueous stripping vapour. The desorber is fitted with structured packing in order to enhance mass transfer.

The reboiler heat duty equals the sum of the energy used for three main purposes: to raise the temperature of the rich solvent to its boiling point, to break the chemical bonds between carbon dioxide and the absorption solvent, and to establish the driving force needed for stripping by generating a aqueous vapour stream (Sak05).The extra steam vapour (6) is condensed at the top of the desorber and recycled back to the column. A pure carbon dioxide current (7) is sent to the compressor, where it achieves the proper pressure to be transported, stored underground or further used.

The lean solvent (2) temperature is reduced in the pre-cooler before reentering the absorber, to increase gas solubility. The treated gas specification limits the equilibrium partial pressure at the top of the absorber. At lower temperatures, the vapour pressure over the lean solvent is lower increasing the mass transfer driving force.

2.6. Carbon Capture Performance Variables

The carbon capture performance is measured by the absorption efficiency with which carbon dioxide is removed from the gas mixture. In PCC plants, the capture performance is determined by the capture rate and the specific energy demand.

The capture rate *CR* is the percentage of carbon dioxide flow volume in the feed gas removed in the capture plant. The *CR* must be set regarding the gas specification in the treated gas current. Since the carbon dioxide removed reacts with the amino acid solvent in the absorber, the CR is proportional to the absorber-desorber working capacity and the liquid to gas ratio, *L/G* (Equation 2.4).

$$CR = \frac{L}{G} \cdot \left(Working\ Capacity\right) \tag{2.4}$$

The CR is normally a fixed variable in carbon capture applications. Steenevelt et al. (Ste06) presented in their CCS technology overview that the economic amount of removed carbon dioxide was between 80 and 95%. Kvamsdal et al. (Kva05) specified that when the *CR* is reduced from 90 to 75%, the absorption efficiency is significantly increased. However, when CR is increased to 95%, the investment costs are much higher.

The specific energy demand *SED* is the ratio between the reboiler heat duty and the removed carbon dioxide mass flow (Equation 2.5). The reboiler heat duty is at its lowest when the final equilibrium is reached in the absorber. The carbon capture plant operates at its optimum, when the solvent flow rate is adjusted to the available contact area to reach the lowest *SED* possible.

$$SED = \frac{Reboiler\ Heat\ Duty}{Removed\ Carbon\ Dioxide} \tag{2.5}$$

2.7. Key Operating Variables

The proper selection of the operation variables that influence the carbon capture performance are key factors for the correct rate promoter testing in the capture process.

2.7.1. Column Packing Height

The packing height defines the amount of interfacial area available for carbon dioxide mass transfer in the absorber and desorber. The packing height is sized regarding the gas uptake velocity. To achieve low energy demands, the V-L system should be close to equilibrium at al points in the absorber and desorber. The addition of an activator to the kinetic-limited solvent may increase the diffusion rate coefficient and therefore reduce the required packing height considerably.

2.7.2. Solvent Flow Rate

The solvent flow rate is directly proportional to the raw gas throughput. The relationship between liquid and gas flow, *L/G* is a standard which depends on the solvent's carbon dioxide uptake capacity per cycle. Its value is optimised by achieving the lowest heat duty in the reboiler for a given gas flow volume and treated gas specification.

2.7.3. Absorber Operating Temperature

The amine-CO_2 reaction liberates energy to the environment. The temperature gradient in the absorber column gives an idea of the absorption rate in each stage. At the top of the absorber column, the partial pressure over the solvent is lowered below the treated gas partial pressure in the lean solvent cooler. As the solvent descends in the column, the absorption enthalpy set free by the chemical reaction with carbon dioxide heats up the solvent. The higher temperature is an indication that more carbon dioxide is being absorbed. At the bottom of the column, the solvent is cooled down by the flue gas stream. At this point, the chance of carbonate precipitation is the highest, since the solvent has a carbonation ratio close to equilibrium at a low temperature.

2.7.4. Solvent Strength

The solvent concentration in the aqueous solution is also commonly known as "strength". The absorption performance increases with the solvent strength. Both the absorption reaction kinetics and the loading capacity are higher. However, a higher concentration also tends to higher material corrosion, carbonate precipitation (especially in AAS solvents) and solvent degradation. Each solvent has an optimal range in which it can be safely operated.

2.8. Carbon Capture Plant Scale-Up

There are several stages a process must overcome before it is commercialised (Table 2.4). After an initial concept is worked out, it is foremost tested at a bench scale. A proof of principle study must demonstrate the technical feasibility of the method. In laboratory absorption-desorption capture plants, packed distillation columns are used to contact the synthetic raw gas with the solvent. The experiment setup is adequate for solvent and rate promoter screening studies, gas-liquid load variation and testing of new process configurations. Due to heat losses, capture efficiency can only be qualitatively measured.

Table 2.4. Examples of different carbon capture from flue gases plant sizes

Plant	Source	Scale	Purpose	Feed [Nm^3/h]	Product [t/d]	Diameter [m]
PostCap™ Lab	Synthetic gas	Mini plant	Solvent screening, load variation, plant configuration testing	3	0.015	0,05
PostCap™ Pilot	Pulverized hard coal	Pilot	Simulation model validation, real FG conditions, material corrosion testing, energy efficiency, risk analysis, emissions	140	1	0.2
OASE Blue™*	Dried lignite	Skid mounted	EOR, beverage industry	1550	7.2	0.6
Bellingham**	Gas fired	Large	CO_2 recovery for beverage industry, EOR, GHG emissions reduction, etc	240000	310	5.6*
Example***	Coal fired	Full		500000	3000	10

*RWE/BASF/Linde test facility at Niederaußem Lignite Power Plant

**Taken from (Cha99)

***Approximate values

Pilot plants are commonly retrofitted to industrial off-gas streams or small-scale fuel burners. The process is tested under real gas conditions, in which cross interaction of the solvent with by-components may alter the plant's operation parameters. The reaction products are known as heat-stable salts, which are removed from the process by solvent reclaiming. The burdened solvent with heat stable salts is qualified for first reclaiming sizing experiments. The performance results serve as proof to validate computer simulation models. Capture efficiency is meaningful despite over-designed absorber and desorber sizes. In the piping internals, material corrosion tests can be accomplished. Potential unwanted emissions in the column head can be measured, to test the solvent stability.

Skid mounted plants are the smallest scale to be constructed for commercial purposes. Within carbon capture, the gas product is destined in the majority of cases to EOR and the beverage industry. These plants became very popular in the 80s when the price of crude oil enabled their construction for EOR. However, they are currently considered as an energy waste, and are normally used as process demonstration at a larger scale.

Finally, the bigger commercial plants are categorised under full scale. Large scale plants fit commercial use of carbon dioxide purposes when bigger amounts are required. Full scale capture plants are those meant to reduce GHG emissions from fossil fuel resources. In the industry, the largest plant retrofitted to a gas fired combustion stream is Bellingham (Cha99). The biggest application retrofitted to a coal fired combustion gas stream is located at the Plant Barry Power Station in Alabama, in which 500 tons of carbon dioxide are recovered daily (MIT12).

3. ABSORPTION RATE MEASUREMENT IN THE STIRRED CELL

The gas uptake velocity of a chemical absorbent may be improved by adding an absorption rate promoter, which either actively participates in the mass transfer of the gas component into the liquid solvent or acts as a catalyst of the slow rate-controlling chemical reaction. In industrial gas treatment, promoters are especially of interest for slow reacting solvents, such as hot potassium carbonate, tertiary and hindered amines. In carbon capture from low pressure gas mixtures, the gas loading range is operated close to equilibrium in order to reduce energy costs. The high carbonation ratios significantly reduce the absorption driving force, requiring higher column sizes to reach the desired capture rate. The activation of the solvent will in this case lead to lower packing heights and reduce investment costs. With the objective of finding a potential absorption rate promoter for the Siemens CCS^{+} solvent, a series of chemical compounds were screened through laboratory tests. The main properties considered in this study were the toxicity, the enhancement performance factor and the price.

The toxicity determines if the promoter compound may cause harm to the environment or to human health. The use of promoters with a high toxicity makes the safety measurements in a full scale capture plant more complex. This causes additional process costs, and causes unnecessary operational risks. The enhancement performance factor is a measure of the increase in the absorption reaction kinetics of the chemical solvent due to the addition of the promoter. The volumetric absorption rate, which is a measure of the solvent kinetics, was determined experimentally by adding a fixed amount of carbon dioxide into a hermetically closed stirred cell reactor containing a certain amount of solvent. The total pressure drop due to chemical absorption of carbon dioxide into the liquid phase was measured and recorded. The velocity increase caused by the promoter addition was defined as the promoter enhancement factor. The promoted solvent was compared to the benchmark run while maintaining a constant solvent strength, an initial carbon dioxide loading and reaction temperature. Previous to the rate promoter investigation, a simple absorption rate measurement was carried out to determine which reaction mechanism was predominant in the different carbonation ratio regions. The prediction of the regions in which the gas diffusion was kinetic-limited, may help for further experiments in the laboratory and pilot plant.

The rate promoters investigated in this work had either an inorganic or organic nature. Organic promoters, such as monoethanolamine, had the disadvantages that most of them are volatile, degradable and may cause corrosion at high concentrations. Inorganic promoters, such as arsenite, serve as catalysts and buffer solutions. Higher rate promoter reactivity is often connected with high toxicity. The environment hazard known to some industry promoters opposed their use in the PostCap^{TM} process. It was therefore within the scope of this work to identify a new compound with similar absorption performance to the industrial compounds (Boc10), bare zero toxicity and have a low price.

3.1. CO_2 Absorption Rate Promoters

The use of absorption rate promoters or activators to enhance the chemical absorption of carbon dioxide with chemical solvents has been investigated since the appearance of the first gas purification processes. The increase in importance of the kinetic-limited hot potassium carbonate process further motivated the development of various new compounds, mainly focused on reducing the gas removal equipment sizes.

3.1.1. Chemical Properties

In this thesis, several chemical compounds with different structures and properties were considered to have an enhancement effect on the CCS^+ solvent. The majority of the compounds were taken from the literature. Some had already obtained positive results and had been commercially implemented in the gas purification industry. Their implementation in amino acid salt solvents was not widely investigated in the literature. The rest of the compounds were deduced to have promoting properties due to similarities with the well-established absorption promoters (Table 3.1). These common properties must be considered when searching for new components. In the following sections, only those compounds which proved to have a kinetic benefit on the CCS^+ are presented.

Table 3.1. Chemical properties in the investigated organic and inorganic promoters

Organic promoters	Inorganic promoters
Heterocyclic molecule	Salt of a weak acid in basic solution
Secondary amino group/-s	pK_A similar to the pH of the CO_2-loaded solvent
Piperazine, imidazole	Arsenite, boric acid, PROM-1, PROM-2

Piperazine is a fast reacting organic heterocyclic secondary diamine. It was already tested in alkanolamine, potassium carbonate and amino acid solvent blends (Mim98; Dang03; Cul04; Cul05; Tan11; Row11). Its use as a promoter is well known in the activated MDEA process (Koh97). Imidazole is an organic heterocyclic secondary amine. It was proposed by Roughton and Booth (Rou38) to have a buffer effect on the carbon dioxide hydration reaction. Its presence together with the enzyme carbon anhydrase in animal hemoglobin speeds up the carbon dioxide hydration in the capillary tissue and the carbonic acid dehydration in the lung tissue (Eds58). Arsenite is the salt of a weak oxyacid. It was extensively investigated by Roughton et al. (Rou38), Sharma et al. (Shar63), McNeil et al. (McN67) and Astarita et al. (Ast81) due to its catalytic behaviour in carbon dioxide absorption. Arsenite was first patented as a absorption promoter for sodium carbonate solvent for washing out weak gaseous acids by Bähr in 1938 (Bäh38). It was industrially implemented in the Giammarco Vetrocoke Arsen process (Gia75), and later replaced by other more benign substances like glycine (Gia84). Although its toxicity makes it unfeasible for large scale PCC plants, it was included in this investigation as a performance standard. The potassium borate + vanadate inorganic mixture was disclosed by Field, J. (Fie74) to activate the uptake capacity and the diffusion rate coefficient of a potassium carbonate solvent in the separation of carbon dioxide from gas feeds. Boric acid has also been confirmed as a potash promoter by Ghosh et al. (Gho08). Further, Endo et al. (End11) discovered that the presence of the boric acid promoter did not affect the CO_2/K_2CO_3 phase equilibrium. Since vanadium oxide is very hazardous, it is unlikely for it to be implemented in a large scale plant. It was therefore replaced in this study by a non-toxic compound with a similar molecular structure, named PROM-2. Finally, PROM-1 is an inorganic promoter included in the hydration catalyst group. It was previously investigated as a catalyst of the $CO_2 + H_2O$ reaction, but has until today not been implemented in the gas industry. Its use for the amino acid solvents was experimentally tested, and the findings have already been disclosed in the framework of this thesis.

3.1.2. Promoter Ranking Criteria

All of the aforementioned compounds were previously considered to have a kinetic benefit on the CCS^+ solvent. In order to establish which of the promoters was ideal for further testing in the laboratory mini plant and pilot plant, they were ranked according to the following categories:

- Toxicity
- Absorption rate enhancement
- Market price (availability)

The most important factors considered in this study were the toxicity and the absorption rate enhancement. The market price was taken into account, but was not decisive in the promoter selection. Regarding the experimentation in the test capture plants within this work, only those promoters with zero toxicity could be investigated due to safety reasons.

3.2. Experiment Setup and Procedure

The absorption rate is the variable used in this work to quantify the performance of each promoter. It was measured in a stirred cell reactor apparatus. The experiment setup and the testing methodology will be explained in the following subchapters.

3.2.1. Experiment Setup

The experiment setup (Figure 3.1) consisted of three main components: a gas meter, a stirred cell submerged in a thermostat bath and a vacuum pump. The gas was supplied by an externally attached gas bottle. The gas feed into the gas meter was regulated by a needle valve. The gas meter consisted of the addition of three metal flasks of different volumes. The gas flow into these flasks was regulated by two spherical valves, placed before and after. The total volume of the gas meter amounted up to 137 ml. The pressure was measured both by a DIN [0-60 bar] analogical gauge and a digital WIKA Metronic Line [0 - 25 bar] gauge. Due to safety features, a pressure relief valve was annexed at the top of the gas meter.

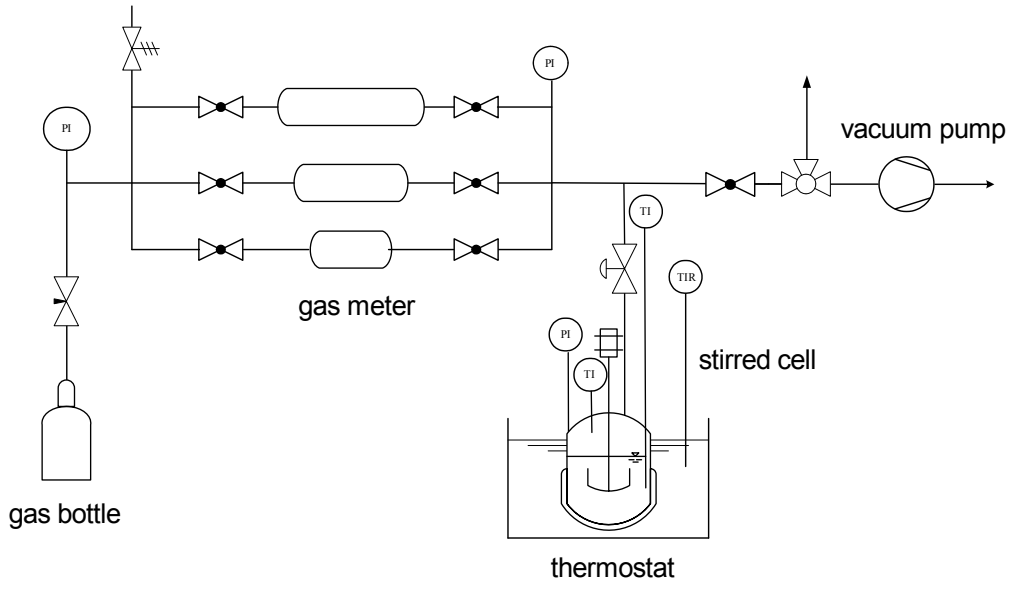

Figure 3.1. Stirred cell experiment layout

The gas meter was connected to the stirred cell through a membrane valve. This valve regulated the flow of carbon dioxide into the stirred cell. The stirred cell reactor (Büchi Labortechnik AG) was fabricated in 1.4503 stainless steel. The total volume of the cell amounted up to 207.7 ml. It could be hermetically closed to the environment to avoid gas leakage. The V-L system was tempered by submerging the stirred cell in a thermostat water bath (LAUDA). The temperature of the V-L system was measured by a Pt-100 thermocouple and the pressure by a digital WIKA Metronic Line [0 - 2.5 bar] gauge. The measurement data acquisition was performed by an AMR ALMEMO 2290-8 device and the respective pressure drop curves were later plotted by the AMR Win Control computer software. The gas outlet was restrained by a spherical valve. A posterior three-way valve regulated either the gas flow to reestablish the ambient pressure at the end of each test run or to connect the system to the vacuum pump for degassing.

In Table 3.2, the measurement uncertainty of the directly measured variables is presented. The values in this table have been provided by the instrument supplier.

Table 3.2. Measurement uncertainty of directly measured variables

Variable	Units	Error
Stirred Cell Pressure	[mbar]	25
Gas Meter Pressure	[mbar]	250
Stirred Cell Temperature	[ºC]	0.5
Weight	[g]	0.0001*

*Standard deviation measured and calculated by (Tol13)

3.2.2. Experiment Procedure

The same experiment procedure was repeated in the stirred cell test runs. An overview of the steps is presented in Table 3.3.

Table 3.3. Experiment procedure

Solution pre-loading	Degassing	Tempering	Gas addition
The fresh AAS solution was pre-loaded with CO_2 in a washing flask.	The inert gas content was removed from the AAS solution by applying vacuum in the stirred cell	The experimental temperature was set by a tempered water bath in which the stirred cell was submerged	The added CO_2 amount was controlled by the initial total gas pressure after closing the gas feed valve.

At the start of each test run, the solvent solution was firstly pre-loaded with carbon dioxide before being added into the stirred cell. The gas pre-loading was done in a 500 ml bubble flask. Afterwards, a sample was titrated and the density was measured, in order to estimate the liquid composition. Further information on the acidic titration analysis method can be found in the Appendix A. The liquid solution was weighed into the stirred cell and afterwards the top, where the stirrer was screwed down. Once closed, the stirred cell reactor was screwed on to its cage support, and connected to the gas meter. The Swagelock® connection was hermetically closed by inserting a sealing gasket between the conduits to avoid gas leakage. The membrane valve that regulated the gas flow into the cell remained at this point closed. The vacuum pump was started, and the three-way valve adjusted so the vacuum pump and gas meter were aligned. Later, the spherical valve was slowly opened until the gas meter was completely emptied, i.e. the total pressure read absolute zero. Only then, the membrane valve was carefully opened, to prevent the solvent in the stirred cell reactor from being ejected from the cell bottom, due to the instant change in pressure. The stirred cell was then fully degassed, until the vapour pressure at room temperature was reached. Finally the membrane valve was closed. The complete degassing of the inert gases was not required for these experiments because they did not interfere directly with the absorption rate measurements.

The lifting platform, where the thermostat was placed was raised, so that the stirred cell would be submerged into the thermostat water bath. The thermostat was finally switched on and the water bath set to the desired temperature. The motor stirrer was switched on and set to 500 rev/min. The V-L system inside the cell slowly warmed up until the experiment temperature was reached. Before noting the starting vapour pressure of the system, the pressure reading had to remain constant for at least 1 hour. The carbon dioxide was added to the gas meter by slowly opening the needle valve until a total pressure of around 6 bar was reached. For these

experiments the entire volume of the gas meter was used. Once the pressure was stabilised, the membrane valve was slowly opened, letting the gas flow from the gas meter into the stirred cell. The temperature and pressure of the gas meter were measured before and after the addition to calculate the amount of carbon dioxide added into the stirred cell for each test run. Finally, when the desired pressure in the cell was reached, the membrane valve was closed. This marked the start of the experiment, and the pressure of the cell was recorded every 5 seconds. The high pressure difference between the gas meter and the stirred cell requires that the opening and closing of the membrane valve was performed in a controlled way.

The total pressure of the stirred cell consisted of the gaseous carbon dioxide and the vapour pressure over the solvent. As the carbon dioxide was chemically absorbed, the total pressure decreases or "drops" forming a descending curve in dependence with the experiment time. Both the pressure and temperature in the stirred cell are measured simultaneously, and shown graphically on the computer. The absorption rate depends on the pressure drop curve gradient at the start of the experiment, i.e. how fast the system advances towards the equilibrium. Once the gas pressure ceases to decrease, the equilibrium has been reached.

3.2.3. Experiment Conditions

In order to simplify the result evaluation, a few assumptions were made:

- Given that the carbon dioxide was added to the stirred cell as a pure gas, the absorption rate was liquid-side controlled.
- The total pressure of the cell was equal to the partial pressure of added carbon dioxide and solvent equilibrium back pressure. The chemical absorption of the gas in the cell decreased PCO_2 and increased PCO_2^*.
- The thermodynamic equilibrium was reached when $PCO_2 - PCO_2^* = 0$.
- The gas amount added was the same for all experiments.
- The temperature variation due to the absorption heat was neglected.

The experiment data were selected between the closing of the membrane valve after gas addition until the equilibrium was reached.

3.2.4. Results Interpretation

The volumetric absorption rate, $R_A \cdot a$ was calculated according to the equation proposed by Vaidya et al. (Vai07) based on the conservation principle and under the assumption that the ideal gas conditions were maintained throughout the experiment (Equation 3.1).

$$R_A \cdot a = \frac{V_G}{V_L \cdot R \cdot T} \cdot \left(\frac{dP}{dt} \right)_{t=0} \tag{3.1}$$

The gas volume V_G was calculated by subtracting the total cell volume minus the liquid volume V_L. The pressure drop curve in the cell was fitted to a 3rd degree polynomial, and the gradient (dP/dt) was calculated by taking the first derivative at *t=0* (Figure 3.2). *T* stands for the system temperature and *R* is the ideal gas law constant.

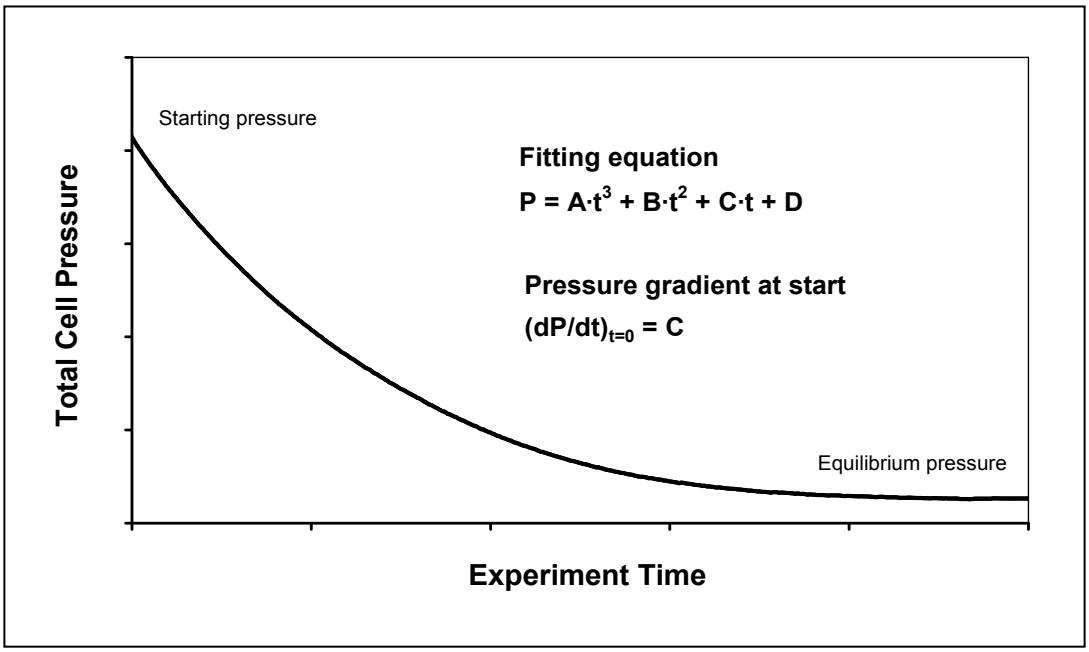

Figure 3.2. Pressure drop curve in the stirred cell

The promoter enhancement factor, E_P was defined as the ratio between the volumetric absorption rate measured with and without promoter (Equation 3.2).

$$E_P = \frac{(R_A \cdot a)_{with\ promoter}}{(R_A \cdot a)_{without\ promoter}} \qquad (3.2)$$

The absorption rate enhancement of the promoted solvent was proportional to E_P.

3.3. Solvent Kinetic Measurement

Before the promoter study, the absorption reaction kinetics of the solvent was measured with increasing carbonation ratio to define how the reaction mechanism developed. The key of this experiment was to see how the carbamate formation effect on the absorption reaction kinetics developed at increasing carbonation ratios. Since the addition of a hydration rate promoter will enhance the carbamate hydrolysis, its implementation at loading regions where carbamate formation is not predominant is a decisive factor. In order to differentiate between carbamate and bicarbonate formation, the same measurement under the same conditions was repeated for a slow-reacting tertiary AAS with a similar chemical structure, named AAS^3. The comparison of both curves will qualitatively reproduce the solvent's reactivity throughout a representative loading range.

In order to investigate a wide range of carbonation ratios, the gas addition was repeated up to ten times on the same solvent. Once the equilibrium was reached, it was established that the cell pressure remained constant for 1 hour before the next addition. The amount of carbon dioxide was approximately the same for each addition. Each value was estimated by a V-L material balance based on the pressure variation in the gas meter before and after each addition. The conditions for all the experiment runs are summarised in Table 3.4.

Table 3.4. Experiment conditions for the solvent kinetic measurements

T, °C	V_L, ml	CO_2 (per addition), mmol	[AAS], wt-%
44.5 - 45.5	35.4	6.5 - 7.5	31.5

The calculated volumetric absorption rates at increasing carbonation ratio are illustrated in Figure 3.3. The absorption rate values are expressed in percentage units. The 100% was set for the fresh CCS^+ absorption rate. The first gas addition accounted for the biggest difference in velocity uptake between the two solvents. The secondary amino acid salt CCS^+ was able to form carbamate since the amino group electron pair is not entirely blocked. The tertiary amino acid solvent AAS^3 acted as a strong base, accepting the proton released from the bicarbonate formation. Under the experiment conditions, it was evident that the carbamate formation is qualitatively two times faster than the bicarbonate formation.

As the carbonation ratio increases, the volumetric absorption rate logically decreases for both solvents. The absorption rate at a 0.6 mol/mol ratio becomes the same. It is confirmed that at this loading the carbamate formation benefit on the uptake velocity no longer exists.

There are two observations that confirm the theoretical assumptions:

- at carbonation ratios between 0.0 and 0.4, the fast carbamate formation in CCS⁺ is predominant and
- at carbonation ratios between 0.4 and 0.7, the controlling mass transfer step is the bicarbonate formation.

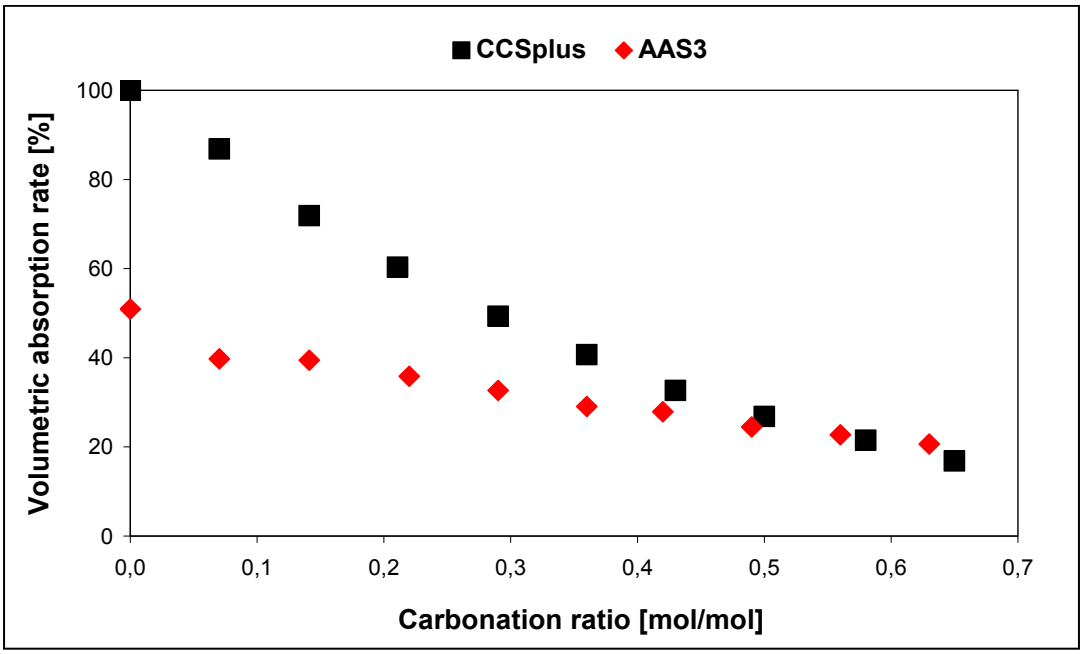

Figure 3.3. Absorption capacity comparison CCS⁺ vs AAS³

In the absorption column, the loading range between the lean solvent entering the top and the rich solvent exiting the bottom is operated close to equilibrium to reduce energy costs. According to the experiment results, at the top of the column, the carbamate formation is predominant, whereas at the bottom only bicarbonate is formed. The slow kinetic of the carbamate hydrolysis requires a higher contact area in the absorber in order to reach equilibrium. It is therefore understood that a more energy efficient process requires higher investment costs. The catalysis of the controlling reaction will significantly reduce the equipment cost.

3.4. Screening Study

The main goal of the screening study was to find out a potential promoter candidate to promote the CCS^{+} solvent. The promoters were first ranked according to their toxicity, in order to determine future hazards which may be transferred to the full scale process. Moreover, only the non-toxic components would be further tested in the laboratory mini plant and pilot plant due to operation safety issues.

3.4.1. Toxicity

The toxicity was the factor considered to determine the environmental impact of the absorption promoters. The promoter toxicity was fundamental in the screening study since it dictated the level of operation safety required in the capture plant. Components with a high toxicity required special safety measurements, which would mean an extra cost in the process equipment and increase the danger risk during operation. Furthermore, only those substances with low toxicity were authorised to be further tested in the laboratory mini plant and in the Staudinger pilot plant. The promoters were ranked regarding their toxicity in Table 3.5.

Table 3.5. Promoter toxicity ranking

Component	Symbol	Toxicity	Rank
Piperazine		Noxious and corrosive, forms stable nitrosamines with NO_x	3
Imidazole		Cat. 3 toxic and corrosive, forms stable nitrosamines with NO_x	4
Arsenite		Cat. 1A toxic, corrosive, noxious and hazardous for the environment	5
Borate + PROM-2		Noxious and cat. 4 dangerous	2
PROM-1		Cat. 4 dangerous	1

Piperazine and Imidazole possess at least one secondary amino group in their molecular structure. Their reaction with the NO_x present in flue gases forms stable nitrosamines, which are carcinogenic chemical structures. Arsenite is also categorised as a very dangerous carcinogenic substance. In the chemical process industry in Germany if the concentration of a carcinogenic compound exceeds 1 wt-% concentration in solution, the process would be regulated under the Hazardous Incident Ordinance. This risk level is not desired for a full-scale carbon capture plant. The borate + PROM-2 mixture was at first considered as a strong potential candidate. Yet, boric acid was recently included in the European Chemicals Agency (ECHA) candidate list of substances with a very high concern for authorisation. Its negative impact on the environment and human health has already been reported (Bow02). PROM-1 was the only substance investigated which did not bring additional hazards into the CCS^+ solvent. Arsenite was ranked as the most dangerous promoter. Piperazine and imidazole were considered as inconvenient for a full scale process due to their high toxicity; however there are process countermeasures, which avoid the nitrosamine formation or favour their destruction. Thee missions to the environment through volatility losses or entrainment may be further controlled with a water wash on the absorber and desorber head (Tay46). Both solutions mean extra equipment investments and increase the process difficulty. The Borate + PROM-2 mixture and the PROM-1 promoters are the only candidates, which were authorised for further testing in the laboratory mini plant and pilot plant.

3.4.2. Promoter Enhancement Factor

The promoter enhancement factor derived from the pressure drop curves measured in the stirred cell. The volume of the liquid and the gas, as well as the pressure increase due to gas addition were set so that the carbonation ratio during the experiment would vary from 0.25 to 0.70 mol/mol. This carbonation range more or less corresponds to the working capacity in the absorber column. The promoter enhancement factor was measured for each rate promoter. In order to generate reproducible results, each test run was repeated three times. The mean value of the volumetric absorption rate was taken. In each test run, the variables recorded were the temperature and the pressure in the stirred cell. The temperature was maintained constant at about 45 - 46 °C by submerging the stirred cell in a tempered water bath. At first, the liquid temperature increased due to the absorption enthalpy set free. Soon after, the temperature returned to its set value and remained constant until the end of the experiment. It was assumed that the vapour pressure of the solvent remained constant, so that the measured pressure decrease represented the carbon dioxide uptake velocity. The experiment conditions are summarised in Table 3.6.

Table 3.6. Experiment conditions for the absorption rate promoter tests on CCS^+

T	V_L	CO_2 per addition	[AAS]	[Prom]	α_{start}
[°C]	[ml]	[mmol]	[wt-%]	[wt-%]	[mol/mol]
45.2 - 45.8	17.7	17.4 - 17.7	30.0	1.0	0.25

The pressure drop curves are represented in Figure 3.4. The diagram qualitatively represents the velocity with which the system advances towards the equilibrium. That system with faster absorption reaction kinetics will reach the final equilibrium pressure in less time. The only difference between the represented curves is the promoter added to the CCS^+ solvent. At the start of the experiment, all curves have the same gradient, due to higher initial gas solubility at a high gas pressure. Soon after, the absorption rate difference between the promoted solvent (red, yellow, and green, blue) and the standard (black) was visible. Arsenite (blue) is clearly the fastest rate promoter. The other three compounds are more similar to one another. The CCS^+ solvent promoted with piperazine reached a lower equilibrium gas pressure in all three test runs (approx. 10% less). Unlike the inorganic compounds, piperazine increased the absorption capacity as well as the velocity uptake.

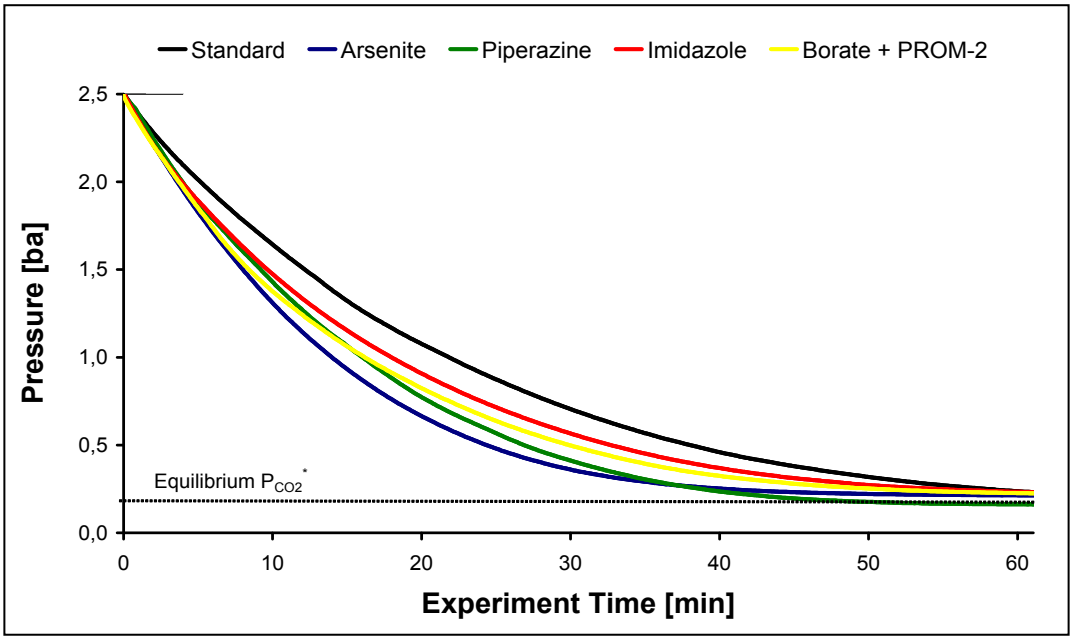

Figure 3.4. Pressure drop curve promoter comparison

PROM-1 was tested in a separate run, at slightly different conditions (Table 3.7). The promoter concentration was lowered due to a worse solubility in the pre-loaded CCS^+ solvent compared to the other compounds. Two different concentrations were tested (0.1 and 0.3 wt-%) to observe if there was any effect on the absorption enhancement performance. In the new test runs, the liquid sample was increased to approx. 26 ml and the starting carbonation ratio to 0.36.

Table 3.7. Experiment conditions for the PROM-1 test on CCS+

T [°C]	V_L [ml]	CO_2 per addition [mmol]	[AAS] [wt-%]	[Prom] [wt-%]	α_{start} [mol/mol]
45.0	26.4	16.4	30.0	0.1 - 0.3	0.36

The pressure drop curves are presented in Figure 3.5. The experimental time was shorter compared to the previous test runs since there was a higher volume of solvent to absorb less CO_2. Furthermore, the solvent was pre-loaded to a higher carbonation ratio. Although the velocity uptake was 20% slower, the system reached the equilibrium pressure in half of the time as the previous experiments. The curves as well as the volumetric absorption rate were not comparable with one another. The standard CCS^+ solvent absorption rate measurement was thus repeated under the new experiment conditions to enable the estimation of a comparable promoter enhancement factor, for the PROM-1 promoted solvent.

At the end of the test runs with 0.3 wt-% PROM-1, a small white solid clump was found in the bottom of the cell. It was not defined if the precipitate was bicarbonate or promoter. This uncertainty was to be cleared up with a preliminary solubility measurement, which will be further discussed in the following section.

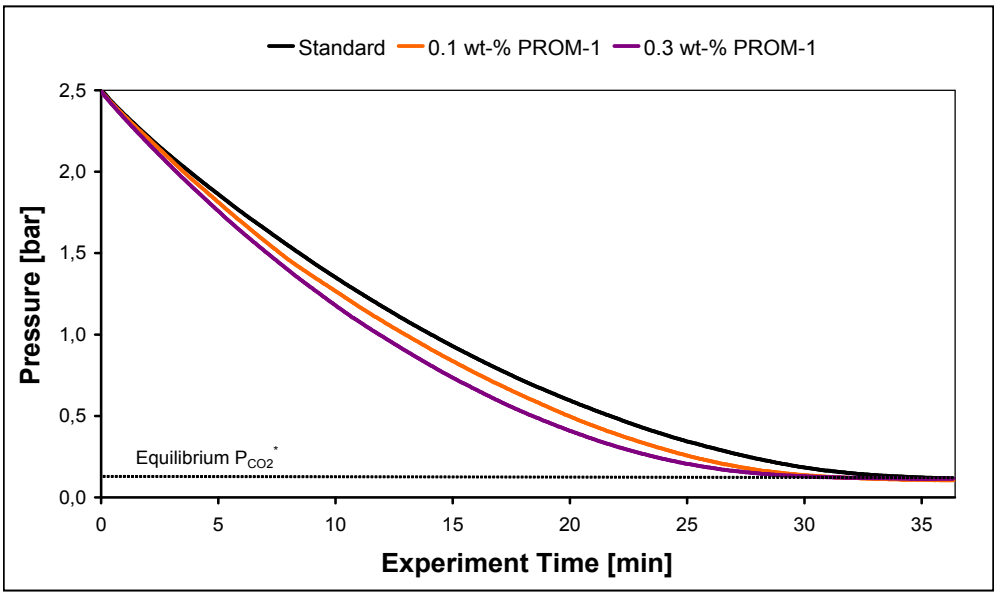

Figure 3.5. Pressure drop curve with PROM-1 at 0.1 and 0.3 wt-%

The measured pressure drop gradient was further converted to the volumetric absorption rate and the promoter enhancement factor according to the procedure described in section 3.2.4. The final promoter enhancement values are depicted in Figure 3.6. Arsenite remains the promoter benchmark regarding absorption rate enhancement. The achieved enhancement factor was two times higher than the rest of the promoters. The rest of the promoters remain more or less at an equal level (*Ep* ~ 1.2). PROM-1 at a 0.1 wt-% concentration achieved the lowest promoter enhancement factor, mainly due to a low promoter concentration.

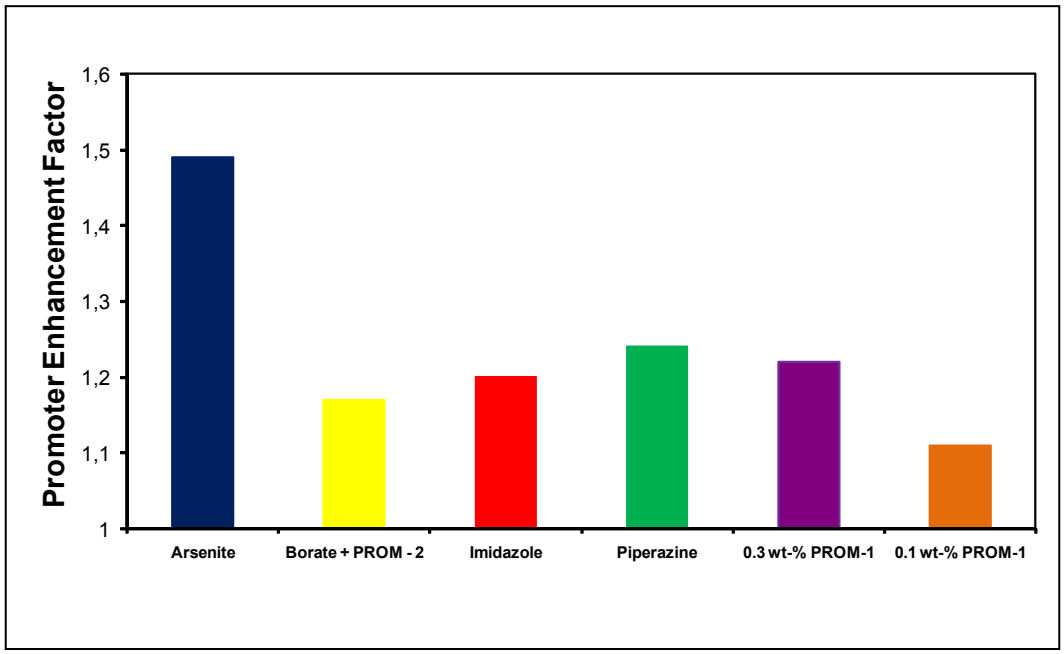

Figure 3.6. Promoter enhancement factor comparison

3.4.3. PROM-1 Solubility

The white precipitate at the end of the pressure drop measurements of CCS+ solvent promoted with PROM-1 made it necessary to investigate the solubility of the promoter under common operation conditions. Therefore, a solubility curve was measured for four different promoted CCS^+ systems: a lean and a rich loading sample at both a low and a high CCS^+ concentration (Table 3.8). For this purpose, the four CCS+ samples were pre-loaded with carbon dioxide to their respective CO_2-loading and saturated with 1 wt-% PROM-1. The liquid phase was stirred in a glass beaker tempered with an external jacket. The temperature was measured directly in the liquid phase. A 5 ml aliquot was taken at each temperature once the liquid temperature measurement remained stable. The sampling was done with a plastic syringe fitted with a particle filter (<2.2 μm). The liquid probe was weighed into a volumetric flask and diluted with distilled water up to 25 ml. The probes were then sent to the analytical laboratory together with a blank sample to measure the concentration of PROM-1.

Table 3.8. Variables in the PROM-1 solubility curve measurement

CO_2-loading [mol/mol]	[CCS^+] [wt-%]	Temperature [°C]
40 - 62	28 - 34	25 - 95

The results from the analytical laboratory were converted back into weight concentration units. The solubility curves measured at 5 temperatures are represented in Figure 3.7.

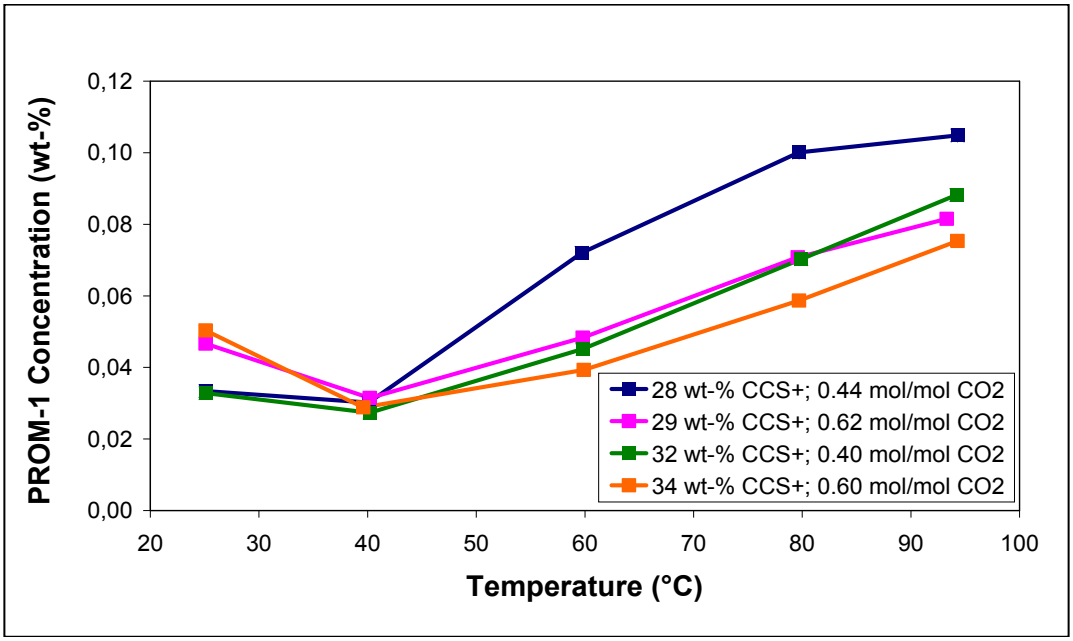

Figure 3.7. PROM-1 solubility curve at different [AAS] and CO_2-loadings

The higher solubility limit was located at about 0.11 wt-% at 95 °C for the lean solvent with a low CCS^+ concentration. The lower solubility limit was located for all solutions at about 0.03 wt-%. The measurement limit was established at 0.008 wt-% (about 10%). For further experimental activities, a concentration of 0.1 wt-% was established for PROM-1.

3.4.4. Market Price

Besides toxicity and performance, the promoters were screened regarding their market price (Table 3.9). The pure substance price (≥ 99%) was inquired in the (ali12) chemical market website. The amount of promoter defined was taken from the concentration used in the pressure drop curves and up-scaled to a full scale carbon capture plant holdup of around 3000 tons. Only the low concentration of PROM-1 was considered, since the higher value exceeded the solubility limit at the operation conditions.

Table 3.9. Promoter price list (ali12) per assumed solvent holdup of 3000 tons

	Arsenite	Borate + PROM-2	Imidazole	Piperazine	PROM-1
Price per metric ton, €/ ton	460	1250 : 560	790	8790	20000
Full scale mass, ton	27.0	8.6 : 25.7	17.6	22.3	3
Full scale price, €	12420	25142	13904	196017	60000
Rank	1	3	2	5	4

Both arsenite and imidazole achieved the lowest market costs at a full-scale carbon capture plant. They were ranked as the most economic promoters to be implemented in the PostCap^{TM} process. The highest market price was found for PROM-1. Nevertheless, its low concentration reduced its full scale price to a feasible amount. The promoted solvent cost would only increase 0.7%, with respect to the standard solvent. The most expensive promoter resulted to be piperazine. Its full scale price was about 15 times higher than the two best ranked promoters. The promoter cost is a factor to consider in the screening study. Nevertheless, if the capital investment savings with the promoted solvent are located in the millions of Euros, the aforementioned promoter costs are no longer a determining factor in the economic analysis.

3.4.5. Promoter Selection

Since all the absorption rate promoters tested increased the absorption reaction kinetics of the CCS^{+} solvent, and the full-scale price was more or less the same; the toxicity became the decisive factor in the selection of the most adequate candidate. In addition, low toxicity also decreased the risk of operation in the continuous absorption-desorption process. Possible solvent leaks through piping connections and pumps had to be considered as possible in the testing facilities. Of all the substances tested, PROM-1 was selected as the promoter to be tested in the laboratory bench- and pilot-scale capture plant.

3.5. Further Pressure Drop Experiments

Once the promoter selection was completed, the effect of other variables on the promoter enhancement factor was further investigated.

3.5.1. Promoter Enhancement Effect at Different CO_2 Loadings

In the AAS solvent kinetic measurements the theory presented in (Ast64) was confirmed, the reaction kinetic regime varied with the increasing carbonation ratio. It was therefore investigated if the PROM-1 promoter enhancement factor also changed with increasing carbonation ratio, i.e. at a slower kinetic regime. Since PROM-1 is classified as a carbon dioxide hydration catalyst, the carbonation ratio range was chosen at loadings higher than 0.5 moles CO_2 per mole AAS. At lower loadings, the predominant carbamate formation reaction was thought to conceal the promoter enhancement effect and was thus excluded from this experiment. The complete experimental conditions are presented in Table 3.10.

Table 3.10. Experimental conditions for the carbonation ratio measurements

T	V_L	CO_2 per addition	[AAS]	[Prom]	α_{start}
[°C]	[ml]	[mmol]	[wt-%]	[wt-%]	[mol/mol]
45.7	35.6	6.6 - 7.4	25.3	0.10	0.55, 0.64, 0.73

Figure 3.8 depicts the results of the pressure drop experiments. The promoter enhancement factor was measured at three different CO_2-loadings.

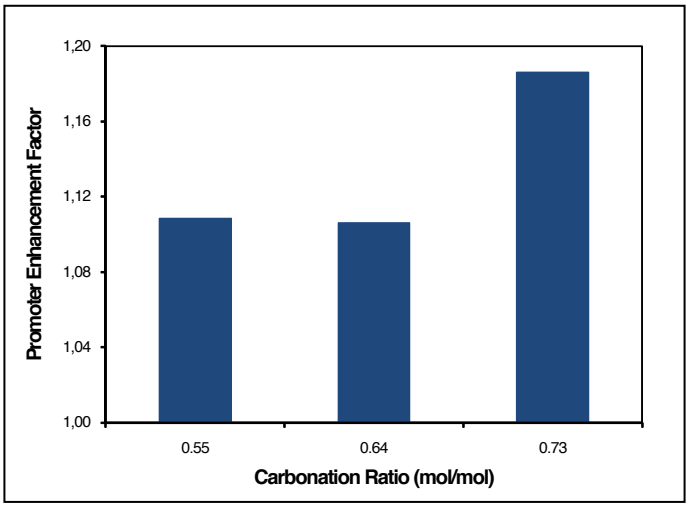

Figure 3.8. Promoter enhancement factor variation with increasing carbonation ratio

The graphic confirms that the promoter enhancement factor increases at higher carbonation ratios. Under the experimental conditions, the first two CO_2 additions achieved the same promoter enhancement factor. The increase happened in the third addition. These results confirmed that PROM-1 has a higher activity at high CO_2-loadings, where the bicarbonate formation is the predominant reaction in the absorption.

3.5.2. Promoter Enhancement Effect on Other AAS Solvents

In order to further confirm the previous findings, PROM-1 was also tested with other amino acid salt solvents, in this case a 1:4 mixture of AAS^2 and AAS^3. The slow reacting AAS^3 solvent was already introduced before. AAS^2 is a secondary amino acid salt, which forms a stable carbamate with carbon dioxide. Its fast reaction kinetics contrasted with its high energy demand and low capacity. The promoter enhancement factor was measured at a high and a low CO_2-loading range. For each range, three CO_2 additions were carried out for the same liquid solvent. Some variables such as the stirrer speed, the solvent concentration and the promoter concentration were varied from one set of CO_2 additions to the other to see their effect on the promoter enhancement factor measurement. The comparison of the promoter enhancement factor at the same carbonation ratio will demonstrate the influence of the changed variables. The experimental conditions are presented in Table 3.11.

Table 3.11. Experimental conditions for the PROM-1 testing on other AAS

T	V_L	CO_2 per addition	[AAS]	[Prom]	α_{start}
[°C]	[ml]	[mmol]	[wt-%]	[wt-%]	[mol/mol]
44.8	35.4	9.4 - 9.5	27.3	0.07	0.23, 0.35, 0.47
45.4	35.4	6.6 - 7.0	24.8	0.10	0.48, 0.57, 0.66

In Figure 3.9, an increasing tendency of the promoter enhancement effect with the carbonation ratio is seen. This trend coincides with the measurements done with the CCS^+ solvent. In the higher CO_2-loading range, this tendency begins to fall. The variables such as stirrer speed, promoter and AAS concentration barely affected the promoter enhancement factor.

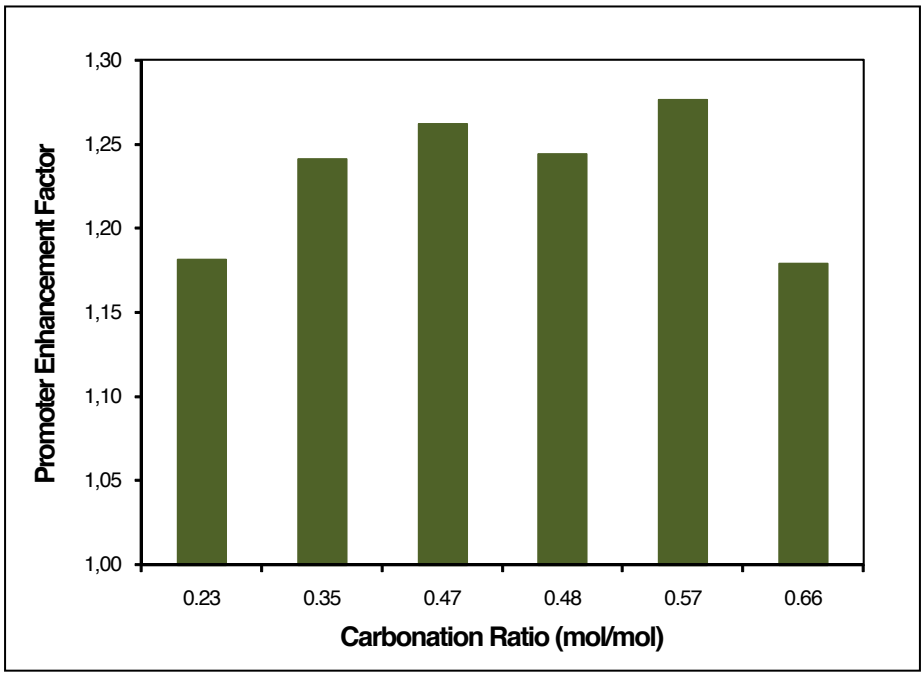

Figure 3.9. Promoter enhancement factor on a 1:4 mixture of AAS^2 with AAS^3

3.5.3. Promoter Enhancement Effect with Co-Promoter

As seen in (Giam84) and (Fiel75), the combination of two different absorption promoters added to the potash solvent increased the carbon dioxide uptake velocity. In previous experiments, it was found that a 3:1 mixture of borate and PROM-2 achieved a promoter enhancement factor similar to piperazine and imidazole. Since PROM-1 has a similar chemical nature to borate, the enhancement effect was also investigated to see if it increased when combined with the co-promoter PROM-2. For this reason, the volumetric absorption rate was for this reason measured in the stirred cell at different carbonation ratios and compared to the standard amino-acid salt solvent.120 g of 25 wt-% CCS^+ solution was pre-loaded to lean solvent conditions (0.4 moles CO_2 per mole AAS). It was later divided into 4 aliquots. One remained as the benchmark and the promoter and/or co-promoter were added to the other three samples to reach a total concentration of 0.1 wt-%. Three different promoter ratios were tested. The four different solvent compositions are presented in Table 3.12.

Table 3.12. Promoter concentration for each case

Test run	[Promoter] [wt-%]
Standard	-
PROM-1	0.130
3 PROM-1+ 1 PROM-2	0.099 + 0.031
1 PROM-1+ 1 PROM-2	0.066 + 0.066

In order to investigate the whole CO_2-loading range in the absorber column (approx. 0.4 to 0.8 mol/mol), three CO_2 additions were carried out for each sample. The gas was added until a total cell pressure of around 1300 mbar was reached. At this point the gas addition valve was closed. The amount of CO_2 added remained more or less constant for each addition. The experimental conditions of the pressure drop measurements are shown in Table 3.13.

Table 3.13. Experimental conditions for the co-promoter effect tests

T [°C]	V_L [ml]	CO_2 per addition [mmol]	[AAS] [wt-%]	[Prom] [wt-%]	α_{start} [mol/mol]
45.4	26.5	8.3 - 8.7	25.0	0.13	0.40, 0.55, 0.70

Figure 3.8 depicts the effect of the co-promoter PROM-2 on the absorption promoter PROM-1 at different ratios. The lower promoter enhancement factor was due to the lower amount of carbon dioxide per addition, which reduced the carbonation range in each measurement, as well as the experimental time required to reach the equilibrium.

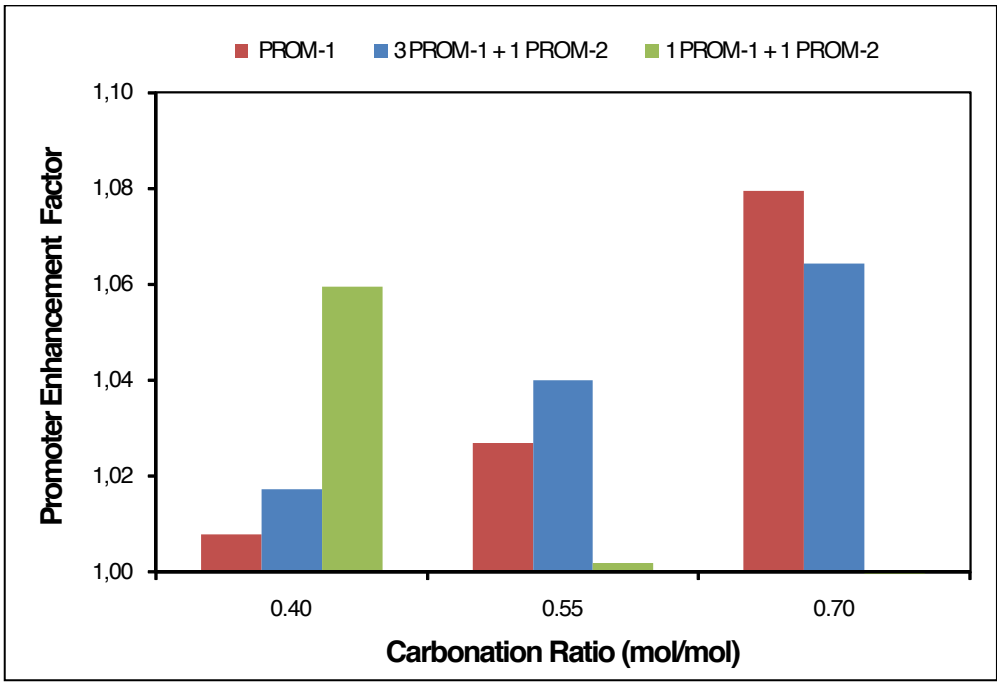

Figure 3.10. Co-promoter effect on PROM-1's promoter enhancement factor

The promoter enhancement factor in the promoted solvent with PROM-1 and PROM-2 (green) at a 1:1 weight ratio was higher at low carbonation ratios and then decreased to zero in the 2nd and 3rd CO_2 addition. The activity of this ratio only takes place in the region, where the fast carbamate formation is the predominant reaction. In the case of the promoted solvent with only PROM-1 (red) and with a PROM-1 and PROM-2 at a 3:1 weight ratio (blue), the promoter enhancement factor increased at higher loadings where the slow bicarbonate formation is the predominant reaction. The slow kinetic regime controls the bottom region of the absorber, and is the limiting factor of the absorber and desorber packing height.

3.6. Conclusion

The promoter qualitative kinetic measurements and screening study carried out for the CCS^+ solvent rendered the following conclusions:

- At the bottom of the absorber where high CO_2-loadings are present, the slow bicarbonate formation controls the carbon dioxide uptake velocity. In this region, the kinetic benefit of the fast carbamate formation is hindered by the low free amino acid salt concentration. To increase the absorption reaction kinetics in this loading region, a catalyst which accelerates the carbon dioxide hydration reaction is preferred.

- The enhancement of the diffusion rate over the operative loading range is possible by promoting the CCS^+ solvent with an absorption rate promoter. Several organic and inorganic compounds commonly used in the gas scrubbing industry were screened regarding their toxicity, performance enhancement factor and price. From all the compounds tested, arsenite achieved the highest enhancement performance factor of all the compounds.

- Although the process cost may be sunk with a high enhancement performance promoter, its hazardous flaws, which are negative for the environment and the human health, complicates the operative security of the process. It was mandatory that the absorption rate promoter combined high performance, low cost and low environmental penalty.

- A new hydration catalyst PROM-1 with zero toxicity was found to produce a kinetic benefit on the carbon dioxide absorption with the CCS^+ solvent. Compared to the other industrial promoters tested, the promoter enhancement factor was marginally lower, due to a lower concentration.

- PROM-1 achieved a higher promoter enhancement factor at high CO_2-loadings. Its activity in the capture plant will occur mainly in the lower absorption stages.

- PROM-1 also had a promoting effect on other amino acid solvents. The findings confirm the fact that PROM-1 is a catalyst of the carbon dioxide hydration reaction.

- The addition of PROM-2 as a co-promoter is favourable at low CO_2-loadings. The enhancement effect at higher loadings is reduced to zero.

Based on these conditions, PROM-1 was selected to be further tested in the laboratory mini plant and in the pilot plant. The ideal concentration in CCS^+ solvent was determined through a solubility measurement to be 0.1 wt-%.

The research on potential absorption rate promoters for carbon capture with amino acid salt solvents must not end with the aforementioned compounds. The results presented in this thesis should be considered as a starting point of a more extensive screening investigation.

4. RATE PROMOTER LABORATORY TESTING IN THE MINI PLANT

The principal cost factors of PCC processes are the energy demand for solvent regeneration and the size of the capture plant equipment; mainly absorber, desorber and direct contact cooler. The energy duty depends on the solvent's loading capacity, and the column size depends on the absorption reaction kinetics. Both factors are interrelated by the capture performance. The minimum energy is achieved only when the rich and lean solvent loadings operate close to thequilibrium. Depending on the solvent's absorption reaction kinetics, reaching the equilibrium loading during absorption and desorption requires enough contact area and residence time. For a defined column diameter, both variables are determined by the absorber and desorber packing height. Fast-reacting amine solvents normally require packing heights of around 10 m to operate at equilibrium, whereas promoted slow-reacting amine solvents require more than 40 m (Mos10). In general, fast-reacting solvents enable lower investment costs, since they can achieve higher loading capacities with lower equipment sizes. Slow-reacting solvents require higher columns to reach the required working capacity. Their use for low pressure gas feeds is not economic from the investment point of view.

In the previous chapter it was observed that the promoted CCS^{+} solvent with inorganic and organic promoters advanced faster towards the equilibrium than the standard solvent. The next step was to test the rate promoter in the Siemens mini plant under variable operating conditions. The absorber packing height was reduced for the promoted solvent to confirm if it was capable to obtain the same capture performance as the standard solvent at full height. In order to investigate a wide range of operating conditions, the solvent flow rate was varied. For the sake of comparability, the reboiler heat duty was adjusted to maintain a constant capture rate for all experimental points. Other process variables such as the solvent concentration, the gas flow, the lean solvent cooling and the rich solvent heating capacity were also maintained constant. Important solvent-specific performance parameters measured in each experiment such as optimal working capacity and energy demand cannot be further used for up-scaling purposes, due to the limited contact area and the high heat losses in the mini plant. However, a relative comparison and a confirmation of the stirred cell results were possible.

Instead of real combustion flue gas, a synthetic gas mixture of nitrogen and carbon dioxide was used. The gas inlet flow rates of each gas were adapted in order to reproduce a coal-fired flue gas composition.

The majority of the experiments presented in this chapter were performed within the framework of the master thesis from J.A. Toledo. Further details to the absorber column modification and error analysis can be found in this work (Tol13).

4.1. Reboiler Heat Duty for CO_2 Desorption

After the absorption, the solvent is regenerated from carbon dioxide by vapour stripping stream in the desorber column. The vapour stream produced in the reboiler lowers the carbon dioxide partial pressure in the gas phase below the equilibrium and the CO_2 mass transfer is reversed from the liquid into the gas causing desorption (Figure 2.2). The reboiler heat duty required to produce the vapour stream can be divided into three main components (Oex10):

a) The heat of desorption q_{des} is equal to the negative value of the heat of absorption. The heat duty in the reboiler reverses the bicarbonate and carbamate reaction to release carbon dioxide, water and free amine. The more efficient amine solvents (primary and secondary amines) require a higher heat of desorption since they form stronger chemical bonds with carbon dioxide.

b) The sensible heat q_{sen} is the energy required to heat up the rich solvent to its boiling temperature. The vapour steam generated in the reboiler condenses on its way up the desorber, which heats up the down flowing solvent. The sensible heat demand is directly proportional to the solvent flow rate and inversely proportional to the rich solvent temperature before entering the desorber.

c) The heat of vaporisation q_{vap} corresponds to the additional vapour steam generated in the reboiler to increase the mass transfer driving force. A more intensive solvent regeneration demands a higher heat of vaporisation. Due to a higher temperature swing, the vaporisation heat decreases faster in efficient solvents (Oex10).

Table 4.1. Reboiler heat duty components

Heat of Desorption	Sensible Heat	Heat of Vaporisation
$q_{des} = \frac{-\Delta H_{abs}}{M_{CO_2}}$	$q_{sen} = \frac{Cp \cdot (T_{reb} - T_{rich})}{\alpha_{rich} - \alpha_{lean}} \cdot \frac{M_{sol}}{M_{CO_2}} \cdot \frac{1}{x_{AAS}}$	$q_{vap} = \Delta h_{vap} \cdot \frac{P_{H_2O}}{P_{CO_2}} \cdot \frac{1}{M_{CO_2}}$
(4.1)	(4.2)	(4.3)

The reboiler heat duty components represented in Table 4.1 are expressed in MJ/kg_{CO2} units. In all equations, M_{CO2} is the molar mass of carbon dioxide. The absorption enthalpy Δh_{abs}, the pressure relation water-CO_2 in the desorber head P_{H2O} / P_{CO2}, the heat capacity Cp and working capacity α_{rich}-α_{lean} are characteristic for the chemical solvent. The working capacity is expressed in moles CO_2 per mole AAS. The average molar mass of the solution M_{sol} and the AAS molar fraction x_{AAS} depend on the solvent strength and the carbonation ratio.

The reboiler heat duty components are interrelated with one another. Their influence on the reboiler heat duty is proportional to the solvent efficiency and the operating parameters. In screening studies of chemical solvents for post-combustion carbon capture, the focus frequently turns to solvents with a low heat of absorption. In most cases, these solvents react via the bicarbonate route, for which higher rich loadings are achievable. This approach is however misguided when the whole process is considered, since a modification of operating parameters like the desorber pressure, may lower the overall energy demand for high heat of absorption solvents. These solvents profit from a higher temperature swing between the absorber and desorber, i.e. higher working capacity for the same temperature range. An increase in the desorber pressure leads to less water vapour loss in the desorber head and thus lower heat of vaporisation (Oex10).

With the focus on identifying the optimal energy efficient solvent for carbon capture from an intermediate partial pressure combustion flue gas (approx. 120 mbar), van Straelen (vStr11) came to the conclusion that those solvents with heats of absorption between 55-65 kJ/mol achieved the best results. The simulation conditions of the study they performed were set to an absorber bottom temperature of 50°C, a rich solvent equilibrium partial pressure of 0.05 bar and a reboiler pressure of 1.15 bar. As in other simulation studies, it was assumed that the solvent-CO_2 system operated at equilibrium. Solvents with lower heats of absorption have much higher vaporisation heat and solvents with higher heats of absorption demand a high heat of desorption. The data gathered in Table 2.2 indicates that the optimal heat of absorption range corresponds to the hindered amines group. The CCS^+ amino acid salt falls into this group, which means that its energy demand is within the lowest in the available current market amine-based solvents. On the downside, solvents with lower than MEA heats of absorption (<80 kJ/mol) usually require higher mass flow rates and/or the absorber must operate at a lower temperature to reach the same capture rate for which the cooling water demand increases (vNie10). In general, solvents with lower heats of absorption have lower absorption reaction kinetics. Higher contact area and longer residence times are required in order for the solvent to operate at equilibrium, which increases the investment costs.

A further optimisation approach is to investigate the specific energy demand variation for a fixed solvent by varying the liquid to gas *L/G* ratio. According to Equation 2.4, the working capacity is inversely proportional to the *L/G* for a constant capture rate. If the equilibrium is reached at all points with increasing *L/G* ratio, the rich loading remains constant and the lean loading is re-adjusted by means of the reboiler heat duty to maintain a constant capture rate.

Nazarko et al. (Naz11) studied the influence of the solvent flow rate and lean loading on the specific energy demand in a carbon capture application with MEA solvent. At lower rates, a higher working capacity is required. Therefore, more additional vapour steam is generated in the reboiler to reduce the carbon dioxide partial pressure and ensure enough desorption driving force required for lower lean loadings. This causes an increase in the heat of vaporisation. At higher rates, the working capacity decreases as well as the vapour loss at the top of the desorber. On the other hand, the sensible heat increases due to a higher solvent flow rate. For the whole lean carbonation ratio range targeted in this study, the heat of desorption remained constant. In other amine solvents which combine carbamate and bicarbonate formation, the heat of absorption may vary with the carbonation ratio (Sie10/13).

Both previous simulation studies from (vNie10) and (Naz11) were carried out considering the fact that the rich equilibrium loading is reached throughout the considered range of operation. In practice, the carbon capture performance is controlled not only by the equilibrium, but also by the absorption reaction kinetics, i.e. how fast the system moves towards the equilibrium. The absorber and desorber height determine the V-L contact area and the residence time for the absorption/desorption to take place. If both variables enable the solvent to operate at equilibrium, then the minimum specific energy demand is achieved. In case the columns are too short or the absorption reaction kinetics too slow, then the absorption reaction rate must be enhanced to reach the optimum value.

This aspect allows combining both factors: energy demand and absorption reaction kinetics to investigate the rate promoter enhancement effect on solvents with slow reaction kinetics. In an underestimated absorber packing height, a solution with higher absorption reaction kinetics will achieve a higher capture rate at the same energy input, or will require lower reboiler heat duty to achieve the same capture rate. The slower absorption reaction kinetics is compensated by increasing the packing height.

4.2. Experiment Setup and Procedure

The experiments under synthetic coal-fired combustion flue gas conditions were carried out in the Siemens mini plant. The absorber column was modified, so that the lean solvent could be bypassed through three different feed stages. This way, the plant could be operated at different absorber packing heights.

4.2.1. Siemens Mini Plant

A simplified flow sheet of the Siemens laboratory carbon capture mini plant is illustrated in Figure 4.1. The plant consisted of an absorber, desorber, plate cross heat exchanger, gas mixing station, two pumps, three thermostats, reboiler, lean solvent surge drum, two filters and infrared gas analyser (Ultramat). The absorber column was made up of six stainless steel DN 50 cylindrical sections with 0.5 m height each. The lean solvent feed was bypassed at 3, 2.5 and 2 m packing height. The column was filled with SULZER-CY structured packing units with a 50 mm diameter. At the top of the absorber there was a condenser, where the majority of the water vapour in the treated gas was condensed and returned directly to the column. At the absorber bottom there was a liquid outlet where samples of the rich solvent could be taken. Above the sump liquid level, the gas mixture was fed into the column. The desorber was made of three 1m insulated glass column sections filled with the same packing units as the absorber. At the top of the desorber there was also a glass condenser, which recovers the upward flowing water vapour. The vaporisation condensate was returned exteriorly to the desorber bottom through a Teflon tube.

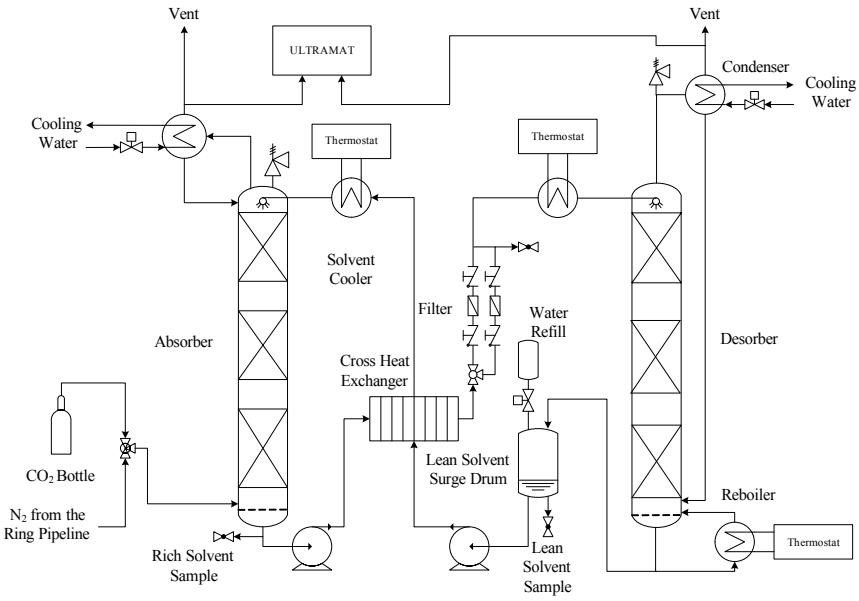

Figure 4.1. Siemens mini plant layout

The desorber bottom was connected to a steel recirculating thermo syphon reboiler. The density difference between the reboiler inlet liquid and the outlet liquid-vapour mixture provided sufficient liquid head to deliver the liquid bottoms into the reboiler. The reboiler heat duty was supplied by a DW-Therm heating oil, which was pumped from the UNISTAT 510 W thermostat oil bath through an internal spiral coil in the reboiler. The heating oil hot temperature set in the thermostat regulated the reboiler heat duty. The gas mixing station specified the composition of the synthetic flue gas flowing into the absorber. The two gas components were carbon dioxide, which was supplied from an AIR LIQUIDE gas bottle and nitrogen, which was supplied by the ring pipeline of the industrial park. The dry gas current entered the absorber and contacted the falling solvent in countercurrent flow. Due to the vapour phase vapour saturation, the water loss in the absorber head (approx. 20 ml/h) had to be continuously refilled. The lean solvent surge drum served as a tank buffer before the lean solvent was pumped back to the absorber continuously. The lean solvent surge drum stabilised the absorber and desorber liquid level. The solvent makeup water was refilled at the top.

4.2.2. Operating Variables

As seen in the previous chapter, the variation of the operating variables affects the specific energy demand in the carbon capture process. The manipulated and fixed variables employed in the experimental test runs are summarised in Table 4.2.

Table 4.2. Operating variables in the mini plant experiments

Manipulated Variables			Constant Variables		
L, kg/h	**h_{Abs}, m**	**T_{Therm}, °C**	**G, kg/h**	**[CCS+], wt-%**	**CR, %**
12 - 25	2; 2½; 3	146 - 155	0.6 (CO_2) 2.9 (N_2)	27 - 29	85 - 87

The base case was established as the standard CCS^+ solvent at a full absorber packing height h_{Abs} (3 m). The test runs with promoted solvent were performed at the three absorber packing heights. The CCS^+ solvent was promoted with 0.1 wt-% PROM-1. The same solution was maintained inside the mini plant for all the promoted solvent test runs. The solvent flow rate *L* was varied over a wide range of values. The interval was selected regarding the gas flow rate *G* so that the regions in which the vaporisation and sensible heat controlled the overall specific energy demand were clearly identifiable. At each solvent flow rate, the reboiler thermostat temperature T_{Therm} was selected until the *CR* value fell into the 85 - 87% range. The solvent strength $[CCS^+]$ remained more or less constant for all the experimental test runs. The lean solvent pre-cooling and rich solvent pre-heating thermostat temperature were kept constant. This caused that the lean solvent temperature at the top of the absorber and the rich solvent temperature at the top of the desorber varied with the solvent flow rate. The absorber inlet temperature varied between 35 - 40 °C and the desorber inlet temperature between 85 - 90 °C.

The influence on the capture performance was neglected, since two experimental points compared with same mass flow rate had the same inlet temperature. It was therefore assumed that the 5 K variation in the inlet temperature to the absorber and desorber could be neglected.

4.2.3. Measuring Procedure

The thermostat temperature and the solvent flow rate were first adjusted by an iterative method. The method was started by setting the heating oil temperature and the solvent flow rate arbitrarily. After the plant operated at a steady state for at least 2 hours, the capture rate (blue diamonds) and reboiler duty (red squares) were measured. In order to calculate the *CR* and further the *SED* for each experimental point (Appendix B), a liquid sample is taken of the lean and the rich solvent. The carbonation ratio and solvent strength were measured with the acid titration method (Appendix A).

The calculation of the initial experimental point is demonstrated in Figure 4.4. In this case, the thermostat temperature was kept constant and the solvent flow rate was varied. As an example of this procedure firstly the hot oil temperature and the solvent flow rate were set to their starting values (19.5 kg/h and 153 °C). The measured capture rate 88% was higher than the targeted range. The solvent flow rate was therefore lowered to 17 kg/h. Due to an increase of the latent heat demand, the capture rate dropped down to 77% and the reboiler duty increased significantly. An increase in the solvent flow rate to 17.5 kg/h brought up the capture rate to 80%. The solvent flow rate was further increased to 18 kg/h and the targeted CR of about 86% was finally accomplished. After taking three samples at the same operating conditions and measuring the capture performance for each one of them, the solvent flow rate was changed to define the next experimental point.

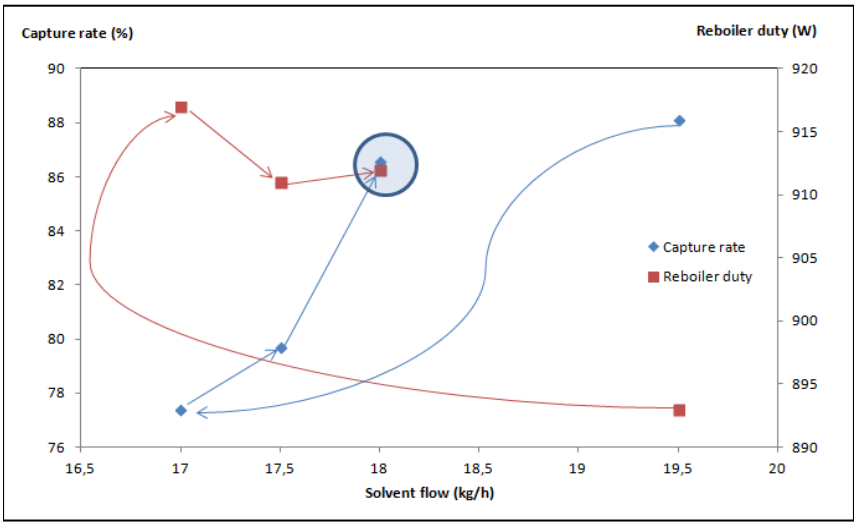

Figure 4.2. Iterative adjustment of the operating variables (Tol13)

4.3. Results and Discussion

According to Equation 2.4, the working capacity decreases with the solvent flow rate at a constant capture rate and gas flow rate. The almost linear trend of the measured values in the mini plant experiments presented in Figure 4.3 ensured a good consistency between the experimental data and the theory. The measurements with promoted CCS⁺ solvent were measured at 2.0, 2.5 and 3.0 m absorber packing height. The base case with standard CCS⁺ solvent was carried out only at 3 m absorber packing height. The solvent flow rate was expressed in % units. The 100% value was set for the optimum solvent flow rate of the base case regarding the specific energy demand.

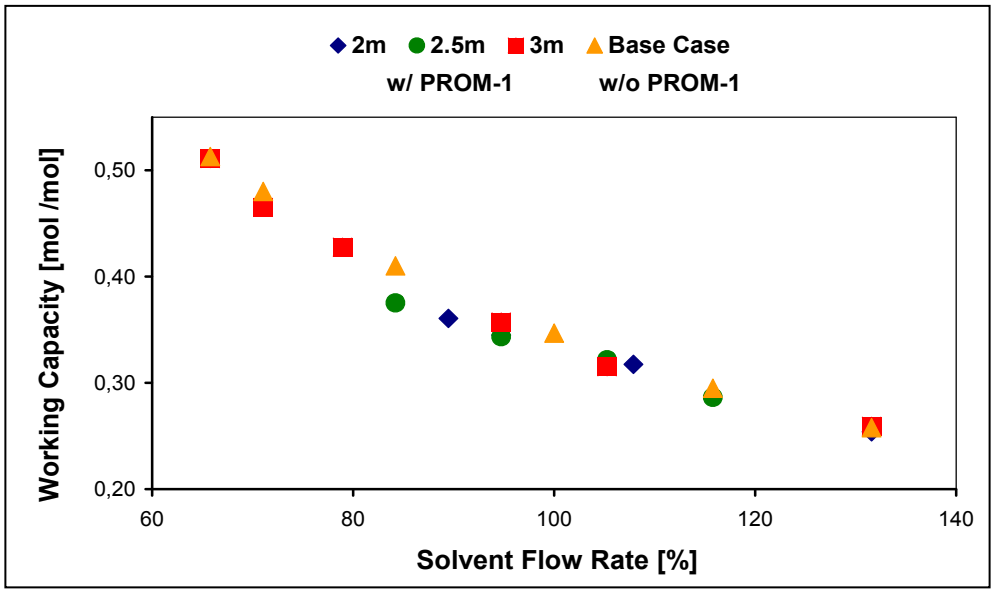

Figure 4.3. Inverse proportion of working capacity to the solvent flow rate

The energy curves at the different absorber packing heights are presented in Figure 4.4. A summary of the experimental data is located in Appendix C. It was observed that the promoted solvent curve at 2.5 m (green dots) achieved the same specific energy demand as the base case (orange triangles) at the optimum solvent flow rate (100 - 110%). At this operating point, the rich-lean loading values also coincide for both test runs. The reduced contact area and lower residence time due to a 17% lower absorber packing height was compensated by the enhancement of the CCS⁺'s absorption reaction kinetics through the addition of PROM-1, which permitted both systems to obtain the same capture performance. At lower solvent rates, the rich loading of the promoted solvent at a 2.5 m absorber packing height was lower than the base case, i.e. the system operated further away from the equilibrium. Under these conditions, a higher working capacity is required to achieve the CR, which made the latent heat the determining factor on the specific energy demand. This caused the big difference in the specific energy demand between the full packing height and the reduced packing height curves. The 2 m curve with promoted solvent obtained higher specific energy demand values throughout the

entire solvent flow rate range. The rich loading measured at the absorber bottom was further away from the equilibrium than the other three curves, which made the desorption more energy intensive to achieve the same working capacity. In all curves, the rich-loading measurements at higher solvent flow rates decreased, which means that the contact area and the residence time became a limiting factor on the capture performance. Due to faster absorption reaction kinetics, the promoted solvent at 3 m (red squares) came closer to equilibrium, compared to the base case, achieving a lower specific energy demand especially at optimum and higher solvent flow rates.

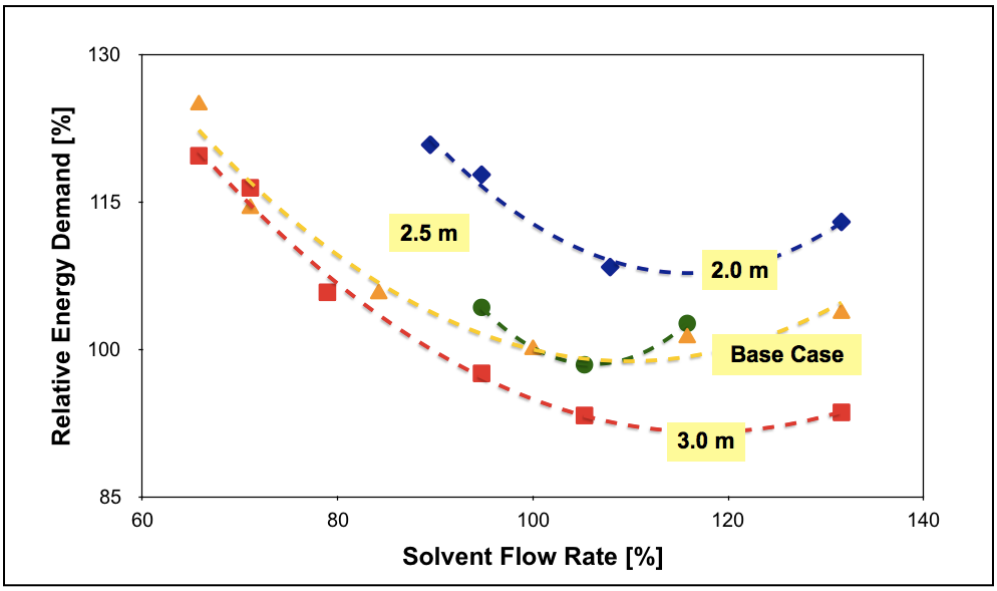

Figure 4.4. Rate promoter testing in the mini plant at different absorber packing heights

For further understanding of the experimental results, the specific energy demand was also plotted against the lean loading (Figure 4.5). In the simulation results for the MEA system presented by Nazarko et al. (Naz11), it was found that the solvent flow rate and lean loading x-axis values were interchangeable. In the simulation, it was considered that all the curve points reached the equilibrium (i.e. the packing height was not a limiting factor). In the practice, at a fixed absorber packing height, the rich loading reached at the bottom of the absorber is lower than the equilibrium, and therefore the curve may be slightly different. Nevertheless, a similar tendency between the simulation and the laboratory results was observed.

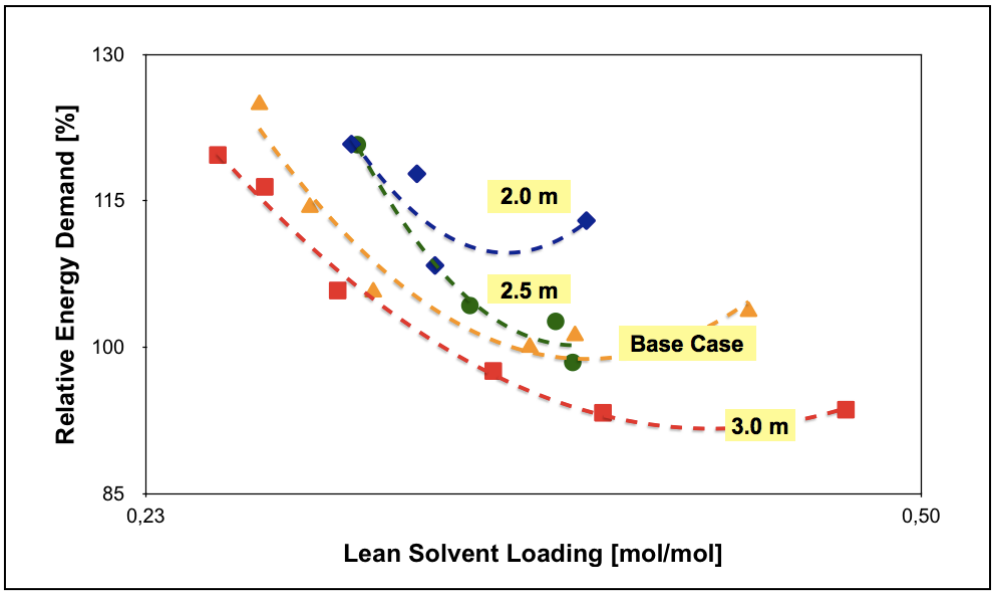

Figure 4.5. Specific energy demand over the lean solvent loading

It can be observed in the graphic that at lean loadings lower than 0.35 mol/mol the base case and the 3 m energy curve with promoted solvent have a similar capture performance. As the lean loading increases, the base case separates from the 3 m and tends to the 2.5 m energy curve with promoted CCS⁺ solvent. It can therefore be pointed out that the rate promoter has a significant effect under the experimental conditions when the curve approaches the operating optimum. In other words, the promoter effect was especially identified at the solvent flow rate range where the latent heat of vaporisation is not the limiting factor of the specific energy demand. In the previous chapter it was established that PROM-1 would have an enhancement effect at higher CO_2-loadings (Table 4.3).

Table 4.3. Promoter effect at different solvent flow rates

Operating range	CO_2-loading range (mol/mol)	Limiting factor on *SED*	Promoter effect
Low solvent flow rate	0.30 - 0.70	Heat of vaporisation	Energy curves at 2.5 and 2.0 m operate at much higher *SED* values
Optimum solvent flow rate	0.35 - 0.70*	Absorption reaction kinetics	The enhanced absorption reaction kinetic of the promoted solvent makes up for 17% absorber packing height reduction
High solvent flow rate	0.40 - 0.65*	Sensible heat	The promoted solvent at a full packing height achieves a much lower energy demand

* The promoted solvent curve at 3 m achieved much higher CO_2-loading values at above optimum flow rates

4.4. Conclusion

The investigation of the specific energy demand curve for the promoted CCS$^+$ solvent at different packing heights rendered the following conclusions:

- The full mini plant packing height was insufficient for the standard CCS$^+$ solvent to reach the equilibrium over the entire investigated solvent flow rate range. This experimental framework was ideal to qualitatively see the effect of a higher absorption reaction kinetic due to the addition of PROM-1 to the solvent.

- Under the mini plant optimum operating conditions, the CCS$^+$ solvent promoted with 0.1 wt-% of PROM-1 required approximately 17% less packing area in order to achieve the same capture performance as the standard solvent. At lower than optimum solvent flow rates, the latent heat demand to achieve a high working capacity was the controlling agent on the specific energy demand.

- At a full absorber packing height, the promoted CCS$^+$ solvent achieved a lower specific energy demand at the optimum operating conditions, since the faster reaction kinetics enabled the system with rate promoter to come closer to equilibrium in the absorber bottom.

After confirming and quantifying the promoter's advantages at a laboratory scale, the focus was turned towards the Siemens pilot plant. PROM-1 was further tested on the CCS$^+$ solvent under real combustion flue gas conditions, in order to generate reliable results that could be further used for up-scaling and economic evaluation.

5. RATE PROMOTER TESTING UNDER REAL GAS CONDITIONS

The laboratory results in the mini plant confirmed the rate enhancement effect in the absorption of carbon dioxide with the promoted CCS$^+$ solvent. The faster absorption reaction kinetics enabled the promoted solvent to achieve the same capture performance as the standard solvent at a reduced packing height (approximately 17%). The next step in the development plan was to reproduce the mini plant experimental results under real combustion flue gas conditions. The Siemens carbon capture pilot plant retrofitted to the hard coal fired power plant Staudinger (Germany) served as the ideal testing location. The operating conditions in the pilot plant were similar to a typical commercial capture plant design, so that the experimental results may be used for up-scaling purposes. A further advantage of the pilot plant was the possibility of reducing the packing height in the absorber and desorber column by leaving out the top structured packing segments in each column. The evaluation of the capture performance at a full and reduced packing height would quantify the enhancement effect of the inorganic promoter on the CCS$^+$ solvent.

The experimental method differed from the mini plant tests in that the reboiler heat duty and the solvent flow rate remained constant for each experimental set. The standard and promoted solvent performance was compared by investigating the effect of the packing height on the capture rate. Under kinetic-limited operating conditions, the packing height reduction was expected to decrease the working capacity, i.e. the swing between the lean and rich loading. At a constant solvent flow rate this translates into a lower capture rate. There was a chance that this negative effect in the capture performance would be compensated by activating the CCS$^+$ solvent with PROM-1. The faster absorption reaction kinetics would make up for the reduced packing height, achieving at least the same capture rate as the standard solvent at a full height.

Furthermore, the experiments were repeated at a lower heat duty in the reboiler, to investigate a slower absorption regime and therefore increase the limiting factor of the packing height. Less stripping steam was generated for desorption, which increased the lean loading and at a constant solvent flow rate decreased the working capacity. Although the capture rate under the operating conditions was lower than the commercial optimum (85 - 90%), these test runs served to validate the promoter effect at higher carbonation ratios, i.e. slower absorption regimes.

The operating parameters were recorded during each experiment by the process control system. The average value of each measured parameter would later be used to develop the Aspen Plus® simulation model to reproduce the promoted CCS$^+$ solvent's new kinetic properties. The prediction of the potential packing height reduction with further cost savings is discussed in the following chapters.

5.1. Pilot Plant vs. Mini Plant

The pilot plant was chosen for the testing of the promoter because the operation factors and variables were more similar to the commercial carbon capture plant. Pilot plants are adequate for confirming the CO_2-AAS laboratory equilibrium measurements or to estimate them indirectly. Moreover, they deliver the basics for the design of the full scale industrial columns. The main differences between the pilot and mini plant are listed in Table 5.1.

Table 5.1. Technical data comparison between mini plant vs. pilot plant

	Mini plant	**Pilot plant**
Specific packing area, m^2/m^3	700	350
Capacity factor, $Pa^{0.5}$	0.45	1.34
Energy supply	Thermostat	Low pressure steam
Optimum L/G, kg/kg	5.5 - 6.0	5.7
Heat loss	Considerable	Negligible
Packing height reduction	Absorber (17 or 33%)	Absorber (20%); Desorber (33%)

The pilot plant structured packing had a lower specific area, enabling a higher gas load in the absorber. Commercial plants will implement a similar packing type, although operated at a higher vapour capacity factor (1.8 and 2.2 $Pa^{0.5}$). In the pilot plant, the reboiler heat duty was supplied by the low pressure steam coming from the coal-fired power plant. The pilot plant was better isolated than the mini plant reducing the total heat losses. The measurement of the specific energy demand in the pilot plant approached the real value. The liquid to gas ratio chosen in the pilot plant fell into the optimum range measured in the mini plant, although the lean and rich loadings were both higher (lower *SED*). The larger pilot plant contact area enabled the AAS-CO_2 system to operate closer to equilibrium.

5.2. Experimental Setup and Procedure

The test runs were carried out in the Siemens PostCap™ pilot plant. The operating conditions like gas and solvent flow rates, solvent strength, lean solvent temperature and reboiler heat duty were adjusted to reach optimal operation conditions at a full packing height. A lower reboiler heat duty was also tested to generate additional results, which would be later compared. By bypassing the top packing sections of the absorber and desorber, the total packing height could be reduced by 25%. The capture performance of the standard solvent was compared to the promoted solvent at a full and reduced packing height.

5.2.1. Pilot Plant Description

The flue gas from Staudinger is typical for a hard coal fired power plant. The vapour composition contains approximately 13 mol-% carbon dioxide (dry). A process flow sheet of the pilot plant is presented in Figures 5.1 and 5.2. The images correspond to two screenshots taken from the process control system (PCS) during operation.

The combustion flue gas coming from the desulphurisation unit was fed into the absorber by the blower (E1011). The rate was regulated by a flow controller (F1010). The flue gas was firstly cooled down in the direct contact cooler (DCC) located below the absorber (K100). The aqueous cooling water was refrigerated in the W101 heat exchanger. The cooling down of the flue gas caused the water vapour content partially to condense into the DCC cooling medium. The absorber was fitted with five segments of Mellapack® 350X structured packing. The top segment could be bypassed, reducing the packing height by 20%. The absorber bottoms were directly fed into the rich solvent surge drum (B101), which served as buffer tank of the absorber pump (E1031). The rich solvent was heated up in the cross heat exchanger (W102) before it was fed into the top of the desorber (K200). The rich solvent rate was regulated by the flow controller (F1032). The desorber was fitted with three Mellapack® 350X packing segments. The top segment could also be run dry, reducing the packing height by 33%.

The stripping vapour steam was generated in the reboiler (W202). The heating energy was supplied by low pressure vapour steam coming from the power plant. The additional vapour to reduce the carbon dioxide partial pressure in the desorber head was condensed in the condenser (W201). Unlike the mini plant, the condensate was recycled back to the desorber top stage. The lean solvent exciting the desorber bottom was pumped through the cross heat exchanger (W102) heating up the rich solvent. The lean solvent temperature entering the absorber was further reduced in the pre-cooler (W103). The set value was regulated by the temperature controller (T1008).

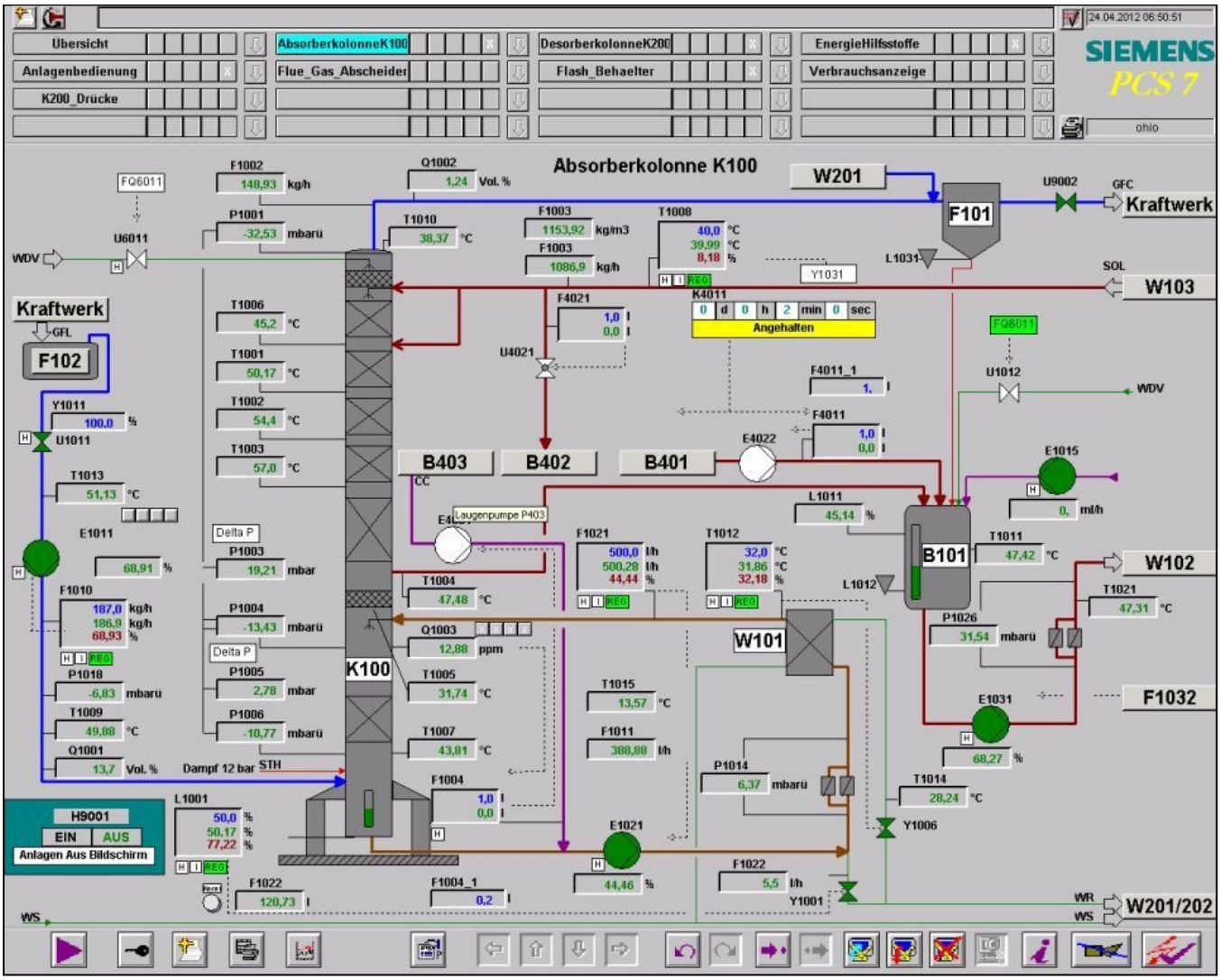

Figure 5.1. PostCap™ PCS: direct contact cooler, absorber and surge drum

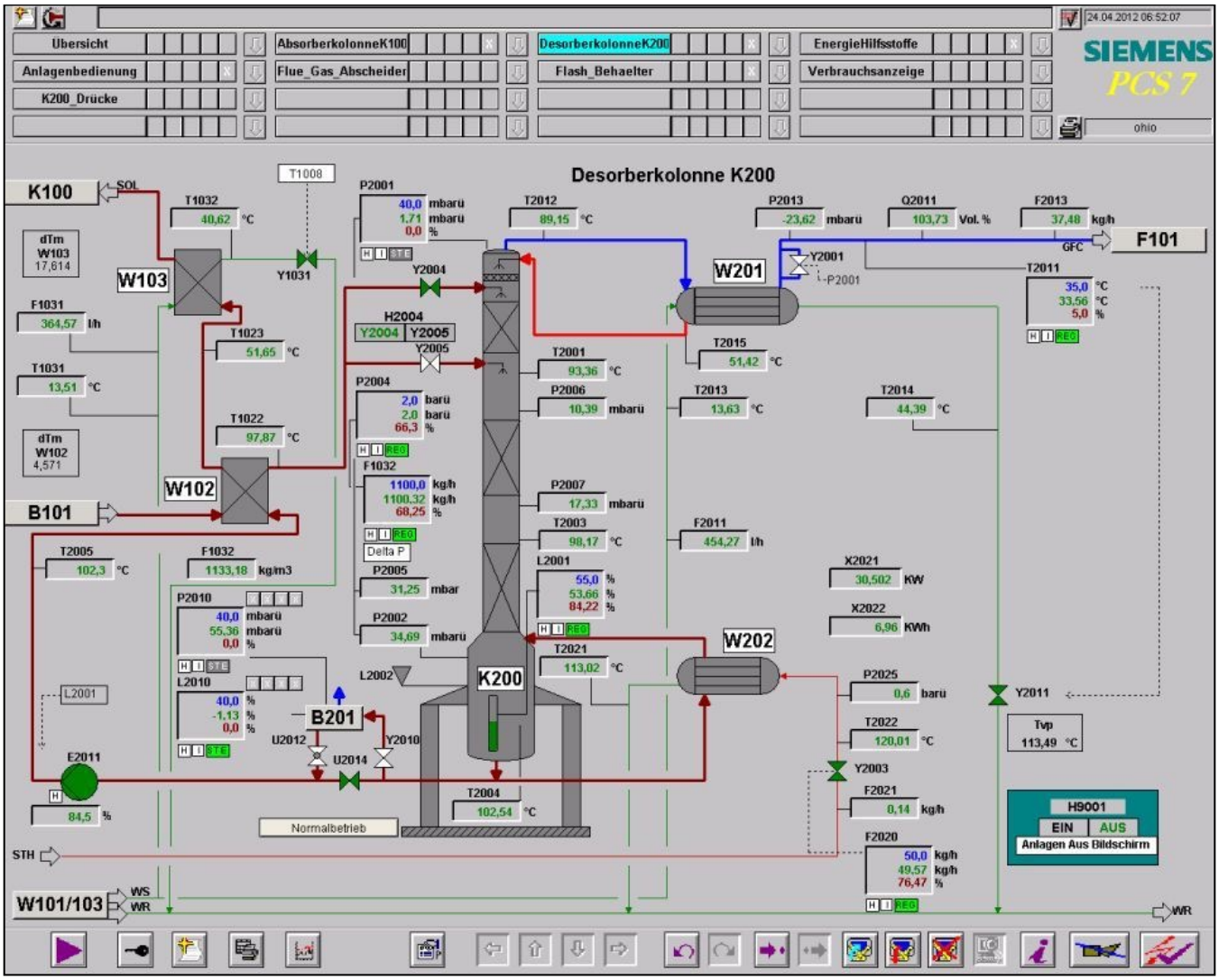

Figure 5.2. PostCap™ PCS: heat exchanger, cooler, reboiler, condenser and desorber

5.2.2. Operating Variables

The fixed operating variables are shown in Table 5.2. The solvent and gas flow rates were set based on the previous test runs performed on the pilot plant (Sie10/13). The reboiler heat duty and the lean solvent feed temperature were selected so that at a full column packing height, the capture rate would be between 85 and 90%. A lower reboiler heat duty was also tested for comparison of the capture performance at higher carbonation ratios. The carbon dioxide mol fraction in the combustion flue gas fluctuated around 13 - 14 mol-%, depending on the power plant operating load.

Table 5.2. Fixed operating variables in the pilot plant

Rich solvent flow rate [kg/h]	Gas flow rate [kg/h]	Reboiler heat duty [-]	CO_2 feed pressure [mbar]	Lean solvent temperature [°C]	Solvent strength [%]
1100	187	Low - High	114 - 119	40	24 - 26

The solvent strength used in the pilot plant was lower compared to the mini plant tests to avoid crystallisation. In any case, the solvent strength and promoter concentration have a big influence in the absorption reaction kinetics, so further investigations must be carried out to find out the optimal value to ensure operation safety and improve the capture performance.

5.2.3. Experimental Procedure

The feed stage height in both absorber and desorber could be lowered, so that the operation at a reduced packing height could be compared to full height. Regarding the effect on the capture performance, it was expected that when using the standard CCS$^+$ solvent, a decrease of the packing height, while the other parameters were kept constant, would likewise decrease the capture rate. The lower contact area and residence time would hinder the rich solvent to reach the equilibrium at the bottom of the absorber, since the reaction kinetics was the limiting agent. In case of the promoted solvent, the reaction kinetics would no longer control the rich solvent loading. The reduction of the packing height was expected to be compensated by the promoter enhancement of the absorption reaction kinetics. Table 5.3 contains a summary of the varied operating variables used in the promoter tests in the PostCap^{TM} pilot plant. All test runs were carried out in a random order, to avoid error propagation. The column titled “Test run” addresses the order with which each experimental run was performed. The full packing height in each column was specified at 100%. When both top packing segments were bypassed, the total packing height decreased to 75%. The first four test runs were performed with standard CCS$^+$ solvent to set the benchmark capture performance. In the following four test runs, 0.1 wt-% PROM-1 was added to the solvent. The reboiler heat duty was set at a “high” value so that at a full packing height the standard CCS$^+$ solvent achieved a capture rate between 85 and 90%. The “low” value supplied 15% less heat to the reboiler, which shifted the rich-lean loading range to higher carbonation ratios.

Table 5.3. Varied operating variables in the pilot plant

Test run [Nr.]	0.1 wt-% PROM-1 [y / n]	Absorber height [%]	Desorber height [%]	Reboiler heat duty [h / l]
1	n	100	100	high
2	n	100	100	low
3	n	80	66	low
4	n	80	66	high
5	y	100	100	high
6	y	100	100	low
7	y	80	66	low
8	y	80	66	high

After each test run, the solvent circulation was shortly interrupted in order to vary the lean solvent feed stage and hence modify the absorber and desorber packing height. Once the operation was restarted, the process variables recorded in the process control system were not considered until the plant reached steady state. Once reached, the operating variables remained constant for a period up to approximately 3 hours. The measured data was evaluated after each test run and the average value of each parameter was estimated. Approximately half an hour before the end of each test run, a liquid sample was taken from the absorber and desorber outlet. The carbonation ratio and solvent strength of the samples were afterwards analysed by acid titration in the laboratory according to the method described in Appendix A. The capture performance was finally calculated according to the calculation procedure described in Appendix B.

5.3. Results and Discussion

The measured values in the promoter testing at the PostCap™ pilot plant are summarised in Table E.1 of Appendix E. The most relevant operation parameters, process variables and capture performance were tabulated. The operating variables were represented by the average value of the measurements recorded during operation. The results were sorted out in a specific manner, so that two tests runs with the same packing height or with the same reboiler heat duty may be directly compared.

5.3.1. Capture Rate

Figures 5.3 and 5.4 represent the capture rate values measured for different reboiler heat duties and packing heights. The capture rate of the standard CCS+ solvent (unpromoted solvent) is compared to the promoted solvent with PROM-1.

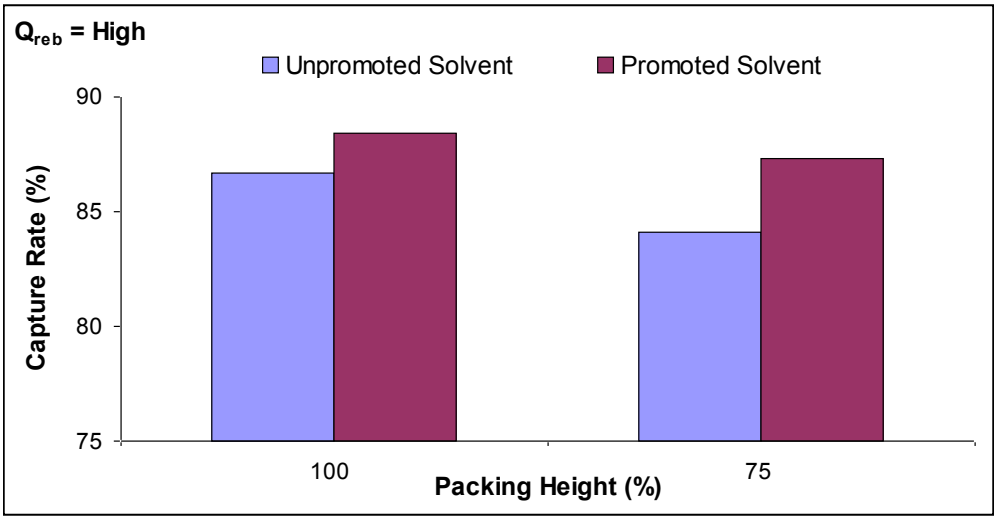

Figure 5.3. Effect of the packing height on the capture rate at a high reboiler heat duty

As expected, the capture rate of the unpromoted solvent decreased at a reduced packing height. This result indicated that the capture performance under the selected operating parameters was kinetic-limited. Due to faster absorption reaction kinetics, the promoted solvent achieved higher capture rates that were only marginally lower for the reduced packing height. For both packing heights tested, the promoted solvent achieved a higher capture rate. At lower reboiler heat duties, the capture rate differences between the promoted and unpromoted solvents were more significant, since the higher carbonation ratios (0.48 – 0.82 mol/mol) were responsible for lower absorption reaction kinetics. The lean loading values were mostly dependent of the reboiler heat duty and therefore remained practically the same. Higher rich loadings, hence working capacities were therefore achieved either at the full packing height or by the promoted solvent. The results demonstrated the same tendency as known from the mini plant experiments.

Under kinetic-limited operating conditions the addition of PROM-1 resulted in a higher capture performance or lower *SED*. In the pilot plant experiments, a higher capture rate was observed.

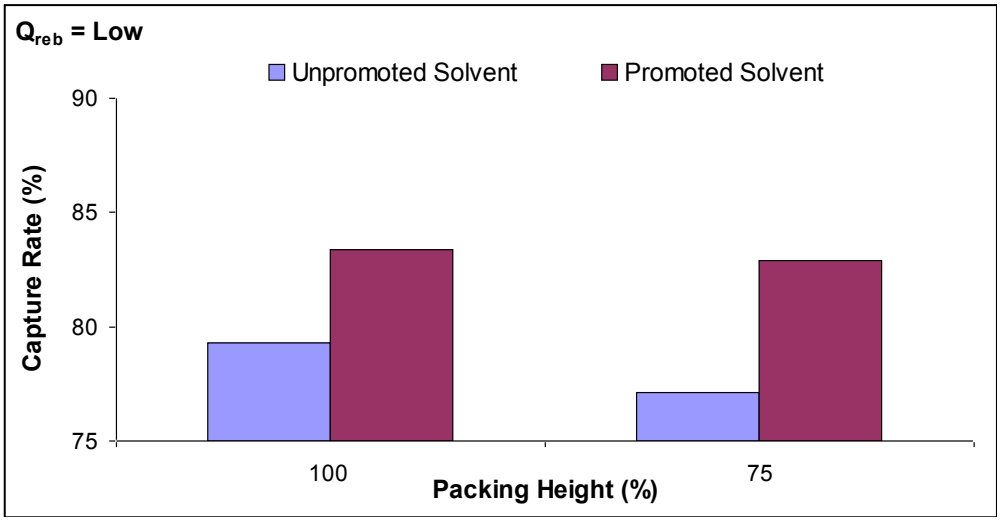

Figure 5.4. Effect of the packing height on the capture rate at a low reboiler heat duty

The experimental results were gained under real combustion flue gas conditions. The obtained results were a step forward towards the capital cost savings. Due to limited availability of the pilot plant, the promoter long-term stability could not be tested, and therefore remains the focus of future research objectives.

5.4. Conclusion

The pilot plant experiments rendered the following conclusions:

- Although the pilot plant operated closer to equilibrium, the capture performance under the operating conditions was kinetic-limited as it was the limiting factor in the mini plant experiments. The reduction of the packing height in the case of the standard CCS$^+$ solvent decreased the capture rate for the same reboiler heat duty. The packing height influence on the capture rate was accentuated at a lower reboiler heat duty.

- The promoted CCS$^+$ solvent achieved a higher capture rate than the standard CCS$^+$ solvent for all the tested operation conditions at the same reboiler heat duty. The reduction of the packing height barely affected the capture performance of the promoted CCS$^+$ solvent for both reboiler heat duties tested. Based on this result, it is assumed that the promoted CCS$^+$ solvent reached the equilibrium rich solvent loading in all of the test runs, which means that a further packing height reduction may be possible. This fact will be further investigated in chapter 6.

After successfully testing PROM-1 in the PostCap^{TM} pilot plant, the focus was set on calculating the potential packing height reduction for full-scale carbon capture plants. Hence, the Aspen Plus® simulation model developed by Siemens for the standard CCS$^+$ solvent was adapted to the promoted CCS$^+$ solvent in order to reproduce the experimental results observed in the pilot plant experiments. The model would be further implemented in an economic evaluation to estimate the total capital cost savings for a commercial plant.

6. PROMOTED CCS+ MODEL DEVELOPMENT IN ASPEN PLUS®

The operating parameters measured in the pilot plant were used to adapt the existing CCS+-CO_2 mass transfer correlation model in Aspen Plus® to the CCS+-PROM-1-CO_2 system. The model would then be implemented to simulate the full scale capture plant and carry out an economic evaluation to estimate the cost savings potential through the reduction of the packing height in the absorber and desorber. A similar approach was realised by Thee et al. for the MEA/K_2CO_3 system (The11).

The standard CCS+ solvent Aspen Plus® model was developed and validated in the first 2 years of the PostCap™ pilot plant operation (Sie10/13). First, the thermo-physical properties of the CCS+ solvent at different concentrations were measured in the laboratory. The results were correlated and recorded in the Aspen Plus® Database. The correlation model chosen was that of Bravo, Rocha and Fair 92' (Bra92), because it fitted the experimental data best.

The interfacial area factor *IAF* and heat transfer factor *HTF* are scalars of the mass and heat transfer equations, which describe the absorption reaction kinetics in the absorption and desorption column. The correlation factors were simulated to fit the promoted solvent kinetic properties by an iterative process. First the reboiler heat duty was adjusted to accomplish the experimental capture rate. Then the *IAF* and *HTF* were varied to match the temperature profile in the absorber and desorber. Finally, two sets of correlation factors were defined for the promoted and standard solvent, in the absorber and desorber. Only the test runs performed at a full packing height were used as a standard for fitting the correlation factors. The simulation model was then validated with the test runs operated at a reduced packing height.

The low mean error resulting from the comparison between simulation and experimental values approved the model to accurately quantify the packing height reduction potential. Hence, PROM-1 was virtually "added" to the CCS+ solvent by changing to the *promoted IAF* and *HTF* correlation factors in the base case simulation at a full packing height. The height per rate of packing was lowered until the capture rate matched the base case. The packing height reduction was estimated for both the high and low reboiler heat duties.

Further details on the model development and economic evaluation may be found in the diploma thesis of M. Wiese (Wie12).

6.1. Basics

Aspen Plus ® is a computer simulation software tool implemented to design and optimise chemical processes. Unlike traditional equilibrium stage models, the rate-based modelling solution ensures accurate modelling of the carbon capture process and prevents over-design of distillation equipment, as well as downstream processing units. The rate-based model has been previously used with the goal to design plants with smaller equipment and lower energy consumption (Asp09).

During the model development for the promoted CCS^{+} solvent, an adequate mass transfer correlation was selected from all those available in Aspen Plus®. The thermo-physical properties and the chemical reaction parameters were adopted from the standard CCS^{+} solvent; since it was assumed that the low concentration PROM-1 did not affect the CO_2-AAS equilibrium. Finally, the column properties were specified for the dimensions of the pilot plant.

6.1.1. Process Flow Diagram

The process simulation starts with the process flow diagram (Figure 6.1). In this window, the block and streams were interconnected with one another according to the capture process layout. To simplify calculations, the CO_2 compression stage after the desorber was left out of the simulation.

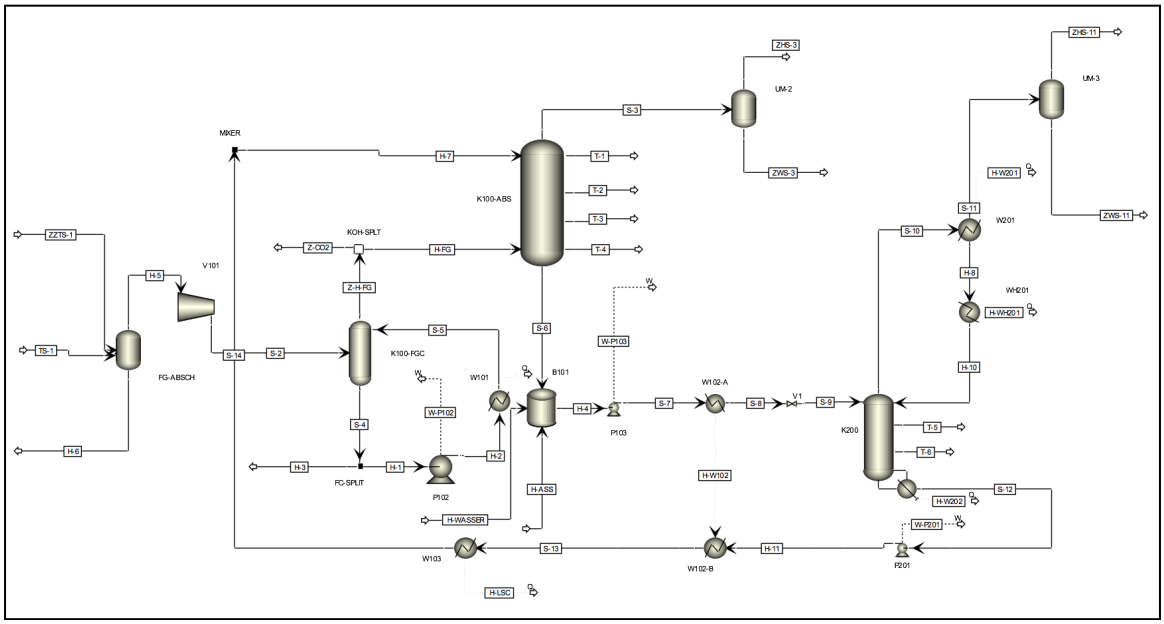

Figure 6.1. Aspen Plus® process flow diagram

6.1.2. Bravo Rocha Fair 92' Mass Transfer Correlation

The mass transfer correlation proposed by Bravo, Rocha and Fair BRF92' (Bra92) has been selected to reproduce the gas diffusion processes occurring in the absorber and desorber columns. This correlation is commonly used in the simulation of distillation processes. The correlation parameters were originally fitted by using a chemical system based on cyclohexane / n-pentane (Raz12). This organic mixture diverges from the AAS-CO_2 electrolyte system; however, the BRF92' achieved the best simulation results among the other correlations tested in the thesis of M. Wiese (Wie12).

The mass transfer correlation may be modified to fit the AAS-CO_2 system by manually varying the mass and heat transfer equation scalars, respectively: the interfacial area factor *IAF* and the heat transfer factor *HTF*. These parameters were noted in the RateSep packing specifications sheet.

The interfacial area factor corrects the amount of area provided by the structured packing for the chemical reaction in relation to the reaction kinetics. The *IAF* directly influenced the diffusion rate at the different column stages. The heat set free by the absorption reaction was likewise proportional to the *IAF*, and it determines the temperature profile in the absorber.

The heat transfer factor was used as a fine adjustment of the temperature profile to match the experimental values. At high carbonation ratios, the slow reaction regime was encountered in the absorber, especially in the lower stages for which IAF values lower than unity were expected.

6.1.3. Thermo-physical Properties

The VLE data for the CCS^+-CO_2 system was obtained from laboratory measurements. The characterisation experiments were performed by I. Schillgallies within the framework of his diploma thesis (Schi08). The Henry coefficients measured for different solvent strengths (23.0, 21.0, 33.5 and 36.8 wt-%) were fitted to a temperature dependent binary interaction parameter law. This law characterised the carbon dioxide solubility in the AAS solution. Wilson was selected as the base property method, since it allows the use of the Henry coefficients and assumes non ideal gas behaviour. The solvent physical properties were adopted from the "pront.ilb" file, which was based on the experimental measurements (Sie10/13). This file is required for any Aspen Plus® simulation that involves the CCS^+-CO_2 system.

6.1.4. Chemical Reaction

In order to simplify the calculations and reduce the input data; the carbamate formation, carbamate hydrolysis and bicarbonate formation were merged into one expression (R-6.1).

$$AAS + CO_2 + H_2O \leftrightarrow AAS - BCBO \quad \text{(R-6.1)}$$

The amino acid salt *AAS* reacts with carbon dioxide CO_2 and water H_2O to form the bicarbonate product *AAS-BCBO*. The reaction product combines the protonated amino acid salt and the bicarbonate ion species. The equilibrium constants were determined from the thermo-physical properties defined beforehand. The absorption reaction kinetics would be afterwards set by the *IAF*.

6.1.5. Column Properties

The absorption and desorption mass transfer calculations were carried out with a rate-based approach (RateSep). In this calculation type, every mass and heat transfer balance is rigorously calculated for each fictional separation stage. Unlike the equilibrium model, the equilibrium between the liquid and vapour streams leaving each theoretical stage is not assumed. The RateSep method is more accurate, but also more time consuming. It is ideal for reproducing the pilot plant results for the standard CCS$^+$ solvent; since under the tested kinetic-limited operating conditions, it was verified that the absorber did not reach the equilibrium (Asp06).

As depicted in Table 6.1, the column dimensions, structured packing characteristics, absorption enthalpy, operating variables and reboiler heat duty were input data that were introduced into the simulation model.

Table 6.1. Column property specifications

RateSep Input Data	Column dimensions	Reboiler heat duty
	Packed height per stage	Condenser capacity
	Number of stages	Film resistance
	Type of packing	Mass transfer correlation

In the vapour phase, the film resistance is set to Film mode since only diffusion resistance takes place. In the liquid phase, the “Filmrxn” mode (Men13) was selected since the AAS-CO_2 chemical reaction occurs. The place where the chemical reaction takes place is weighted by the reaction condition factor; 0 corresponds to the interface and 1 to the bulk phase.

6.2. Modelling Procedure

The goal of the promoted CCS+ model development in Aspen Plus ® was to determine a *promoted* interfacial area and heat transfer factor that best fitted the experimental results. The *IAF* corrects the amount of V-L contact area offered by the column packing that truly participates in the carbon dioxide mass transfer. It was previously expected, that the promoted solvent would imply a higher (enhanced) *IAF* than the base case, due to faster absorption reaction kinetics. The correlation factors were estimated by simulating those cases at a full packing height and different reboiler heat duties. The main reason for this was to avoid the complexity of varying more than one parameter. The stream and block experimental input data were introduced in the data browser once the global settings, the property method, the reaction chemistry, the equilibrium constants and the column properties had been defined. The simulated output data were compared with the experimental values for model validation (Table 6.2).

Table 6.2. Model parameters: input data, manipulated variables and output data

Experimental Input data	Manipulated variables	Simulated Output data
Gas and liquid flow rate	Interfacial area factor	Lean CO_2-loading*
CO_2 flue gas concentration	Heat transfer factor	Rich CO_2-loading*
Pressure profile	Reboiler heat duty (→CR)	Capture rate
Process heat loss		Absorber and desorber temperature profile
Solvent strength		
Rate packing properties		

It was defined as a simulating condition that the capture rate and the temperature profiles of the absorber and desorber had to coincide with the experimental values. After entering the experimental input data for the base case, the reboiler heat duty was determined. In the first simulations there was a discrepancy between the simulated and experimental *CR* values when using the same reboiler heat duty, which remained unaffected from the interfacial area factor variation. Therefore, the experimental reboiler heat duty was increased. To avoid interdependency, the correlation factors were set to unity. Once the capture rate coincided, the correlation factors were varied to match the temperature profile in the absorber and desorber. The modelling procedure was repeated for the standard and promoted solvent at full packing height and alternate reboiler heat duty, i.e. cases 1, 2, 5 and 6 (Table 5.3). Further on, the fitted parameters were validated with the rest of the cases at a reduced packing height, i.e. cases 3, 4, 7 and 8 (Table 5.3). It was possible to reproduce all the experimental values except the reboiler heat duty. This discrepancy might be due to error sources in the experimental procedure or in the fitted equilibrium data. The effect on the modelling procedure was neglected.

6.3. IAF and HTF Fitting

The modelling procedure was first carried out for the base case: standard solvent at a high reboiler heat duty and full packing height (case 1). Once the *IAF* and *HTF* were established, the promoted solvent at a full packing height and high reboiler heat duty experimental input data were simulated (case 5). As expected, the new experimental capture rate and temperature profiles differed from the simulated results. Therefore, the *IAF* and *HTF* factors were increased until both profiles corresponded to one another and the capture rates matched. In the meantime, it was observed that the *IAF* variation in the desorber was not as significant as in the absorber. Wiese (Wie12) discussed in his diploma thesis that this is caused by the higher desorber temperatures (90 - 100°C). These temperatures have a lower effect on the dynamic viscosity variation throughout the mass transfer area than the intermediate absorber temperatures (40 - 60°C). According to the Stokes-Einstein equation, the dynamic viscosity is a factor of the Reynolds and Schmidt number. A higher viscosity opposes resistance to diffusivity; hence it is indirectly proportional to the absorption reaction kinetics. The same correlation factor fitting method was repeated for the low reboiler heat duty cases (cases 2 and 6), which operated at approximately 20% less energy input. The final modelling results are presented in Table 6.3.

Table 6.3. IAF and HTF fitting final results

Case	Reboiler heat duty	Promoter	Absorber		Desorber	
			IAF	HTF	IAF	HTF
1	high	no	0.15	20	0.60	5.0
2	low	no	0.12	20	0.40	0.2
5	high	yes	0. 20	20	0.75	5.0
6	low	yes	0.20	20	0.75	5.0

The standard CCS$^+$ solvent factors decreased at a lower reboiler heat duty. Due to slower absorption reaction kinetics, the available packing area was less effectively used for mass transfer. The temperature profile in the desorber was better matched with a reduced *HTF*, fact which does not have any thermodynamic explanation. This fact was neglected since it does not have any direct effect on the packing height reduction. As in the pilot plant results, the promoted solvent absorption efficiency did not decrease with the reboiler heat duty. The high absorption reaction kinetics prevailed through the low and high carbonation ratio range, eliminating the kinetic-limitation. Only a lower capture rate was achieved for the low reboiler heat duty due to a higher lean loading, namely reduced working capacity. The promoted solvent achieved a higher *IAF* in both the absorber and desorber, which agreed well with the previous laboratory results.

The correlation factors were maintained constant for the remaining cases with a reduced packing height simulation. The comparison between the simulated and experimental capture rate is presented in Table 6.4.

Table 6.4. Comparison of simulated and experimental CR at a reduced packing height

Case	Reboiler heat duty	Promoter	Capture rate (exp.)	Capture rate (sim.)	Error, %
4	high	no	84.1	84,7	0,71
8	high	yes	87.3	86.5	0.92
3	low	no	77.1	76.5	0.78
7	low	yes	81.4	82.3	1.09

The simulated results deviate from the measured values with an average error of 0.87%, demonstrating a good agreement between the correlation factors and the CCS^{+} absorption kinetics. The fitted correlation factors were accurate enough to make a realistic estimation of the potential packing height reduction for the promoted solvent under the pilot plant operating conditions. The only negative factor was the disagreement in the reboiler heat duty. The connection between the equilibrium model, the absorption enthalpy and steam flow measurement in the pilot plant must be further examined.

6.4. Packing Height Reduction

It was previously demonstrated in the laboratory mini plant experiments that a packing height reduction is possible for the promoted solvent. The same capture performance was reached at a lower investment cost. The pilot plant offered a higher contact area so that the CO_2-AAS system operated closer to equilibrium, bringing about a higher height reduction potential. To quantify this potential, the simulation model was developed for the standard and promoted solvent in Aspen Plus®. The base case capture rate without promoter and full packing height was established as designed specification. The promoter was “added” by changing the corresponding correlation factors *IAF* and *HTF*. The packed height per stage was reduced until the reference capture rate was reached, and the temperature profiles were then more or less matched. The packing height reduction results are located in Table 6.5.

At a high reboiler heat duty the packing height reduction is lower, since the system is further from the equilibrium. Therefore, the absorption reaction kinetics had a smaller influence on the capture performance. The mini plant experiments were operated at very similar conditions, and the potential packing height reduction was also similar (83.0 vs. 78.5%). The mini plant desorber packing height could not be reduced, which explains the difference between both testing facilities.

Table 6.5. Packing height reduction for a constant CR at alternate reboiler heat duties

CCS⁺ solvent	Reboiler heat duty	Capture rate, %	Packing height, %		Total packing reduction, %
			Absorber	Desorber	
w/o PROM-1	high	86.7	100	100	22.5
w/ PROM-1			75	80	
w/o PROM-1	low	79.3	100	100	43.5
w/ PROM-1			60	53	

At a lower reboiler heat duty, the packing height reduction was higher. According to the simulation, it should be possible to reduce the total packing height to about the half of the pilot plant, and still obtain the same capture performance with the promoted solvent. This result would favor those operation cases in which a 90% CR is not required.

6.5. Conclusion

The simulation model development in Aspen Plus® produced the following conclusions:

- The promoted CCS^{+} solvent absorption performance was better reproduced with enhanced interfacial area and heat transfer values compared to the base case. The faster absorption reaction kinetics virtually increased the usage of more packing area by the promoted solvent. At a lower reboiler heat duty, the correlation factors in the promoted solvent were maintained constant. No kinetic-limitation was introduced due to weaker solvent regeneration. Only the equilibrium rich loading impeded that the solvent reached the same capture rate as the higher reboiler heat duty case.

- The model accuracy achieved had an average relative error of 0.87%. The fitted correlation model accurately reproduced the relationship between absorption reaction kinetics of the CCS^{+} solvent (with and without promoter) and packing height.

- The promoted CCS^{+} solvent enabled a total packing height reduction of 22.5% for a high reboiler heat duty and 43.5% for the low value. The cost savings will further be calculated in the economic evaluation of the following chapter.

The simulation model needs to be further optimised by correcting the divergence between the equilibrium constant data and reality by using more accurate correlating data, so that the reboiler heat duty and the lean and rich loadings coincide with the experimental values.

7. ECONOMIC EVALUATION

The main goal of this thesis is to establish the total amount of costs savings in the Postcap™ carbon capture process, achievable through the promoter addition to the CCS+ solvent. The laboratory experiments produced a potential candidate, PROM-1, which significantly enhanced the carbon dioxide absorption reaction kinetics. It has already been proven experimentally that the promoted CCS+ solvent achieved a reduction of the total structured packing height of about 17% in the laboratory mini plant and 25% in the pilot plant while still maintaining the same capture performance. The rest of the operating parameters, such as solvent strength, reboiler heat duty and gas flow rate, were kept constant. In order to calculate the capital investment savings at a reduced packing height, an economic evaluation was carried out for the full scale capture plant. The capital and operation costs were estimated for the standard solvent at a full packing height and compared to the promoted solvent at a reduced packing height. The Aspen Plus® simulation model developed in the previous chapter was used for this purpose. The cost estimation was carried out with the “Calculator” tool located under Flowsheeting Options.

The step between equipment sizing and costing was based on the well-established modular cost estimation method developed by Guthrie (Gut69) that was later on reviewed by Biegler (Bie99). The modular cost estimation method was initiated by calculating the equipment bare cost *BC*. Further, the cost component estimation within the capital investment expenditures and operating and maintenance costs were all proportional to the *BC*. The proportion was established by empirical percentage factors, which Guthrie correlated by considering the costs of about 40 industrial chemical plants. His modular cost estimation method has an accuracy of 25 to 40%, which was sufficient for the preliminary design of the carbon capture plant. The Guthrie equipment sizing and costing method was designated only to full scale chemical plants. Therefore, the pilot plant was up-scaled to commercial dimensions. The equipment capacities and operating variables were adapted to fit the coal-fired flue gas conditions of a reference example used in the doctor thesis of M. Abu Zahra (Abu09). Both in the simulation and cost estimation of the commercial plant, the CO_2 compression stage was also included. The capital investment savings were first estimated for the base case and the promoted solvent under the standard operating conditions.

Furthermore, the influence of the utility costs on the operating variable design was studied by considering two different scenarios. In the first scenario, carbon dioxide would be removed from a coal-fired power plant operating in Middle East, where the low steam and electricity costs cause the capital investment expenditure to play the major role in the plant economy. In the other scenario, the capture plant was to be built in Europe, where the focus was directed to reducing the energy consumption within the carbon capture process.

Due to confidentiality regulations, the entire economic evaluation results are expressed in relative units. The reference values (100%) were established for the base case, i.e. standard CCS+ solvent at a full packing height. Some technical data required for the cost calculation has been provided from the (Sie10/13) source.

7.1. Modular Cost Estimation

The capital investment expenditure (CAPEX) are the fixed cost that finances the engineering, procurement, construction and startup of the capture plant. The operation and maintenance expenditure (OPEX) are the annual cost that finances the capture plant's working expenses. In Guthrie's modular cost estimation method, first the equipment bare costs are calculated based on the capacity or size of each unit (Figure 2.6). The rest of the investment costs as well as the operation and maintenance *O&M* costs are proportional to the total equipment bare costs. Finally the utility costs were estimated from the electricity and steam consumption obtained from the simulation.

7.1.1. General Bare Costs

In the modular cost estimation method used in this thesis, first the equipment bare costs *C* were calculated by a nonlinear power law expression (Equation 7.1).

$$C = C_0 \cdot \left(\frac{S}{S_0} \right)^{\alpha} \tag{7.1}$$

The equipment bare costs were calculated by multiplying the component reference cost C_0 and a scaling factor. The scaling factor was the relationship between the capacity of the component *S* and the reference case capacity S_0. The capacity relation was exponentially scaled by α ($\alpha < 1$). The nonlinear variation of the equipment costs is known as an economy of scale, where incremental costs decrease with larger capacities (Bie99). Table 7.1 gives an overview of the scaling factors of different types of equipment. The common values for the reference case costs and capacities, as well as for the index can be found in Table E.1 of Appendix E.

Table 7.1. Scaling factor for the different equipment components in the capture plant

Equipment	Scaling factor	Units	Factor
Blower / Pumps / Compressor	Power	W	$\left(\frac{P}{P_0} \right)^{\alpha}$
Cross Heat Exchanger / Coolers / Reboiler / Condenser	Area	m^2	$\left(\frac{A}{A_0} \right)^{\alpha}$
Absorber / Desorber / Direct Contact Cooler / Piping	Height, Diameter	m	$\left(\frac{d}{d_0} \right)^{\alpha} \cdot \left(\frac{h}{h_0} \right)^{\beta}$

Once the costs were calculated for each of the capture process components, a series of scalars were included in the equation (7.2) to make the final estimation adjustments:

- The material and pressure factor *MPF* was developed empirically to evaluate particular properties of the equipment beyond the standard layout. The *MPF* accounted for special construction materials and high pressures.
- The module factor *MF* implied the extra costs for installation, piping, labor, shipping, taxes and supervision. The *MF* and *MPF* values of the capture plant components are presented in Table E.2 of Appendix E.
- The update factor *UF* compensated the price increase over the years due to inflation. It was defined as the relationship between the present and the base cost index. The yearly cost index variation has been documented in the *Chemical Engineering* magazine. With a base cost index of 115.0 (1968) and present cost index of 585.7 (NSTU), the update factor equaled 5.1. The high *UF* might have caused inaccuracies in the final cost calculation of the capture plant components. Nevertheless, the goal of the economic evaluation was to establish a first preliminary comparison between the standard and promoted solvent, for which the cost precision is of relative importance.

To sum up, all three scalars transform the equipment bare costs into the updated modular bare costs *UMBC*:

Uninstalled cost = *(BC) x (MPF)*

Installation = *(BC) x (MF) – (BC) = BC x (MF - 1)* (calculated in a carbon steel basis)

Total installed cost = Uninstalled cost + Installation = *BC x (MPF + MF - 1)*

$$UBMC = UF \cdot BC \cdot (MPF + MF - 1) \tag{7.2}$$

7.1.2. Equipment specifications

a) Columns

The costs of the absorber, desorber and flue gas cooler were split into the structured packing and the pressure vessel. The sump and column head volume was independent from the packing height. It was fixed to a constant value of 9161 m^3 (Sie10/13). The packing costs were fixed at a rate of 4000 €/m^3. The packing height had a greater influence on the column's bare cost than the vessel size.

b) Heat Exchangers

The heat transfer area was the scaling factor used to calculate the bare costs of the reboiler, condenser, cross heat exchanger, lean solvent pre-cooler and the cooling water cooler. The area was the relation between the transferred heat *Q* and the heat transfer coefficient *U* times the hot-cold log mean temperature difference ΔTln (7.3). The cooling water cold temperature was fixed at 19 °C and the hot temperature at 29 °C (Sie10/13).

$$A = \frac{Q}{U \cdot \Delta T\, ln} \tag{7.3}$$

The heat transfer coefficients used for each component are summarised in Table 7.2.

Table 7.2. Heat transfer unit specifications (Sie10/13; VDIA)

Component	Heat Transfer Unit, kW/(m^2·K)
Reboiler	1.0
Condenser	0.6
Cross Heat Exchanger	3.7
Lean Solvent Pre-Cooler	3.0
Cooling Water Cooler	3.0

c) Steam and Condensate Piping

The steam and condensate piping costs were estimated based on the piping inner diameter and total length. First, the pipeline cross sectional area A_p was calculated by dividing the flow rate m obtained from the simulation by the fluid density ρ and the fluid velocity v (7.4). The vapour steam velocity was established at 50 m/s and the condensate at 2 m/s.

$$A_p = \frac{m}{\rho \cdot v} \tag{7.4}$$

The piping inner diameter d_p was finally estimated by (7.5).

$$d_p = \sqrt{\frac{A_p \cdot 4}{\pi}} \tag{7.5}$$

The total piping length was fixed at 200 m (Sie10/13).

7.1.3. Total Capital Investment

The addition of all the updated modular bare costs for each component produced the total *UMBC*. The majority of the economic evaluation calculation was directly or indirectly based on this value. The fixed capital investment *FCI* was divided into the direct costs, which considered the infrastructure, contingency and fees of the carbon capture plant; the indirect costs, which accounted for the engineering and construction; and the CO_2 compression cost. The *FCI* cost elements were estimated as a percentage from the total UMBC. The total capital investment *TCI*, was calculated by adding the total *UMBC* and the *FCI*, as well as, the working investment, the first CCS^+ solvent fill-up and construction insurance. All costs were calculated as a percentage of the *UMBC*. The percentage factors established by Guthrie are all summarised in Tables E.3 and E.4 of Appendix E.

7.1.4. Operation & Maintenance Costs

The operation and maintenance cost excluding the utilities: steam and electricity expenses, were estimated according to Guthrie's cost estimation method as a percentage from the *FCI*. The percentage factors are tabulated in Table E.5 of Appendix E. Only the solvent and promoter makeup and utility costs were calculated separately. A solvent makeup factor of 1.5 kg solvent per separated ton of carbon dioxide was taken from Abu Zahra's work (Abu09). The promoter cost was set at 20000 €/ton (ali12) and the solvent cost at 2700 €/ton (Sie10/13). The final cost of the promoted CCS^{+} solvent with 0.1 wt-% PROM-1 was established at 2720 €/ton. At 7500 annual operating hours, and $3.66 \cdot 10^5$ tons of CO_2 separated per hour, the final solvent makeup costs were rounded to 1.1 M€/y Since the economic evaluation framework was placed in two different scenarios, namely Europe and Middle East, the utility costs varied from one region to the other. The reference values of the utility costs in each region are summarised in Table 7.3. The data were taken from a Siemens intern source and the "Bundesamt für Wirtschaft und Technologie" (BWT).

Table 7.3. Fixed utility prices (Sie10/13; BWT)

Location	Electricity, €/MWh	Steam, €/ton
Europe	100	50
Middle East	7	30

7.2. Full Scale Capture Plant Parameters

The design parameters selected to represent the full scale plant in this economic evaluation were taken from a reference case by Abu Zahra et al. (Abu09).The settings corresponded to a carbon capture plant retrofitted to a coal-fired 600 MW_e power plant. The higher flue gas flow rate required the up-scaling of the absorber and desorber diameter. The new diameter was designed to fit the capacity factor and the new flue gas flow rate. The vapour capacity factor was set up to 2.1 in the absorber and 1.8 in the desorber. Although these values significantly exceed the pilot plant (Table 5.1), they were adequate for operating with industrial column packing types. The solvent flow rate was fitted to reach a trickling density in the absorber of 30 $m^3/(m^2 \cdot h)$. The liquid to gas ratio remained approximately the same as in the pilot plant test runs. Due to a higher carbon dioxide feed and a higher solvent rate, the reboiler heat duty was adjusted, so the capture rate reached 90% in the base case. The process parameters are summarised in Table 7.4. The packing height was the varied parameter in the economic evaluation. The base case settings corresponded to the same full packing height as in the pilot plant. The promoted solvent case was simulated with the same reduced packing height values determined at a high reboiler duty (Table 6.5). In the optimised scenarios, the packing height was either reduced or increased, to respectively decrease the capital investment expenditures or lower the reboiler energy demand. The correlation factors *IAF* and *HTF* were those established in for the high reboiler heat duty (Table 6.3).

Table 7.4. Full scale capture plant design parameters

Full scale parameters	Units	Value
Flue gas flow rate	[kg/s]	616
Vapour capacity factor (Absorber)	$[Pa^{0.5}]$	2.1
Vapour capacity factor (Desorber)	$[Pa^{0.5}]$	1.8
Trickling density (Absorber)	$[m^3/(m^2 \cdot h)]$	30
Diameter (Absorber)	[m]	20
Diameter (Desorber)	[m]	18
CO_2 product flow	[kg/s]	102
CCS^+ concentration	[%]	24.5
Solvent flow rate	[kg/s]	3667

7.3. Simulation Results and Discussion

The economic evaluation of the promoted carbon capture process was focused on determining the cost savings caused by a reduced packing height. Hence, the pilot plant operating conditions were up-scaled to a full scale capture plant and simulated in Aspen Plus®. The modular cost estimation method factors were inserted in the “Cost” tool. This application permits the writing of the simulation results in an MS Excel worksheet, where the percentage factors and costing equations were already correlated.

7.3.1. Cost Savings with the Promoted Solvent

The base case with CCS⁺ solvent and a full packing height was simulated first. The capital investment and maintenance costs were calculated. These costs were set as the base case. Afterwards the packing height was reduced according to the same values as in Table 6.5. The mass transfer model correlation factors were modified to match the promoted CCS⁺ solvent values (see Table 6.3). A first fill and a full annual refill of the promoter were included in the fixed and variable costs respectively.

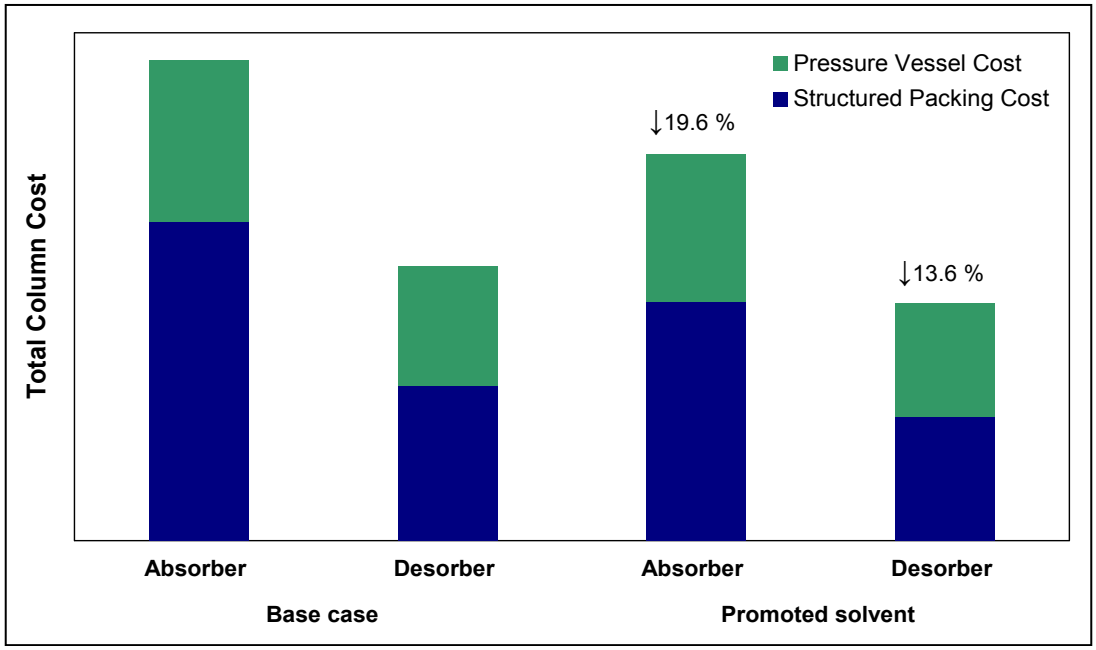

Figure 7.1. Total column cost reduction for the promoted solvent

As it is observed in Figure 7.1, the structured packing costs had a bigger influence on the total column costs than the pressure vessel. The pressure vessel costs were not reduced significantly by the promoted solvent. Considering only the bare costs, the promoted solvent achieved a reduction of 19.6% in the absorber and 13.6% in the desorber. The cost savings progression in the modular cost estimation method is further presented in Table 7.5. The promoted case ended up having 9.5% lower total investment costs than the base case.

Table 7.5. Investment cost savings for the promoted solvent

	Promoted Solvent Cost Savings, %
Total Column Costs	17.4
UBMC	11.8
FCI, TCI	**9.5**

The *O&M* costs decreased 1.7% for the promoted case (Table 7.6). In the calculation process, the steam and electricity prices were set to be those from Europe (see Table 7.3). This fact was irrelevant since the reboiler energy demand and solvent flow rate remained the same for the base and promoted solvent cases. The outcome from the economic evaluation is that it is possible to reduce about 10% of the total capital investment expenditures of a full scale carbon capture plant by adding PROM-1 to the solvent.

Table 7.6. O&M cost savings for the promoted solvent

	Promoted Solvent Cost Savings, %
OMC	9.6
Electricity	0.0
Steam	0.6
O&M	**1.7**

7.3.2. Cost Savings in CAPEX and OPEX Optimised Designs

After calculating the full scale cost savings due to the promoter addition, it was meant to modify the boundary conditions to investigate the promoted solvent in other operative scenarios. The costs of the utilities may be a limiting factor when it comes to designing the carbon capture plant equipment size and operation. In oil & gas producing countries where fuel is less expensive; it is better to increase the reboiler heat duty for two reasons: so that a faster absorption kinetic requires lower contact area and a higher working capacity reduces the solvent flow rate. This case was referred to in this thesis as “C-optimised”. In countries where fuel is more expensive

and the concern towards carbon emissions higher; it may be better to invest more capital in constructing larger equipment (higher packing height and residence times) so that the CO_2-AAS chemical system can operate closer to equilibrium and therefore reduce the energy demand. This case was referred to in this thesis as “O-optimised”. The utility costs for both scenarios for the O&M cost estimation were presented in Table 7.3.

❖ Promoted C-optimised

There has been previous evidence in this work that the capture performance of the carbon capture process was mainly influenced either by the reboiler heat duty or by the column packing height. The C-optimised settings focused on reducing the equipment size, since the low steam and utility costs made the process CAPEX-limited. While maintaining the capture rate constant, a sensitivity analysis was carried out in Aspen Plus® to estimate the amount of reboiler heat duty that had to be extra introduced in the process to compensate the loss of packing height. The promoted solvent case served as the starting point. First the desorber packing height was decreased from 80 to 50%. This required an 8% increase in the reboiler heat duty. Afterwards, the absorber packing height was reduced to 64%, which increased the reboiler heat duty further up to 21% more than the base case. In his diploma thesis, M. Wiese (Wie12) explained that a further decrease of the absorber packing height would result in a further exponential increase in the reboiler heat duty, which is economically not feasible. The results of this analysis are expressed in Table 7.7.

Table 7.7. Sensitivity analysis to determine the optimum CAPEX settings, %

	Absorber	**Desorber**	**Reboiler heat duty**
Base case →	100	100	100
Promoted solvent case →	75	80	100
	75	50	108
Promoted C-optimised case→	64	50	121
Promoted C-optimised reduction			**Reboiler heat duty: -21.0%** **Total packing height: 42.2%**

The C-optimised case achieved about the half of the total packing height compared to the base case. The decrease in the packing height led to exponential increments in the reboiler heat duty. This will surely save a big amount of capital investment expenditures; although as seen before, the absorber and desorber cost savings would eventually be evened out with by the rest of the cost estimation components. The comparison between the promoted C-optimised and the base case costs is presented in Figure 7.2. Considering only the bare costs, the C-optimised absorber costs were reduced by 28.2% and the desorber costs by 34.1%.

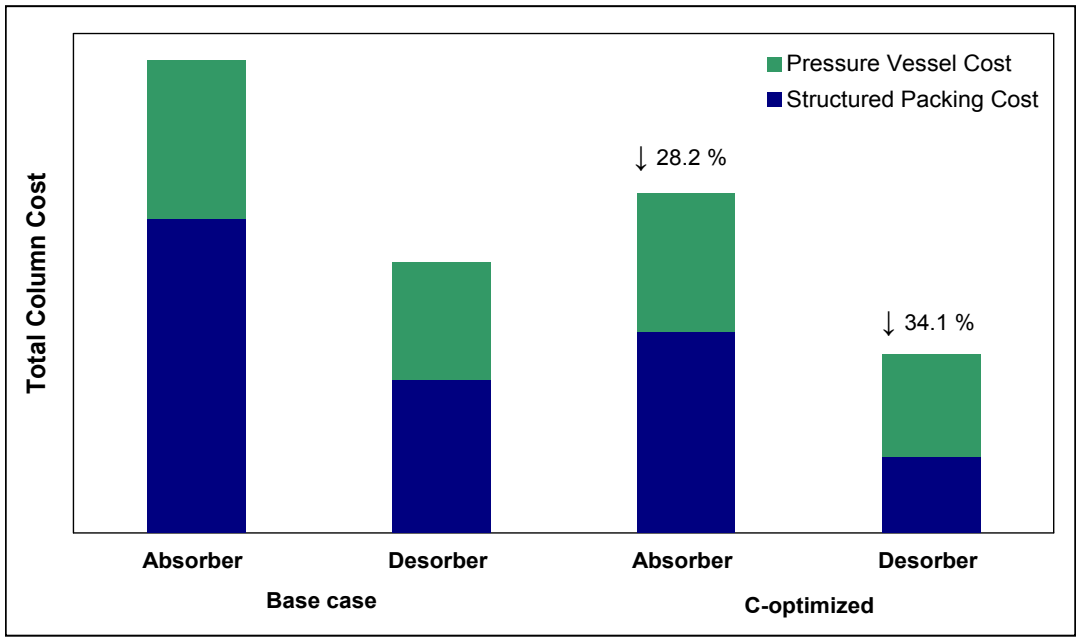

Figure 7.2. Total column cost reduction for promoted solvent with C-optimised settings

The total costs savings for the absorber and desorber added up to 30.3%. As in the previous figure, the pressure vessel costs remained the same, for the full and reduced packing height. The further estimation of the investment savings is presented in Table 7.8. The promoted C-optimised case ended up reducing the total capital investment expenditures by 14.9%.

Table 7.8. Investment cost savings for the promoted solvent with C-optimised settings

	C-optimised Cost Savings, %
Total Column Costs	30.3
UBMC	18.4
FCI, TCI	14.9

Moreover, the O&M costs for the C-optimised promoted case are presented in Table 7.9. Although the reboiler heat duty for the reduced packing height was increased by 21%, due to lower OMC costs, the yearly operation and maintenance of the capture plant was reduced by 2.6%. The fact that a higher energy demand increases the carbon dioxide emissions has been neglected in this calculation. The low utility prices in the Middle East render a high importance of the investment costs. It has been demonstrated in the economic evaluation that it is worth to operate the capture plant with a higher steam demand in places where it is less expensive, but therefore significantly reduce the fixed costs. In the end, both fixed and variable costs will be lowered.

Table 7.9. O&M cost savings for the promoted solvent with C-optimised settings

	C-optimised Cost Savings, %
OMC	14.9
Electricity	0.0
Steam	-20.4
O&M	**2.6**

❖ Promoted O-optimised

In Europe, the prices of steam and electricity are higher than in the oil & gas producing regions. There is a higher interest in lowering the energy demand for carbon capture in this scenario. The determining factor to reduce steam consumption is to increase the absorption capacity. In general, the capture process that achieves the lowest specific energy demand with feasible invest costs will be the one which will succeed at a commercial scale in the future. For this purpose, the base case operating conditions and settings were varied. The strategy to reduce steam demand was to increase the packing height. This method is only effective if the rich solvent has not reached the equilibrium rich loading at the bottom of the absorber. For this purpose, a sensitivity analysis was carried out in Aspen Plus®, to determine the absorber packing height at which the rich loading reaches the equilibrium.

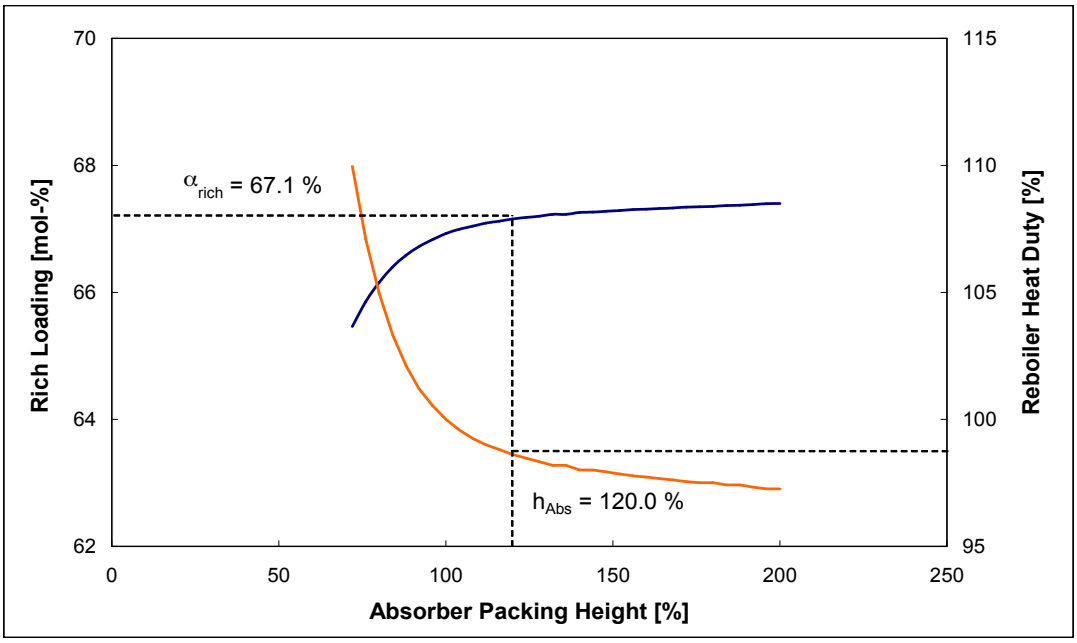

Figure 7.3 Decrease of the reboiler heat duty with the packing height (Wie12)

In Figure 7.3, it can be observed how by increasing the packing height in the absorber, the rich solvent loading approaches a constant value, which at the same time reduces the reboiler heat duty. Both curves tend to move towards an equilibrium region where the packing height increments have little effect on the rich solvent loading and the reboiler heat duty. The selected packing height defined as O-optimised is that at which the loading increment curve changes to be linear. It was assumed that at this packing height, a rich loading very close to equilibrium is reached, so that from this point on the system is not any more kinetic-limited. The reboiler heat duty was not significantly decreased. It has already been demonstrated that the promoter does not enhance the absorption capacity, but only the gas uptake velocity.

The optimum solvent flow rate may have been altered due to an increase in packing height. Hence, a sensitivity analysis was carried out to determine the operating point at which the energy demand was lowest (Figure 7.4). The values expressed are still relative to the base case.

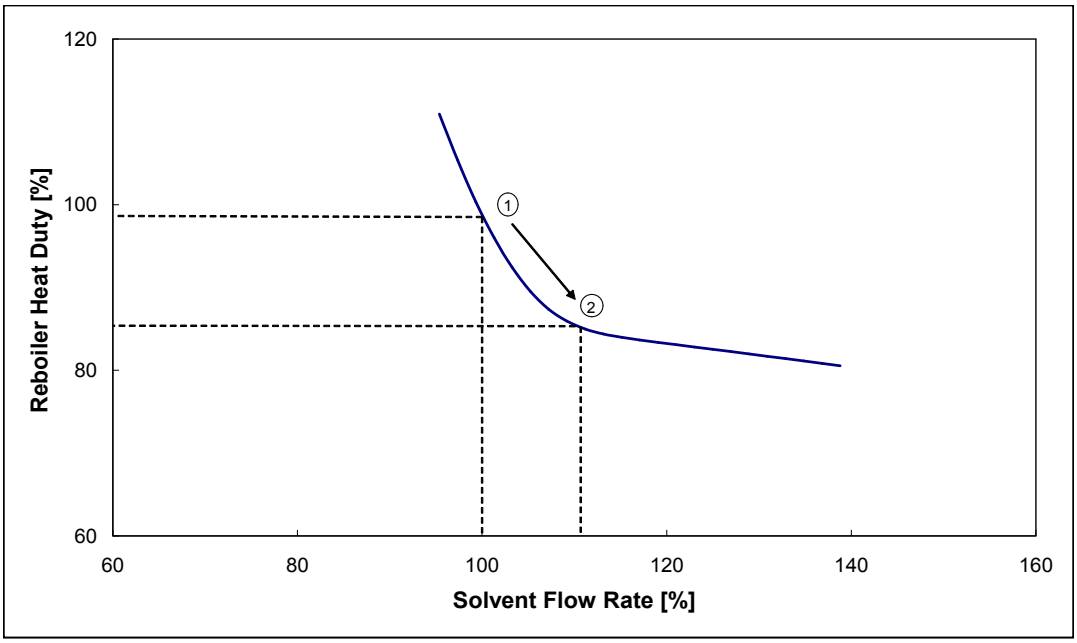

Figure 7.4. Decrease of reboiler heat duty with increasing solvent flow rate (Wie12)

The starting point (1) corresponded to the promoted solvent case with 120% packing height. The flow rate increase lowered the latent heat of vaporisation significantly. The optimal operating point (2) was selected at the ending of the curve region. Compared to the energy curves shown in Figures 4.1, 4.2 and 4.6; the simulation trend continues decreasing at flow rates higher than 110.5%. In his thesis, Wiese (Wie12) explains in his thesis that at these rate values Aspen Plus® has convergence problems since it approaches flooding conditions and the simulation results were therefore unreliable. The modified operating parameters for the promoted O-optimised case are presented in Table 7.10.

Table 7.10. Operating conditions base vs. promoted O-optimised case

Case	Base case	Promoted O-optimised case
Absorber packing height, [%]	100	120.0
Solvent flow rate, [%]	100	110.5
Reboiler heat duty, [%]	100	85.0

A lower reboiler heat duty required an increased packing height and solvent flow rate. The heat exchanger sizes and electricity demand of the pumps were therefore increased. Since the desorber height did not demonstrate a strong influence on the capture performance, the same packing height was maintained as for the promoted solvent case. The absorber and desorber bare cost results of the O-optimised case are depicted in Figure 7.5.

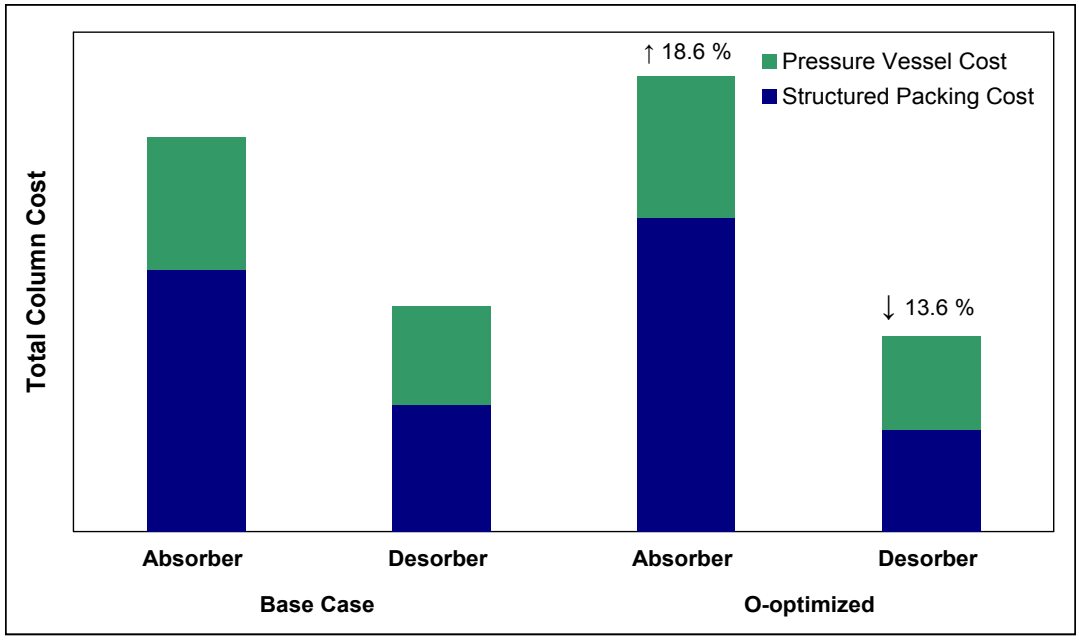

Figure 7.5. Total column cost reduction for promoted solvent with O-optimised settings

The absorber bare costs increased by 18.6% whereas the desorber costs decreased by 13.6% (same as in the promoted case). The further cost factors in the total capital investment expenditures are summarised in Table 7.11. The increase in the absorber packing costs was nearly compensated by the desorber reduction, levelling out a CAPEX increase of 1.5%.

Table 7.11. Investment cost savings for the promoted solvent with O-optimised settings

	O-optimised Cost Savings, %
Total Column Costs	-6.9
UBMC	-1.9
FCI, TCI	-1.5

The lower steam demand had a significant repercussion on the steam costs (Table 7.12). The steam savings were in part compensated with a marginal increase in the OMC and electricity costs. The OMC increase was due to higher bare module costs. The increase in the electricity consumption of the pumps was caused by a higher solvent flow rate. The overall O&M cost reduction resulted in 11.1%.

Table 7.12. O&M cost savings for the promoted solvent with O-optimised settings

	Promoted Solvent Cost Savings, %
OMC	-1.5
Electricity	-0.6
Steam	15.0
O&M	11.1

The final results of the economic evaluation are all summarised in Table 7.13.

Table 7.13. Final simulation results

[%]	Base case	Promoted CCS^{+} solvent		
		Standard	C-optimised	O-optimised
Absorber height	100.0	75.0	64.0	120.0
Desorber height	100.0	80.0	50.0	80.0
Total packing height	100.0	76.9	57.0	100.0
Solvent flow rate	100.0	100.0	100.0	110.5
Reboiler heat duty	100.0	100.0	121.0	85.0
TCI	100.0	90.5	85.1	101.5
O&M	100.0	98.3	97.4	89.9

7.4. Conclusion

The simulation results rendered the following conclusions:

- Under the full-scale PostCap^{TM} operating parameters with coal fired flue gas conditions, the CCS^{+} solvent promoted with 0.1 wt-% PROM-1 obtained a total column packing height reduction of 17.4%. Based on the modular cost calculation method from Guthrie, the investment costs savings summed up to 9.5%. The *O&M* expenses were also decreased slightly due to the lower *OMC* value.

- In regions where the utility (steam & electricity) prices are less expensive, such as in the Middle East, the packing height could be reduced further by increasing the reboiler heat duty. Combined with the promoted CCS^{+} solvent, the C-optimised promoted solvent achieved a packing height reduction by 43.0% and investment costs savings of 14.9%. Although the steam consumption increased by 21.0%, the *O&M* expenses were also decreased due to lower *OMC*.

- In regions where the utility prices as well as the concern towards carbon dioxide emissions are high, such as in Europe, higher packing height is meant to improve the absorption capacity and lower the energy demand. Nevertheless, it was evidenced that the effect of the promoted solvent on the reboiler heat duty was minimal, due to the fact that the capture performance was equilibrium-limited. Thus, the solvent flow rate was increased to reduce the latent heat of vaporisation. The new O-optimised operating parameters reduced the reboiler heat duty by 23.3%, which was translated in *O&M* costs savings of 11.1%. The lower desorber packing height evened out the total capital investment to be higher by only 1.5% compared to the base case.

8. CONCLUSION AND OUTLOOK

The main contributors to the cost of carbon capture are the size of the absorption equipment and the high energy demand for solvent regeneration. An improvement of the solvent's absorption efficiency, which contemplates both the absorption reaction kinetics and uptake capacity, is therefore the key factor to reducing overall costs. To reduce steam consumption in post combustion CO_2 capture amine plants, the rich-lean loading range is operated close to the thermodynamic equilibrium. At carbon loadings higher than 0.5 mol CO_2 per mol amine, the Siemens amino acid solvent CCS$^+$ has similar absorption reaction kinetics as a tertiary amine. In this loading range the fast carbamate reaction does not influence the gas diffusion rate through the liquid phase. The two main reactions that take place are the carbamate hydrolysis and bicarbonate formation. Both pathways belong to the slow reaction regime and are responsible for the high packing height requirements in the absorption and desorption columns.

In order to maintain a low reboiler heat duty and at the same time reduce the high investment costs related to high packed towers, the absorption reaction kinetics were enhanced by the addition of a rate promoter. Taking into consideration the requirements of carbon capture from power generation flue gases, besides low cost, it was the focus of this work to avoid any additional environmental impact. Therefore, the compound which best suited the amino acid solvent CCS$^+$ and the PostCap^{TM} process was that which possessed zero toxicity and had a catalytic effect on the reaction with carbon dioxide under optimal operation conditions. From a group of potential promoters, the chemical compound named PROM-1 was selected after doing different absorption reaction kinetic measurements in the laboratory. It was demonstrated that the promoter had a catalytic effect in the CO_2 absorption with CCS$^+$, especially at high CO_2 loadings. Most important of all, PROM-1 scored top marks in the environmental ranking list elaborated with all of the potential candidates. It was further discovered that PROM-1 had a catalytic effect in CO_2 absorption with other amino acid salt solvents with different chemical structure than AAS$^+$. It was deduced from the experimental results that the promoter acted as a catalyst of the carbon dioxide hydration reaction. Solubility measurements pointed out that the optimal promoter concentration to avoid precipitation under process operation temperature conditions was 0.1 wt-%.

The CCS$^+$ solvent promoted with PROM-1 was further tested in the laboratory mini plant. Carbon dioxide was captured from a synthetic flue gas stream with an experimental absorber-desorber configuration. A wide range of reboiler specific energy demand range was investigated by varying the mass flow rate and the absorber packing height. The performance of the standard CCS$^+$ solvent was compared to the promoted case at the same amine concentration. At energy optimum operation conditions, the promoted CCS$^+$ solvent required 17% less packing height in order to achieve the same capture performance. This result was very promising for studying the cost reduction potential of the inorganic additive.

The investigation was continued in a pilot scale plant retrofitted to the flue gas exhaust of a hard coal fired power plant. Here the energy input in the reboiler, the liquid and the gas flow rates were maintained constant and the performance of the standard CCS$^+$ solvent was compared to the promoted solvent. In all the tested operation points, the promoted solvent achieved a higher capture rate than the standard solvent. A total packing height reduction of 25% was possible for the promoted AAS$^+$ solvent at the same capture performance. The mini plant tests did not render such a high result as the pilot plant since only the absorber packing height was varied.

The cost reduction potential of the PROM-1 promoter had been demonstrated in two different testing plants. The exact packing height that could be reduced in a full scale plant along with the cost savings it would imply was calculated by adapting a simulation model to the promoted AAS$^+$ solvent by using the Aspen Plus® industrial process simulation program. In the development of the simulation model, an enhanced interfacial area factor was used to reproduce the faster absorption reaction kinetics of the promoted CCS$^+$ solvent. The packing height reduction was estimated considering the same capture rate, solvent flow and reboiler heat duty for the standard and promoted solvent. A good consistency between experiment and simulation produced an average relative error of 0.87%.A packing height reduction of 22.5% was estimated for the promoted solvent at 86.7% capture rate. The packing height potential reduction increased with a decreasing performance, being a 43.5% reduction possible for 79.3% capture rate.

The simulation model served as the basis for the final economic evaluation. In this study three cases were contemplated: the standard case, in which the cost reduction was estimated for a full scale capture plant; the C-optimised case, in which low utility costs moved the focus towards reducing equipment size at the cost of increasing steam consumption; and the O-optimised case, in which high utility costs and emission concern, required the lowest achievable steam demand. Under standard operating conditions, the total investment savings summed up to 9.5%. A lower OMC brought down the *O&M* expenses 1.7%. The C-optimised settings achieved investment savings of 14.9% and *O&M* savings of 2.6%. The O-optimised standards lowered the *O&M* expenses by 11.1% at the expense of an investment increase of 1.5%. The promoted solvent performed best at reducing the investment costs of a full scale PCC amine plant. In countries where the utility costs are low, the investment savings can be further increased if the energy input is marginally increased, such as in the C-optimised case.

Future work continuing the investigation line of this thesis must focus on researching new chemical catalysts, especially inorganic compounds, with similar chemical properties as PROM-1. The absorption rate measuring techniques and testing procedures in the mini and pilot plant described in this work are adequate to undertake an extended promoter screening procedure. Furthermore, it is also necessary to investigate the benefits of combining absorption rate promoters with energy demand improved process layouts such as the split loop configuration. The investment savings due to enhanced absorption reaction kinetics may in this case be combined with lower reboiler heat duties, for an overall process cost reduction purpose. To avoid promoter loss in the amine process, the process of immobilising the promoter on the structured packing is a possible solution and ought to be tested at a pilot scale.

9. REFERENCES

(Abu09) Abu Zhara, M., Carbon Dioxide Capture from Flue Gas – Development and Evaluation of Existing and Novel Process Concepts, Ph.D. Thesis, University of Delft, Netherlands, 2009.

(Alv12) Alvis, R.S., Hatcher, N.A., Weiland, R.H. CO_2 Removal from Syngas Using Piperazine Activated MDEA and Potassium Dimethyl Glycinate, Proceedings of the Nitrogen + Syngas Conference in Athens, Greece, February 20-23, 2012.

(ali12) www.alibaba.com (available on February 2012)

(And11) Andrés Kuettel, D., Fischer, B., Joh, R., Kinzl, M., Schneider, R., Schramm, H. Carbon Capture with Low Environmental Impact: Siemens PostCap™ Technology, Proceedings of the 2nd ICEPE: Efficient Carbon Capture for Coal Plants Conference in Frankfurt am Main, Germany, June 20-22, 2011.

(And12) Andrés Kuettel, D., Fischer, B. Removal of Acidic Gases and Metal Ion Contaminants with PostCap™ Technology, Proceedings of the 11th International Conference on Greenhouse Gas Control Technologies in Kyoto, Japan, November 18-22, 2012.

(Aspe09) Aspen Tech, "Fortune 500 E&C Firm Helps Customers Reduce CO_2 Emissions and Lower Costs", Aspen Technology, 2009.

(Aspr11) Asprion, N., Clausen, I., Lichtfers, U., Wagner, R. Carbon Dioxide Absorbent Requiring Less Regeneration Energy, U.S. Patent 8,034,166.

(Ast64) Astarita, G., Marrucci, G., Gioia, F. The Influence of Carbonation Ratio and Total Amine Concentration on Carbon Dioxide Absorption in Aqueous Monoethanolamine Solutions, Chemical Engineering Science, 1964, Vol. 19, pp. 95-103.

(Ast67) Astarita, G. Mass Transfer with Chemical Absorption, Elsevier, 1967.

(Ast81) Astarita, G., Savage, D., Longo, J. Promotion of CO_2 Mass Transfer in Carbonate Solutions, Chemical Engineering Science, 1981, No. 36, pp. 581-588.

(Ast83) Astarita, G., Savage, D.W., Bisio, A. Gas Treating with Chemical Solvents, John Wiley and Sons Inc., 1983.

(Bäh35) Bähr, H., Mengdehl, H. Separation of Hydrogen Sulfide from Gaseous Mixtures Containing the Same, U.S. Patent 1,990,217.

(Bäh38) Bähr, H., Mengdehl, H., Wenzel, W. Washing Out of Weak Gaseous Acids from Gases Containing the Same, U.S. Patent 2,137,602.

(Beh12) Behr, P., Maun, A., Tunnat, A., Gönner, K. Optimization of CO_2 Capture from Flue Gas with Promoted Potassium Carbonate Solutions, Proceedings of the 11th International Conference on Greenhouse Gas Control Technologies in Kyoto, Japan, November 18-22, 2012.

(bel14) www.bellona.org/ccs/ccs-news-events/news (available in January 2014)

(Ben59) Benson, H.E., Field, J.H. Method for Separating CO_2 and H_2S from Gas Mixtures, U.S. Patent 2,886,405.

(Bie99) Biegler, L.T., Grossmann, I.E. Westerberg, A.W. Systematic Methods of Chemical Process Design, Prentice Hall PTR, 1999.

(Boc10) Bock, F.J. Zur Entfernung von CO_2 aus Prozessgasgemischen – ein Überblick aus sicherheitstechnischen Sicht, TÜV Nachrichten, 2010, Nr. 11/12, pp. 27-36.

(Bot38) Bottoms, R. Process for Separating Acidic Gases, U.S. Patent 1,783,901.

(Bow02) Bowler, R., Gysens, S., Hartney, L., Rauch, S., Midtling, J. Increased Medication Use in a Community Environmentally Exposed to Chemicals, Industrial Health, 2002, No. 40, pp. 335-344.

(Bra85) Bravo J.L., Rocha J.A., Fair, J.R. Pressure-drop in Structured Packing, Hydrocarbon Process, 1985, No. 65, pp. 45-49.

(Bra92) Bravo J.L., Rocha J.A., Fair, J.R. A Comprehensive Model in the Performance of Columns Containing Structured Packing, Distillation and Absorption, Institution of Chemical Engineers Symposium Series, 1992, Vol.1, No. 128.

(Bro09) Brouwer, J.P., Feron, P.H.M., Asbroek, N.A.M. “Amino Acid Salts for CO_2 Capture from Flue Gases”, TNO Science & Industry, 2009.

(BWT) Bundesamt für Wirtschaft und Technologie (www.bmwi.de)

(Cap68) Caplow, M. Kinetics of Carbamate Formation and Breakdown, Journal of the American Chemical Society, 1968, Vol. 90, No. 24, pp. 6795-6803.

(Chak88) Chakraborty, A.K., Astarita, G., Bischoff, K.B. and Damewood, J.R., Jr. Molecular Orbital Approach to Substituent Effects inAmine-CO_2 Interactions., Journal of American Chemical Society, Vol. 110, No. 21, pp. 6947-6954.

(Chap99) Chapel, D., Ernest, J., Mariz, C. Recovery of CO_2 from Flue Gases: Commercial Trends, Proceedings of the Canadian Society of Chemical Engineers Annual Meeting in Saskatchewan, Canada, October 4-6, 1999.

(Cul04) Cullinane, J.T., Oyenekan, B.A., Lu, J., Rochelle, G.T., Aqueous Piperazine / Potassium Carbonate for Enhanced CO_2 Capture, Proceedings of the 7th International Conference on Greenhouse Gas Control Technologies, Vancouver, Canada, September 5-9, 2004.

(Cul05) Cullinane, J.T. Thermodynamics and Kinetics of Aqueous Piperazine with Potassium Carbonate for Carbon Dioxide Absorption, Ph.D. Thesis, University of Austin Texas, U.S., 2005.

(Danc50) Danckwerts, P.V., Absorption by Simultaneous Diffusion and Chemical Reaction. Transactions of the Faraday Society, 1950, Vol. 46, pp. 300-304.

(Dang03) Dang, H.Y., Rochelle, G.T., CO_2 Absorption Rate and Solubility in Monoethanolamine / Piperazine / Water, Separation Science and Technology, 2003, Vol. 38, No. 2, pp. 337-357.

(Ech97) Echt, W. “Chemical Solvent-Based Processes for Acid Gas Removal in Gasification Applications”, Dow, 1997.

(Eds58) Edsall, J., Wyman, J. Carbon dioxide and Carbonic Acid, Biophysical Chemistry Vol. I, Ch. 10, pp. 550-590, Academic Press Inc., 1958.

(Eid09) Eide Haugmo, I. Environmental Impact of Amines, Energy Procedia, 2009, Vol. 1, pp. 1297-1304.

(End11) Endo, K., Nguyen, Q.S., Kentish, S.E., Stevens, G.W. The Effect of Boric Acid on the Vapour Liquid Equilibrium of Aqueous Potassium Carbonate, Fluid Phase Equilibria, Vol. 309, pp. 109-113.

(Ewi80) Ewing, S.P., Lockshon, D., Jencks, W.P. Mechanism of Cleavage of Carbamate Anions, Journal of the American Chemical Society, 1980, Vol. 102, No.9, pp. 3072-3084.

(Fau24) Faurholt, C. Studier over Kuldioxid og Kulsyre og over Karbaminater og Karbonater, Ph.D. Thesis, University of Copenhagen, Denmark, 1924.

(Fer01) Feron, P.H.M., Asbroek, N. “New Solvents Based on Amino Acid Salts for CO_2 Capture from Flue Gases”, TNO Environment, Energy and Process Innovation, 2001.

(Fie75) Field, J.H. Separation of CO_2 from Gas Mixtures, U.S. Patent 3,907,969.

(Fis13) Fischer, B. Investigation of the Reactions when Applying Amino acid Salts for Post Combustion Carbon Capture Processes - Degradation Pathways, Environmental and Economic Impact, Ph.D. Thesis, University of Duisburg-Essen, Germany, in press.

(Gho08) Ghosh, U.K., Kentish, S.E., Stevens, G.W. Absorption of Carbon Dioxide into Potassium Carbonate Promoted with Boric Acid, Proceedings of the 9th International Conference on Greenhouse Gas Control Technologies, Washington D.C., U.S., November 16-20, 2008.

(Gia75) Giammarco, G., Giammarco P. Process for the Removal of Carbon Dioxide and/or Hydrogen Sulfide and other Acidic Gases from Gas Mixtures, U.S. Patent 3,897,227.

(Gia84) Giammarco, G., Giammarco P. Absorption of CO_2 and H_2S Utilizing Solutions Containing Two Different Activators, U.S. Patent 4,434,144.

(Gut69) Guthrie, K.M. Data and Techniques for Preliminary Capital Cost Estimating, Chemical Engineering, 1969, Vol. 76, No. 6, pp. 114-122.

(Hig35) Higbie, R., The Rate of Absorption of a Pure Gas into a Still Liquid During Short Periods of Exposure, Transactions of the American Institute of Chemical Engineers, 1935 Vol. 35, pp. 36-60.

(Hoc07) Hockley R., "Aspen RateSep", Aspen Tech Corporate Presentation, 2007.

(Hoo97) Hook, R. An Investigation of Some Sterically Hindered Amines as Potential Carbon Dioxide Scrubbing Compounds, Industrial and Engineering Chemistry, 1997, Vol. 36, pp. 1779-1790.

(IEA09) International Energy Agency (IEA), Technology Roadmap - Carbon Capture and Storage, Paris, France, 2009.

(Joc09) Jockenhoevel T., Schneider R., Rode H., Development of an Economic Post-Combustion Carbon Capture Process, Energy Procedia, 2009.

(Kir04) Kirk-Othmer Encyclopedia of Chemical Technology, 5th Edition, Vol.I, pp. 26-98, John Wiley and Sons Inc., 2004.

(Koh97) Kohl, A.; Nielsen, R., Gas Purification, 5th Edition, Gulf Publishing Company, 1997.

(Kum02) Kumar, P.S. Development and Design of Membrane Gas Absorption Processes, Ph.D. Thesis, University of Twente, Netherlands, 2002.

(Kva05) Kvamsdal, H., Mejdell, T., Steineke, F., Weydahl, T., Aspelund, A., Hoff, K.A., Skouras, S., Barrio, M. Tjelbergodden Power/Methanol - CO Reduction Efforts, SP2 CO_2 Capture and Transport, Technical Report, SINTEF Energy Research Trondheim, ISBN 82-5942762-1.

(Led76) Leder, F., Shrier, A.L., Montclair, N.J. Method and Composition for Removing Acidic Contaminants from Gases, U.S. Patent 3,932,582.

(Mat12) Mathias, P. M., Reddy, S., Smith, A., Afshar, K., A Guide to Evaluate Solvents and Processes for Post-Combustion CO_2 Capture, Proceedings of the 11th International Conference on Greenhouse Gas Control Technologies in Kyoto, Japan, November 18-22, 2012.

(McN67) McNeil, K.M., Danckwerts, P.V. The Absorption of Carbon Dioxide into Aqueous Amine Solutions and the Effects of Catalysis, Transactions of the Institute of Chemical Engineers, 1967, Vol. 45, pp. T32-T49.

(Meld77) Meldon, J.H., Smith, K.A., Colton, C.K. The Effect of Weak Acids upon the Transport of Carbon Dioxide in Alkaline Solutions, Chemical Engineering Science, 1977, Vol. 32, pp. 939-950.

(Men13) Mendez, M. "Achieve Better Designs and Commercial Viability", Aspen Tech's Carbon Capture Modeling, Engineering Collaboration Webinar Series, February 20, 2013

(Mim98) Mimura, T., Shigeru, S., Ijima, M., Mitsuoka, S. Method for the Removal of Carbon Dioxide from Combustion Exhaust Gas, U.S. Patent 5,744,110.

(Mos10) Moser, P., Schmidt, S., Sieder, G., García, H., Stoffregen, T., Rösler, F. Versuchsergebnisse aus der Post Combustion Capture Pilotanlage in Niederaußem, Sichere und nachhaltige Energieversorgung 12-13.10.2010, TU Dresden, Institut für Energietechnik.

(Naz11) Nazarko, J., et al. Einfluss der Betriebsparameter der CO_2 Abtrennung mittels MEA-Wäsche auf den Regenerationsbedarf, Buchbeitrag, Kraftwerkstechnik, Band 3; Neururuppin, TK Verlag Karl-Thome Kozmiensky, 2011, pp. 183-198.

(Not09) Notz, R. CO_2-Abtrennung aus Kraftwerksabgasen mittels Reaktivabsorption, Ph.D. Thesis, University of Stuttgart, Germany, 2009.

(NUST) Norwegian University of Science and Technology (www.ntnu.edu)

(vNie11) van Nierop, E.A., Hormoz, S., House, K.Z., Aziz M.J. Effect of Absorption Enthalpy on Temperature-Swing CO_2 Separation Process Performance, Proceedings of the 9th International Conference on Greenhouse Gas Control Technologies, Washington D.C., U.S., November 16-20, 2008.

(Oex10) Oexmann, J., Kather, A. Minimizing the Regeneration Heat Duty of Post-Combustion CO_2 Capture by Wet Chemical Absorption: The Misguided Focus on Low Heat of Absorption Solvents. International Journal of Greenhouse Gas Control, 2010, No. 4, pp. 36-43.

(Per97) Perry, R., Green, D. Perry's Chemical Engineers' Handbook, 7th Edition, McGraw Hill, 1997.

(Pux11) Puxty, G., A Rational Approach to Amine Mixture Formulation for CO_2Capture Applications, 2nd ICEPE International Conference on Energy Process Engineering, Frankfurt, Germany, 2011.

(Raz12) Razi N., Bolland O., Svendsen H. Review of Design Correlations for CO_2 Absorption into MEA Using Structured Packing, International Journal of Greenhouse Gas Control, 2012.

(Rig89) Riggs, O. L. Jr. Process for Recovering Acidic Gases, U.S. Patent 4,869,884.

(Row11) Rowland, R., Yang, Q., Jackson, P., Attalla, M. Amine Mixtures and the Effect of Additives on the CO_2 Capture Rate, Proceedings of the 10th International Conference on Greenhouse Gas Control Technologies in Amsterdam, Netherlands, September 19-23, 2011.

(Roc01) Rochelle, G.T., Research Needs for CO_2Capture from Flue Gas by Aqueous Absorption / Stripping, US Dept of Energy Report, 2001.

(Rol12) Rolker, J., Thibaut, L., Seiler, M.A. New Chemical System Solution for Acid Gas Removal, Chemie Ingenieur Technik, 2012, Vol. 84, No. 6, pp. 849-858.

(Rou38) Roughton, F., Booth, V. The Catalytic Effect of Buffers on the Reaction $CO_2 + H_2O = H_2CO_3$, Biochemistry Journal, 1938, No. 32, pp. 2049-2069.

(Sak05) Sakwattanapong R., Aroonwilas A., Veawab A. Behavior of Reboiler Heat Duty for CO_2 Capture Plants Using Regenerable Single and Blended Alkanolamines, Industrial and Engineering Chemistry Research, 2005, Vol. 44, No. 12 pp. 4465-4473.

(San92) Sander, M. T., Mariz, C. L. The Fluor Daniel Econamine FG^{TM} Process: Past Experience and Present Day Focus, Energy Conversion Management, 1992, Vol. 33, No. 5-8, pp. 341-348.

(Schi) Schingnitz, M., Franke G., Gall, R. Absorptive Entfernung von Kohlendioxid aus Synthesegasen, Communication from the VEB Ingenieurtechnischen Zentralbüro Böhlen, (available in the internet on January 2013).

(Schi08) Schillgallies, I. Optimierung der CO_2-Abtrennung aus Rauchgasen zur Realisierung eines CO_2-freien Kraftwerkes, Diploma Thesis, University of Oldenburg, 2008.

(Schi10) Schillgallies I. Abschlussbericht zum Projekt CO_2 Post Combustion Capture, Institute for Natural and Applied Chemistry, University of Oldenburg, 2010.

(Shao09) Shao, R., Stangeland, A. Amines used in CO_2 Capture, 2009, Bellona Report.

(Shar63) Sharma, M., Danckwerts, P. Catalysis by Brönsted bases of the reaction between CO_2 and water, Transactions of the Faraday Society 1963, 59, 386-395.

(Shri74) Shrier, A.L., Danckwerts, P.V. Promoting Scrubbing of Acid Gases, U.S. Patent 3,856,921

(Sie10/13) Information and engineering values discussed internally within Siemens.

(Smi78) Smith, K.A., Meldon, J.H., Colton, C.K. Gas Absorption, U.S. Patent 4,080,423.

(Spe26) Sperr, F. Jr. Gas Purification Process, U.S. Patent 1,592,648.

(Ste06) Steeneveldt, R., Berger, B., Torp, T.A. CO_2 Capture and Storage Closing the Knowing-Doing Gap, Chemical Engineering Research and Design, 2006, No. 84, pp. 739-763.

(Sto11) Stolten D., Scherer, V. Efficient Carbon Capture for Coal Power Plants, Wiley-VCH, 2011.

(sul12) www.sulzer.com (available in October 2012)

(Tan11) Tang, Z., Fei, W., Oli, Y. CO_2 Capture by Improved Hot Potash Process, Proceedings of the 10th International Conference on Greenhouse Gas Control Technologies in Amsterdam, Netherlands, September 19-23, 2011.

(Tay46) Taylor, J.E., Boonton, N.J., Haslam, J.H. Separation of Carbon Dioxide from Gases, U.S. Patent 2,592,762.

(The12) Thee, H., Suryaputradinata, Y.A., Mumford, K.A., Smith, K.H., da Silva, G., Kentish, S.E., Stevens, G.W. A Kinetic and Process Modeling Study of CO_2 Capture with MEA-Promoted Potassium Carbonate Solutions, Chemical Engineering Journal, 2012, Vol. 210, pp. 271-279.

(Tol13) Toledo Soto, J.A. AAS based CO_2 Capture Process Energy Demand and Capital Cost Reduction by Adding an Inorganic Promoter, Master Thesis, Technical University of Berlin, 2013.

(Vai65) Vaidiya, P.D., Kenig, E.Y., Gas-Liquid Reaction Kinetics: A Review of Determination Methods, Chemical Engineering Communication, 2007, No. 194, pp. 1543-1565.

(VDI) VDI Wärmeatlas

(Ver11) Versteeg, G.F., Kumar, P.S., Hogendoorn, J.A., Feron, P.H.M. Method for Absorption of Acid Gases, U.S. Patent 7,927,403.

(vHol06) van Holst, J., Politiek, P.P., Niederer, J.P.M., Versteeg, G. F. CO_2 Capture from Flue Gas Using Amino Acid Salt Solutions, Faculty Science and Technology, University of Twente, Netherlands, 2006.

(Vor10) Vorberg, G., Katz, T., Sieder, G. Absorption Medium for Removing Acid Gases which Comprises Amino Acid and Acid Promoter, U.S. Patent 2010/0186590 A1.

(vStr11) van Straelen, J., Geuzebroek, F. The Thermodynamic Minimum Regeneration Energy Required for Post-Combustion CO_2Capture, Proceedings of the 10th International Conference on Greenhouse Gas Control Technologies in Amsterdam, Netherlands, September 19-23, 2011.

(Wie12) Wiese, M. Aspen Plus® Simulation of CO_2-Absorption Enhancement with Inorganic Promoters from Pilot Plant Results, Diploma Thesis, RWTH Aachen, 2012.

(Wol94) Wolsky, A. M., Daniels, E. J., Jody, B. J., CO_2 Capture from the Flue Gas of Conventional Fossil-Fuel Fired Power Plants, Environmental Progress, 1994, Vol. 13, No. 3, pp. 214-219.

APPENDIX A: ACID TITRATION ANALYSIS

The sample analysis within the experiment activities in this thesis was done by acid-base titration in order to determine the liquid phase composition. The titration analysis is a volumetric analytical method in which a liquid mixture with an unknown composition was neutralised using a standard solution or titrant. Since the solvents investigated have an alkaline nature; the titrant used was 1M aqueous solution of hydrogen chloride. The addition of the standard in the carbonated AAS mixture causes the pH to decrease. Within the scope of this work, a double titration method was used to accurately measure the carbonation ratio and the AAS concentration of each sample.

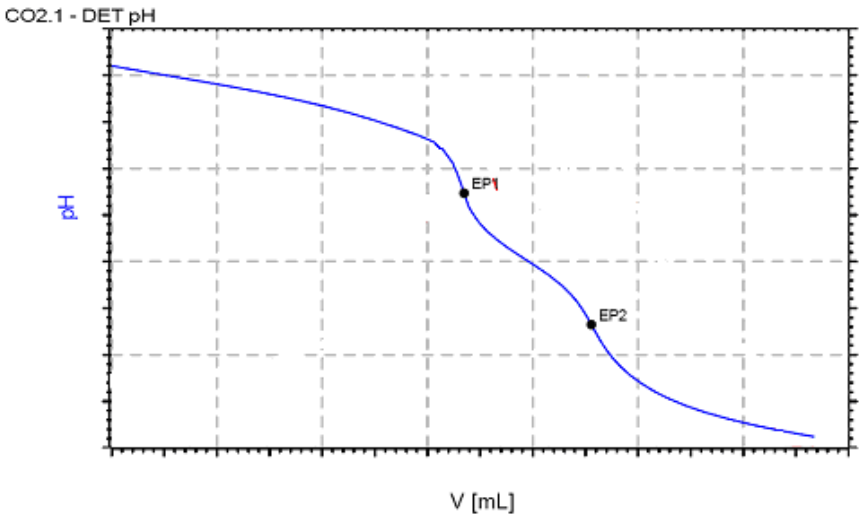

First pH-curve to determine the bicarbonate content

After taking the sample from the stirred cell, the mini plant or the pilot plant, an amount of approximately 2 g was poured into a glass beaker and measured in a weighing scale. After noting the sample weight, it was diluted with 50g of distilled water. The pH-electrode was submerged in the submerged in the analyte solution and the dosing process was started. The solution homogeneity was guaranteed by a magnet stirrer. As the acid was fed into the beaker; the solution pH decreased. This was due to the neutralisation reaction between the non-reacted AAS and the solvent alkali excess with the standard. The pH curve reaches the first equivalence point, where the curve gradient increases notoriously. At this point, all of the non-reacted AAS and alkali excess have been neutralised. As the standard was further added, the bicarbonate content reacted back to carbonic acid. The formation of carbon dioxide bubbles in the analyte was observed. Since the standard concentration was 1 M and the reaction stoichiometry between hydrogen chloride and bicarbonate was 1:1, the volume difference between the first and second equivalent points equals the molar content of bicarbonate in the sample.

After the first titration, the sample was degassed from the rest of carbon dioxide that may remain physically solved by applying vacuum. A diluted alkali mixture, 10 wt-% sodium hydroxide was added in excess to increase the pH of the sample to 12. It was therefore ensured that all the AAS was reacted back to the dissociated form. The AAS content in the sample was determined by the second titration.

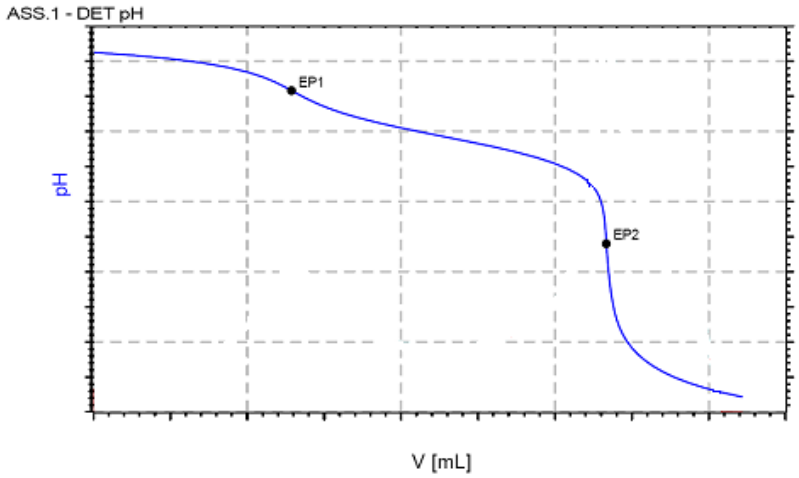

Second pH-curve to determine the AAS content

The addition of the standard on the degassed sample will decrease the pH as in the first titration curve. In the second curve (Figure 3.4), the first equivalent point was reached when the excess alkali added was consumed. The standard volume consumed between both equivalent points determines the AAS content in the sample. The alkali amount corresponds to the total volume used in the first titration minus the AAS volume in the second titration. The carbonation ratio was the relation between the bicarbonate volume in the first titration and the AAS volume in the second titration (Table 3.1).

Table A.1: Determination of the AAS content and carbonation ratio in the solvent sample

Component	Equation
AAS content, mol_{AAS}	$AAS = (EP2 - EP1)_{AAS}$ (A.1)
Carbonation ratio (α),mol_{CO2}/mol_{AAS}	$\alpha = \frac{(EP2 - EP1)_{CO_2}}{(EP2 - EP1)_{AAS}}$ (A.2)

The titration equipment consists of a 888 Titrando model from Metrohm, which includes a pH-electrode and a dosing device to add the precise standard volume. The alkali was added with a 725 Dosimat model from Metrohm. The degasification system consists of a vacuum pump CVC 3000 Vacuubrand, a stirrer Ikamag® RCT and a hermetic glass recipient. The vacuum pressure in the recipient was adjusted by a needle valve.

APPENDIX B: CAPTURE PERFORMANCE ESTIMATION

During the capture plant operation, the capture performance was defined by the capture rate *CR* and the specific energy demand *SED*. *CR* was the relation between the carbon dioxide molar flow rate in the treated gas stream $n_{CO2removed}$ and the carbon dioxide molar flow rate in the flue gas stream $n_{CO2feed}$ (Equation B.1).

$$CR = \frac{n_{CO_2removed}}{n_{CO_2feed}} \tag{B.1}$$

The carbon dioxide molar flow rate removed from the flue gas was obtained by multiplying the absorber - desorber working capacity and the respective in / out solvent mass flow rate in the absorber. The carbonation ratio was measured by analysing through acid titration the samples taken from both columns' sumps. The solvent mass flow rate in / out of the absorber was measured, monitored and recorded by the Siemens process control system (Equation B.2).

$$n_{CO_2removed} = \alpha_{CO_2}^{\ rich} \cdot L_{Solvout} - \alpha_{CO_2}^{\ lean} \cdot L_{Solvin} \tag{B.2}$$

The carbon dioxide molar flow rate fed into the absorber was dependent on the carbon dioxide mol fraction y_{CO2} in the flue gas and the flue gas flow rate fed into the absorber *G*. It must be considered only in the pilot plant experiments that the flue gas, which comes from the desulphurisation unit, was saturated with water vapour. The water vapour portion must be subtracted from the total flue gas mol flow rate in order to estimate the carbon dioxide molar flow rate. The saturated water vapour partial pressure p_{H2O}^{s} at the temperature of the flue gas entering the absorber can be easily found in the literature. The relation between p_{H2O}^{s} and the total gas pressure yields the water mol fraction in the flue gas (Equation B.3).

$$y_{H_2O} = \frac{p_{H_2O}^{\ s}(T)}{P} \tag{B.3}$$

In order to convert the flue gas mass flow rate into mol units, the average molecular weight of the flue gas (CO_2, H_2O and N_2) M_{wFG} must be estimated. However, in the pilot plant, the carbon dioxide mol fraction $y_{CO2}$was measured for the dry flue gas stream. If the oxygen amount was neglected (the FG contains only carbon dioxide and nitrogen), the average molecular weight of the dry flue gas stream M_{dFG} can be calculated (Equation B.4).

$$M_{dFG} = y_{CO_2} \cdot M_{CO_2} + (1 - y_{CO_2}) \cdot M_{N_2} \quad \text{(B.4)}$$

Following the same procedure, but now implementing M_{dFG} and y_{H2O}; M_{wFG} was estimated (Equation B.5).

$$M_{wFG} = y_{H_2O} \cdot M_{H_2O} + (1 - y_{H_2O}) \cdot M_{dFG} \quad \text{(B.5)}$$

Finally, the relation between the flue gas mass flow rate G and M_{wFG} gives n_{FG} (Equation B.6).

$$n_{FG} = \frac{G}{M_{wFG}} \quad \text{(B.6)}$$

To determine the dry flue gas molar flow rate n_{dFG}, the water content was subtracted from n_{FG} (Equation B.7).

$$n_{dFG} = n_{FG} \cdot (1 - y_{H_2O}) \quad \text{(B.7)}$$

The CO_2 molar flow rate fed into the absorber was finally gained (Equation B.8).

$$n_{CO_2feed} = y_{CO_2} \cdot n_{dFG} \quad \text{(B.8)}$$

Further, the specific energy demand was the relation between the reboiler heat duty Q_{Reb} and the carbon dioxide flow rate removed from the flue gas stream (Equation B.9).

$$SED = \frac{Q_{Reb}}{n_{CO_2removed}} \quad \text{(B.9)}$$

The reboiler heat duty in the mini plant consisted in the sensible heat exchange between the heating oil that circulated inside the spiral coil in the reboiler, and the AAS solvent on the outside. The heating oil flow rate m_{Oil} was measured in a Venturi meter. The temperature of the heating oil was measured before T_{in} and after T_{out} entering the reboiler. The heat capacity Cp was correlated at the heating oil average temperature. The correlation was taken from the DW-Therm heating oil user's guide (Equation B.10).

$$Q_{Reb} = m_{Oil} \cdot Cp \cdot (T_{in} - T_{out}) \tag{B.10}$$

The reboiler heat duty in the pilot plant was supplied by low pressure steam vapour coming from the power plant. The heat was proportional to the latent heat produced by the condensation of the steam vapour in the reboiler. The vapour overheating and undercooling effects during the heat transfer were also considered in the energy balance (Equation B.11). The reboiler heat duty was directly calculated and recorded by the process control system.

$$Q_{Reb} = Overheating + LatentHeat + Undercooling \tag{B.11}$$

APPENDIX C: MINI PLANT EXPERIMENTAL RESULTS

Table C.1. Laboratory mini plant experimental results

Solv. Type	Abs. height	*L*	*[AAS]*	α*_lean*	α*_rich*	*CR*	*SED**
[-]	[m]	[kg/h]	[wt-%]	[mol/mol]	[mol/mol]	[%]	[%]
Base Case	3	12.5	27.6	0.27	0.78	87.4	125
		13.5	28.2	0.29	0.77	87.7	114
		16	27.9	0.31	0.72	87.9	106
		19	27.6	0.35	0.71	87.8	100
		22	28.0	0.38	0.67	87.2	101
		25	28.2	0.44	0.70	86.1	104
Promoted solvent w 0.1 wt-% PROM-1	2	17	29.2	0.30	0.66	86.2	121
		18	28.9	0.32	0.67	86.6	118
		20.5	28.0	0.33	0.65	86.7	108
		25	27.8	0.38	0.64	84.6	113
	2.5	16	29.0	0.30	0.68	83.9	120
		18	28.9	0.34	0.69	86.2	104
		20	27.9	0.38	0.70	87.2	98
		22	28.3	0.37	0.66	85.8	103
	3	12.5	28.6	0.25	0.77	86.8	120
		13.5	28.2	0.27	0.74	85.0	116
		15.0	28.3	0.30	0.72	86.0	106
		18.0	28.1	0.35	0.71	86.0	97
		20.0	28.1	0.41	0.70	85.4	93
		25.0	28.5	0.47	0.73	85.6	94

* Due to confidentiality issues, *SED* is expressed in relation to the base case minimum

APPENDIX D. PILOT PLANT EXPERIMENTAL RESULTS

Table D.1. Pilot plant experimental values

Test run		Operating variables												Capture performance	
Nr.	[Prom]	Packing height	Solvent strength	Reboiler heat duty	Gas flow rate	CO_2 in FG	CO_2 feed pressure	Feed CO_2 flow rate	Lean solvent flow rate	Rich solvent flow rate	Rich CO_2-loading	Lean CO_2-loading	Rem. CO_2 flow rate	Capture rate	Specific energy duty
	[wt.%]	[%]	[wt.%]	[-]	[kg/h]	[mol.%]	[mbar]	[kg/h]	[kg/h]	[kg/h]	[mol.%]	[mol.%]	[kg/h]	[%]	[%]
1	-	100	24.6	High	187.2	13.66	135	34.32	1079	1118	77.3	40.9	29.76	86.7	100.0
5	0.1	100	24.4	High	187.1	13.73	136	34.17	1078	1120	78.2	40.9	30.20	88.4	96.8
4	-	75	25.0	High	186.8	13.52	138	33.70	1066	1105	76.1	40.7	28.33	84.1	102.6
8	0.1	75	24.9	High	186.7	13.79	137	34.20	1073	1114	76.8	40.5	29.87	87.3	96.8
2	-	100	23.8	Low	187.2	13.44	132	33.58	1082	1121	80.9	47.8	26.63	79.3	90.2
6	0.1	100	25.0	Low	186.1	13.30	133	33.11	1082	1120	82.7	48.8	27.62	83.4	86.8
3	-	75	25.6	Low	186.7	13.21	138	32.90	1078	1114	78.2	48.9	25.36	77.1	94.2
7	0.1	75	24.5	Low	187.2	13.30	133	32.52	1073	1106	82.8	48.3	27.54	82.9	87.0

* Due to confidentiality issues, *SED* result values are proportional to the base case results in experiment Nr. 1

APPENDIX E: ECONOMIC EVALUATION FACTORS

Table E.1. Component reference values for size, cost and scaling index

Component	Scaling factor	Reference size	Reference cost (€)	Scaling index
Absorber	Height, Diameter, (m)	1.22, 0.91	779	0.81, 1,05
Desorber	Height, Diameter, (m)	1.22, 0.91	779	0.81, 1,05
Direct contact cooler	Height, Diameter, (m)	1.22, 0.91	779	0.81, 1,05
Condensate piping	Height, Diameter, (m)	1.22, 0.91	779	0.81, 1,05
Steam piping	Height, Diameter, (m)	1.22, 0.91	779	0.81, 1,05
Cross heat exchanger	Transfer area, (m^2)	37.2	3896	0.65
Lean-solvent cooler	Transfer area, (m^2)	37.2	3896	0.65
Reboiler	Transfer area, (m^2)	37.2	3896	0.65
Condenser	Transfer area, (m^2)	37.2	3896	0.65
Cooling water cooler	Transfer area, (m^2)	37.2	3896	0.65
CO_2-compressor	Power, (W)	74570	17920	0.77
Blower	Power, (W)	74570	17920	0.77
Rich-solvent pump	Power, (W)	8700	1169	0.64
Lean-solvent pump	Power, (W)	8700	1169	0.64
Cooling water pump	Power, (W)	8700	1169	0.65

Table E.2. Material pressure factor and module factor for each plant component

Equipment	Material pressure factor	Module factor
Cross heat exchanger	2.00	3.18
Lean solvent cooler	2.00	1.83
Reboiler	3.38	3.18
Condenser	2.00	3.18
Cooling water cooler	2.00	1.83
Flue gas blower	1.00	3.11
Rich solvent pump	1.93	3.38
Desorber pump	1.93	3.38
Cooling water pump	1.93	3.38
CO_2 compressor	2.90	2.93
Absorber	3.85	4.07
Desorber	3.85	4.07
Direct contact cooler	3.85	4.23
Steam piping	3.85	4.12
Condensate piping	3.67	4.23

Table E.3. Fixed capital investment: direct and indirect costs as a function of UBMC

	% UBMC
Direct costs	
Buildings, services and land	40.0
Contingency	15.0
Fee	3.0
Indirect costs	
Construction overhead	
Fringe benefits	2.0
Labor burden	2.9
Field supervision	2.4
Temporary facilities	1.2
Construction equipment	2.0
Small tools	0.5
Miscellaneous	2.3
Engineering	
Project and process engineering	1.3
Design and drafting	1.8
Procurement	0.2
Home office construction	0.2
Office indirects and overhead	3.9

Table E.4. Total capital investment factors as a function of FCI

	% FCI
Working investment	25.00
Start-up and solvent cost (first fill)	10.00
Construction insurance	0.75

Table E.5. Operational and maintenance costs excluding utilities, OMC

	Abbreviation	%	of
Fixed charge	**FC**		
Local taxes		2.0	FCI
Insurance		1.0	FCI
Direct production costs	**DP**		
Solvent makeup		1.1 M€/y	
Maintenance	M	4.0	FCI
Operating labor	OL	2.2 M€/y	
Supervision and support	S	30.0	OL
Operating supplies		15.0	M
Laboratory charges		10.0	OL
Plant overhead cost	**PO**	**60.0**	**M+OL+S**
General expenses			
Administrative cost		15.0	OL
Distribution and marketing		0.5	OL
R&D cost		5.0	OL